Submitted to Reports on
Progress in Physics

LBL-645
Preprint

ACCELERATORS FOR NUCLEAR PHYSICS

D. J. Clark

April 1972

AEC Contract No. W-7405-eng-48

LBL-645

ACCELERATORS FOR NUCLEAR PHYSICS†

D. J. Clark

Lawrence Berkeley Laboratory
University of California
Berkeley, California 94720

ABSTRACT

This article describes the principal charged particle accelerators being used today for research in nuclear physics in the energy range up to about 1000 MeV. The accelerators include Van de Graaffs, sector cyclotrons and linear accelerators for both positive ions and electrons. For each type of accelerator a brief treatment is given of the recent history, operating principles, some special techniques, a typical facility, and some examples of experimental data from that type of accelerator. Descriptions are also given of new types of machines under construction, such as Pelletrons, frequency modulated sector cyclotrons, separated sector cyclotrons, and superconducting linear accelerators. New ideas for the future are mentioned, including multi-stage tandem-cyclotrons, and the electron ring accelerator. The reader is assumed to have no experience in accelerators or nuclear physics, and many references are given to more detailed treatments of the topics covered.

TABLE OF CONTENTS

1. Introduction

1.1 What is an accelerator?

An accelerator is a device for accelerating charged particles to high energies by using electromagnetic fields. To be useful in experiments the particles should emerge from the accelerator as a "beam" with small size and divergence. The particles most often used are protons and electrons, since they are easy to produce, stable and elementary. The third elementary particle found in matter, the neutron, has not been used because it has no charge and its magnetic moment is too weak to be used in a practical accelerator.

Electron accelerators range in size from electronic radio "tubes" or "valves" which accelerate and modulate electrons of several hundred volts energy, to the 2 mile long linear accelerator (linac) completed in 1966 at Stanford University, California, USA, for high energy physics studies. Of intermediate size are direct current electron accelerators used to produce X-rays and study radiation effects in solids, and microwave linear accelerators used to produce high energy X-rays for medical work and electrons, positrons and photons for nuclear structure studies.

Proton accelerators come in a similar large variety. Small machines, which usually accelerate deuterons also, are used in nuclear physics studies. The deuteron beams from small acceleration tubes 30 cm long can be used effectively to produce a higher energy neutron beam by bombarding a tritium target. Proton accelerators go upward in size through the direct current Van de Graaffs to the circular cyclotrons, and synchrotrons hundreds of meters in diameter. Some of the uses for these machines are producing isotopes for medical studies, the study of

nuclear structure, and the production of new unstable particles. The largest of these will be a synchrontron 4 miles in circumference being completed near Chicago, U.S.A., and a similar facility being planned at CERN, Geneva, Switzerland. There have been many detailed books and reviews on accelerators, such as those by McMillan (1959a), Livingood (1961), Livingston and Blewett (1962) and Blewett (1967), which describe the principles and construction of particle accelerators. Kernan (1968) wrote an introductory booklet on accelerators.

1.2 Accelerators for nuclear physics.

Of the great variety of existing accelerators mentioned above, we will choose those used for the study of nuclear structure and reactions as the subject of this article. In the study of nuclear structure one investigates the nuclear force, which acts between nucleons (neutrons and protons) and the arrangement of the nucleons in the nucleus. Since the diameter of the nucleus is less than 10^{-12} cm, the structure cannot be studied with a microscope, but only by using particles of nuclear size, such as other nucleons or electrons, as a probe, to fire at the nucleus under investigation, and then observe how they are scattered and what other particles emerge from the interaction. By observing the outgoing particle energies and angular distributions, one can deduce the size and shape of the nucleus, and the forces existing inside the nucleus. The projectiles are supplied very efficiently by modern accelerators.

The minimum energy of particle beams required for these studies is the order of the binding energy of nucleons in the nucleus: several million electron volts (MeV). An electron volt is the energy given to an electron or proton when accelerated across a potential of one volt. This

energy can be contrasted with the much lower range of a few electron volts up to a few thousand electron volts (keV) used in atomic physics for the study of the electron structure around the nucleus, which is about 10^{-8} cm in size.

The energy range most used for nuclear structure or "nuclear physics" studies is 1-1000 MeV (1 GeV). In the lower part of this region, 1-100 MeV, positive ion beams interact with the nucleus as a whole, or with several of the nucleons. In the 100-1000 MeV region the proton "wave-length" decreases to interact with individual nucleons in the nucleus, giving more precise information about each nucleon. At energies over 1000 MeV, the dominant process is the production of short lived particles such as mesons. The study of the production and decay of these unstable particles forms the field of "high energy" or "particle" physics. This paper will review the principal current accelerators for positive ions and electrons being used for "nuclear physics" including their operating principles, performance, special techniques and some of the experimental results. It will also describe the new machines being constructed and planned. The energy range under consideration here will be roughly 1-1000 MeV, although the accelerators in the 500-10,000 MeV range are used both for nuclear structure and particle physics. The principal accelerators used in nuclear physics, to be described here, are D.C. machines such as the Cockroft-Walton and the Van de Graff, cyclotrons, and linear accelerators for electrons and heavy ions.

1.3 Historical background

Soon after the discovery of radioactivity by Becquerel in France in 1896, physicists began to use the alpha-particles from the radioactive

elements to study the structure of the atom and the nucleus. This work is described in many books such as Ratner (1964). In the forefront of this endeavor was Ernest Rutherford in England. In the period 1908-1913, Rutherford and his associates used α-particles from natural radioactivity to bombard thin gold foils. They observed that the number scattered backwards was much larger than expected. This could only be explained by the hypothesis that all the positive charge was contained within a radius of about 10^{-12} cm, rather than being distributed throughout the atom of radius 10^{-8} cm, as previously supposed. Thus the concept of the nucleus was born.

In 1919 Rutherford set out to split the nucleus by bombardment with natural α-particles. He chose nitrogen as a target because it has small nuclear charge, and thus is more easily penetrated than gold. He showed that protons were knocked out and therefore were one constituent of the nucleus. This was the first nuclear reaction ever induced in the laboratory. Rutherford had succeeded in performing the first man-made transmutation of the elements, by using projectiles of sufficient energy -- α-particles of several MeV. We would write this reaction $^{14}N(\alpha,p)^{17}O$.

In these experiments the acceleration of the α-particles was produced by a radioactive nucleus. The particles came out in all directions, and with limited energy and intensity. Rutherford (1927) expressed the importance of having a high intensity source of high energy particles in an address to the Royal Society of London: "It has long been my ambition to have available for study a copious supply of atoms and electrons which have an individual energy far transcending that of the α-

and β-particles from radioactive bodies. I am hopeful that I may yet have my wish fulfilled...". Calculations of the energy necessary to penetrate the nucleus showed that protons with less than .5 MeV of energy could penetrate light nuclei. In the late 1920's and early 1930's various laboratories in the world were trying to produce these particle beams. This development work is well documented by Livingston (1966). The main types of accelerators under development were the transformer-rectifier voltage multiplier in England, the cyclotron and the Van de Graaff in the U.S.A. The race was won by the voltage multiplier built by Cockroft and Walton (1932) at Rutherford's Cavendish Laboratory in Cambridge, England. In the first nuclear reaction produced by an accelerator, protons were accelerated and struck a lithium target. At energies of 100-500 keV α-particles were produced: $^{7}Li(p,\alpha)\alpha$. A few months later Lawrence et al. (1932) at Berkeley, California confirmed and extended these results with 1 MeV protons from an early cyclotron with an 11-inch diameter pole.

In the succeeding decades accelerators were pushed higher in energy. As described by Livingston (1959) and McMillan (1959b) Lawrence's group at Berkeley exploited the cyclotron, which used the same voltage many times to accelerate ions to high energy. By 1936 a 27 inch model was producing 6 MeV deuterons and there were about 20 other cyclotrons around the world. New pole pieces were installed to make a 37-inch cyclotron which gave 8 MeV deuterons in 1937. The 60-inch cyclotron was completed in 1939, and served as a model for many others throughout the world. After World War II scientists returned to the accelerator field from wartime research. The 184-Inch synchrocyclotron

was completed in 1946, giving 190 MeV deuterons. Many other synchro-cyclotrons were soon built around the world in the 1950's. The possibility of using sector focusing in cyclotrons proposed by Thomas (1938) was finally put into practice in a new generation of sector-focused cyclotrons which grew during the 1960's.

In the field of D.C. accelerators voltages of up to 1.5 million volts were produced by R. J. Van de Graaff (1931) using a silk charging belt in an electrostatic generator. In 1936 he completed two large generators which operated at +2.5 MV and -2.5 MV, to give 5 MV between them. Van de Graaff's high voltage generators up to this time had no accelerating tubes. At the Carnegie Institution in Washington, D.C., M. A. Tuve et al. (1935) used Van de Graaff's principle to build accelerators of .6 and 1.3 MV for hydrogen ions. The steady D.C. voltages were a great advantage over the pulsed voltages of Tesla coils previously used. A great advance in the suppression of sparking around the high voltage terminal of Van de Graaff accelerators was made by placing them in pressurized vessels. This was demonstrated by Barton et al. (1932) who generated 1 MV in a compact generator operating in 7 atmospheres pressure without an accelerating tube. The development of pressurized Van de Graaff accelerators was carried on by R. G. Herb's group at the University of Wisconsin, U.S.A., starting with .4 MeV in 1934, and getting 4 MeV ions in 1940. At M.I.T. in Massachusetts, U.S.A. the group under J. G. Trump and R. J. Van de Graaff developed high voltage techniques and built electron accelerators to produce X-rays. This field up to 1948 was summarized by them (Van de Graaff et al. 1948). In 1947 Trump, Van de Graaff and others formed the High Voltage Engineering

Corporation for the commercial production of "Van de Graaff" accelerators. This company has done much technical development on higher voltage electrostatic accelerators and has built most of the Van de Graaff accelerators being used throughout the world. In the 1960's the tandem principle was brought into operation, which doubled the beam energy produced by a given value of high voltage.

The third main type of accelerator being developed during this same time was the linear accelerator. The positive ion linac was born in Berlin where R. Wideröe (1928) accelerated sodium and potassium with an rf drift tube to demonstrate resonant acceleration by using the same voltage twice. It was this experiment which gave Lawrence the idea for the cyclotron in Berkeley. At Berkeley the work of Wideröe was extended by Sloan and Lawrence (1931) to accelerate mercury ions to 1.2 MeV, but these heavy ions were of too low an energy to be practical for experiments. During World War II high frequency radar power sources were developed. At Berkeley Alvarez (1946), et al.(1955) used surplus military equipment to supply the first proton linear accelerator of 32 MeV energy. Several proton linear accelerators were later built for nuclear physics use but most have been shut down because of their low duty cycle and limited particles and energies.

Electron linear accelerators were also made possible by World War II radar work. Because of the small electron mass, the velocity quickly approached that of light, and very high frequencies of accelerating voltage were required. Studies were done at Stanford University in California under W. W. Hansen, at M.I.T. in Massachusetts under J.C. Slater, and in England at the Telecommunications Research Establishment under

D. W. Fry, and later at the Atomic Energy Research Establishment at Harwell. These early studies and operation of a linac of 1.5 MeV at Stanford are summarized by the Stanford group (Ginzton et al. 1948). Stanford has led the field by building successive accelerators at 20 MeV, 100 MeV, 600 MeV, 1000 MeV in 1960, and 20 GeV in 1966. The status up to 1955 was summarized by Chodorow et al. (1955), when the electron energy was 630 MeV.

A special accelerator used in a few laboratories is the betatron. It uses the induction principle to accelerate electrons. The first model at 2.3 MeV is described by Kerst (1941). These machines were developed by Kerst at the University of Illinois to an energy of 300 MeV.

In the push toward higher energies the principle of phase stability, discovered independently by Veksler (1945) in Russia, and McMillan (1945) at Berkeley, provided the key to building synochrocyclotrons of hundreds of MeV, and electron and proton synchrotrons of many GeV energy. Finally the discovery of alternating gradient or "strong" focusing by Courant, Livingston and Snyder (1952) made possible the reduction in size of synchrotron magnets and acceleration chambers, to make economically feasible the construction of electron synchrontons up to 6 GeV and proton synchrotrons up to 500 GeV.

In the energy range up to 1000 MeV which we are considering in this article, the principal nuclear physics accelerators are now Van de Graaff generators, cyclotrons and linear accelerators. In Figure 1 we see the number of these accelerators for protons and deuterons between 10-1000 MeV which have been operating in the last 30 years (Burrill 1965), (Howard 1958), (Howard 1967), (Howard 1969), (Gordon et al. 1963),

(F. Chmara 1971, private communication). The trend shows an increasing number of tandem Van de Graaffs and sector cyclotrons, whose excellent beam porperties will be described in later sections of this article. In addition to these positive ion machines there are a number of electron linacs and few betatrons in this energy range also.

2. Requirements for nuclear physics experiments.

2.1 Types of experiments.

The experimental research programs at modern nuclear physics accelerators are sophisticated extensions of the early work done by Rutherford. They seek answers to many questions: What is the size and shape of the nucleus? What are the details of the forces between nucleons, which hold the nucleus together? What are the various energy levels within each nucleus? How many nuclei are stable and how do the unstable ones decay? How does the nuclear scattering, excitation or reaction process induced by a bombarding particle proceed? Descriptions of the present status of the field of nuclear physics are given in many texts, such as Harvey (1969) and Marmier et al. (1969). An illustration of the structure of nuclei is given by the energy level diagrams of a light and a heavy nucleus shown in Figures 2 and 3. The levels are given in MeV. They represent excited states of the nucleus, in which a nucleon is lifted above its ground state in the nuclear shell structure, or a group of nucleons is vibrating or rotating within the nucleus. In the typical light nucleus such as ^{7}Li shown in Figure 2, the levels are usually due to excitation of 1 or 2 nucleons, and are 1-2 MeV apart. Heavy nuclei such as ^{238}U in Figure 3 typically show much closer level spacing of 1-200 kV. These levels are usually due to collective excitation of many nucleons.

To answer the questions about nuclear structure and forces, a great variety of experiments is being done. A main division may be made between the beams produced at accelerators for positive ions

and those provided by electron accelerators.

The positive ion beams of protons, deuterons, α-particles, carbon, oxygen, etc. are themselves nuclei, and so can interact with the target with the nuclear or "strong" interaction. At low energies however the interaction of these ions with a target is dominated by the long range electrostatic repulsion, or Coulomb force. The projectile and target don't come close enough together to feel the short range nuclear forces, which operate inside 10^{-13} cm. The distance of closest approach is proportional to the charge of the projectile and of the target, and inversely proportional to projectile energy. So for example, the nuclear force is felt by protons over .1 MeV on lithium, and by oxygen over 80 MeV on heavy targets. This threshold energy necessary to penetrate the Coulomb repulsion region is usually called the "Coulomb barrier". Interesting "Coulomb excitation" experiments have been done below the Coulomb barrier, by using the Coulomb force to excite many nuclear states. The higher nuclear levels can be excited by using heavier ions as projectiles, because of their higher nuclear charge. The energies and other properties of the excited nuclear states are determined by the γ-rays from de-excitation, and by the energies and angular distribution of the outgoing particles.

At energies above the Coulomb barrier the strong nuclear force comes into play. These experiments can thus give information about the strong force by study of the angular distribution of scattered particles. The target nucleus can be easily excited to

various energy levels by these projectiles, and these levels can be studied by looking at outgoing particles and γ-rays. The bombarding particle may produce a transfer reaction, in which one or more nucleons are transferred to or taken from the target nucleus. In this case the reaction process can be studied, and the levels of the new residual nucleus can be found. These experiments have been done at many bombarding energies, because the nuclear force varies with energy, and also because each nuclear reaction has a particular energy of which it has the highest probability (cross-section) of occurring. Thresholds for multi-nucleon transfer may be 50-100 MeV. Experiments on nuclear structure have been done at proton energies up to several GeV.

In the past several years the search for "super-heavy" elements has become a popular field for research (Seaborg 1968), (Henahan 1971), (Flerov 1972). These elements form a group of stable isotopes which is predicted near the closed shell "magic" proton number Z=114 and neutron number N=184. This stable island is separated from the highest known stable element, Z=105, by a group of unstable elements in the "sea of instability". A promising method for reaching these islands is the bombardment of heavy targets, $Z > 90$, by heavy ions, to synthesize the new elements by fusion, fusion-fission, or nucleon transfer. A projectile energy high enough to overcome the Coulomb barrier is required. This energy is about 7 MeV/nucleon as shown by the curves "CB" in Figure 4. Some of these experiments are now being done, and others will be possible with the next generation of heavy ion accelerators.

When a charged particle beam hits a target, neutrons are one of the most common reaction products. These can be collimated through apertures in absorbers and used as a secondary beam for further experiments. The primary beam most often used is of protons or deuterons. For example 14 MeV neutrons can be produced by bombarding tritium with deuterons of only 100keV: $^{3}H(^{2}H,n)\alpha$. At higher energies proton beams of several hundred MeV are pulsed onto a heavy target. The neutron energies can be identified by their time of flight through several hundred meters, between pulses. The neutron is a useful projectile since it is not charged and thus interacts mainly with the strong force. It does not feel the Coulomb repulsion, and so can easily enter target nuclei at electron volt energies to react or scatter. Its detection, like its production must be done indirectly, by a collision or reaction producing charged particles.

It has been found that particles with "spin" such as the proton or deuteron interact differently with a target, depending on whether their spin is "up" or "down", when they are scattered left and right. For example, the spin-up projectiles may scatter more to the left and those with spin-down more to the right. This spin dependence of nuclear forces can be investigated using a "polarized" beam of mostly spin-up or spin-down particles. The early beams of polarized ions were produced by scattering a primary beam from a well chosen target at an optimum angle, using the known spin dependence of the scattering to give a secondary polarized beam.

Since 1960 modern accelerators have begun to use sources of polarized ions (Haeberli 1967) in the injection stage of the accelerator. These sources separate out ions of one spin direction by using the atomic magnetic moment in a magnetic field. The polarized sources give orders of magnitude more polarized beam intensity at the accelerator output end than the old secondary beam scattering method of production. Polarized neutron beams can be produced as secondary beams emerging at certain angles from either positive ion (Walter 1970) or photon (Baglin 1971) reactions on certain targets. These beams are of low intensity but give unique nuclear information.

The use of electrons as bombarding particles gives a different kind of information, since they don't interact with the strong force, but primarily with the well-known electromagnetic force. Thus the scattering of electrons can give clear information about the size and shape of nuclei and their constituent nucleons without disturbing their structure (Wilson et al. 1964). As the energy of the electrons increases, their "wavelength" decreases, giving better resolution. A 50 keV electron beam in an electron microscope has a wavelength of 10^{-9}cm, so it can only resolve thousands of atoms. The 20 GeV beam of the 2 mile Stanford linac can reveal the internal structure of nucleon with its wavelength of 10^{-14} - 10^{-15} cm. Another useful property of high energy electron beams is that they produce X-rays, created as bremsstrahlung, especially in a target of high atomic number. These can be

used as a projectile for nuclear reactions, or to produce neutron or positron beams in a heavy target. The short pulse capability (several nanoseconds) of the electron linac makes the neutron time-of-flight experiments attractive. The positron beams are usually produced by inserting a target part way along the electron linac. The positrons are accelerated by the remaining length of the linac and can be used to make photon (γ-ray) beams by decay in flight in a light target. These monoenergetic photon beams are useful in making more precise measurements in nuclear structure studies than are possible with the photons produced simultaneously over a broad energy spectrum as bremsstrahlung. Sources of polarized electrons (Baglin 1971) can also be used to inject electron linacs. The resulting polarized beams can be used as projectiles to study spin dependent electron scattering effects, or they can be converted to polarized bremsstrahlung in a thin target, for use in other experiments.

At energies over several hundred MeV protons and electrons can convert their kinetic energy into mass when they hit a target, to create π-mesons, and many other short-lived particles. Their properties are being measured by the high energy experimentalists, and their place in this complex field of subnuclear physics being investigated by high energy theorists. They can also be used as projectiles for studies of nuclear structure, if their intensity is high enough. Also the negative μ and π mesons can replace electrons in a target atom, but much closer to the nucleus. The X-rays emitted as these mesons cascade down through the atomic shells, give

valuable information about the size and shape of the nucleus. Over the past decade a number of proposals for "meson factories" have appeared (Rosen 1966). Several are now being built, such as the Los Alamos 800 MeV proton linac (Rosen 1969). It will provide about 1000 times more primary proton beam intensity than previously available, and thus 1000 times more μ and π meson secondary beam intensity also.

2.2 Beam requirements

2.2.1 Particles and energies.

Since the forces and structure of nuclei are so complex, it is useful to have a large variety of projectiles at various energies available. Beams of nuclei, electrons, photons, or unstable particles each give a unique type of information. High maximum energy of an accelerator is always an advantage, of course, because it allows investigation of nuclear forces in a wide energy range, and makes possible reactions with high threshold energies. Some interactions proceed through a narrow energy level in the intermediate "compound nucleus" of the temporarily fused projectile plus target. These "resonance" interactions can be observed by varying the energy in small steps across the resonance, and thus require an accelerator beam of precise and easily variable energy. The requirements on beam characteristics for various experiments have been described for example by Conzett (1966a) and Conzett *et al.* (1966b).

2.2.2 Energy spread.

The spread in energy of an accelerator beam determines what

types of experiments are possible with the beam. For the study of closely spaced energy levels or narrow resonances the beam must have a spread, ΔE, less than the level spacing, or the levels will be washed out. This is illustrated by Figure 5, showing the γ-ray yield from 5-12 MeV protons on aluminum. The 15 keV resolution at the bottom shows many more details of the interaction, than if the resolution were several hundred kV, as simulated by averaging over larger intervals, in the upper curves. It is often useful to measure the width of a nuclear level, which can be done only if the beam energy spread is of comparable size or less than the level width.

There are several other advantages in having beams of narrow energy spread. One is that a peak in the energy spectrum of scattered particles due to a weak reaction can be better separated from the background. Another is to make sure that the energy being used does not overlap with a nearby resonance where the interaction is greatly enhanced or reduced in strength.

The importance of energy spread is its effect on the experiment. There are several ways in which a relatively large energy spread from an accelerator can be greatly reduced in its effect on the experimental data. One is by use of a high resolution analyzing magnet, which selects only a small part of the accelerator beam within a desired energy interval for use in the experiment. Another technique is to spread the energy out linearly across the target using the dispersion of an analyzing magnet, and

then bring the various energies back to a focus with another magnet after the target. This is often called "dispersion matching" of the two magnets. These techniques will be illustrated in later sections of this paper.

2.2.3 Beam emittance.

A beam of charged particles is composed of a large number of individual particles, each with its position and velocity. For an accelerator beam the particles will usually all have the same speed within 1%, and the same direction within 1° of the axis. A schematic representation of a beam is shown in Figure 6. The Z-axis is the direction of travel, and the X-axis is one transverse direction. This group of particles is also shown as a "phase plot" in the X-X' plane, called phase space in the usual language of beam transport or beam "optics" (Banford 1966). The X-dimension gives the distance from the axis and X' gives the divergence of each particle from the axis. Since the divergence angles are normally small, the tangent dX/dZ is a good approximation for the angle. Sample points are shown to illustrate the correspondence between X-Z and X-X' space. It is convenient to assume that the boundary of the beam envelope is an ellipse in phase space, because the ellipse transforms to other ellipses with equal area as the beam is transported along the beam line. The area of the ellipse in phase space is usually called the "emittance". Smaller emittance beams are easier to transport and make possible better quality experiments. The units of emittance are millimeter-milliradians, centimeter-radians, etc. When a beam is accelerated, the momentum

increases along the axis, but the transverse momenta do not change, so X' and emittance are inversely proportional to momentum. So in stating the emittance of a beam it is important to specify its momentum or energy.

The transport of a beam through a simple beam transport system is shown schematically in Figure 7, in both X-Z and phase space. The source of particles from an accelerator is shown on the left. Four sample rays are shown being transported down the beam line to an image point by two focusing lenses. This image can be at the target, or at an intermediate point which serves as a source for succeeding lenses. The lenses are usually magnetic quadrupoles for energies in the MeV range. The phase plots at points along the line in Figure 7 show the changes in shape due to drift lengths and focusing lenses. The area of the ellipse stays constant according to Liouville's Theorem (Banford 1966). The image has larger size but smaller divergence than the source because it is further from the nearest lens. The lens positions or strengths can be adjusted to give any desired image size, but the area, or $(\Delta X)(\Delta X')$ of the upright ellipse remains constant.

The beam arriving at an experimental target is shown in Figure 8, a diagram similar to that of Conzett (1966b). The ideal scattering or reaction experiment would have an incoming beam of zero divergence as in Figure 8A. The outgoing particles are measured by a detector at angle θ to the beam line. A real experiment uses a beam of finite divergence as in Figure 8B or 8C. In Figure 8B the last focusing lens is adjusted to give a wide parallel beam

on the target. However the scattering angle seen by the detector varies from θ_1 to θ_2. If the experiment is sensitive to scattering angle, as in the case where high energy resolution is required and the energy of the scattered particle varies considerably with angle, then this variation of scattering angle may not be tolerable. The last lens could be adjusted to focus beam on the target, as in Figure 8C. In this case the beam spot is small and the previous type of angular spread does not occur. But a different angular spread now appears, θ_1 to θ_2, due to a variation of incoming divergence on the target. This is just as bad as the previous spread. So the incoming divergence produces an angular spread in scattered beam due either to spot size or divergence on target. In practice the lens would be set at an intermediate point between Figure 8B and 8C to minimize both effects. Thus the incoming divergence, one component of the emittance, sets a lower limit on the angular spread of the beam at the detector. If this spread is too great, the beam must be collimated, with a loss in intensity. So the emittance, as well as the intensity, is a very important parameter of accelerator beams. The above example was simplified, since there would also be a finite source size, as well as divergence, which would also contribute to the beam size on target, and thus the angular spread at the detector.

2.2.4 Time structure.

The time structure of the accelerator beam is important for some experiments. For example if the accelerator beam is on only

.1% of the time, as in a typical pulsed electron linear accelerator, then all the interactions occur within that short fraction of time and outgoing particles of high cross-section reactions may overload the detector unless the beam intensity is reduced. This sort of small duty cycle is especially serious when coincidence experiments are done. Here two outgoing particles from the reaction are detected simultaneously to study their correlation or to separate them from other reaction products which have the same energy. Many more accidental coincidences from reactions occuring at slightly different times occur within the resolving time of the detectors, when all of the beam comes in short bursts, than if the same average beam intensity were spread out smoothly in time (Conzett 1966a), (Griffiths et al. 1966). The duty cycle or fractional "on time" of accelerators is often described as "macroscopic" duty cycle for time structure in the microsecond or larger region, and "microscopic" for time structure in the submicrosecond region. Accelerator beams are pulsed in the macroscopic region for several reasons. In electron linacs there are practical limitations on radiofrequency power for the accelerating voltage. In higher energy proton machines such as synchrocyclotrons or synchrotrons, the accelerating frequency or magnetic field is modulated in cycles. The microscopic pulsing occurs in linear accelerators and cyclotrons because the beam is accelerated just at the peaks of the sine-wave high frequency voltage. The frequencies used vary from 5-20 MHz for cyclotrons to several GHz for electron linacs. From the experimental point of view the macroscopic-microscopic descrip-

tion is useful because detector time resolution can normally be made shorter than a microsecond, so pulsing in the macroscopic region is more likely to be a limitation on coincidence experiments. In the microscopic region the pulse separation would be .1-.001 μ-sec. This structure would not be as serious for experiments, since it is more difficult to resolve two events on this time scale. The best accelerators for coincidence experiments are those with a steady D.C. beam, such as Cockroft-Waltons and Van de Graaffs.

For other types of experiments, the pulsed nature of some accelerator beams can be put to good use. As mentioned previously the production of neutron beams is often done by a pulsed positive ion or electron beam hitting a target. The neutron energies are then easily measured by time-of-flight to a detector. Here the requirement is for a maximum primary beam intensity within as short a time interval as possible, to obtain good neutron intensity and energy resolution. The natural macroscopic pulse feature of electron linacs and synchrocyclotrons is often used for these experiments. For cyclotrons and proton linacs the microscopic pulses can be narrowed, and some pulses suppressed to give high intensity pulsed beams at useful repetition rates. With D.C. accelerators, such as Van de Graaffs, pulsing systems have been built to provide useful pulsed beams.

3. D. C. accelerators

3.1 Single stage systems

3.1.1 Transformer-rectifier voltage multipliers.

The operating principle of the transformer-rectifier voltage multiplier is shown in Figure 9. A transformer feeds about 100 kV of A.C. voltage to the rectifier-capacitor stack shown in Figure 9A. Some of the early electron accelerators of the 1920's used the first stage with one rectifier and one capacitor to accelerate electrons as high as 350 keV, usually to produce X-rays. Later in the 1930's ion accelerators started using the single stage up to about 200 keV. The upper part of the rectifier-capacitor stack of Figure 9A multiplies the voltage up to nV, where n is the number of rectifiers. Thus n times the transformer voltage appears at the top, with only 2V appearing across any of the capacitors or rectifiers. This circuit was adopted from previous circuits by Cockroft and Walton (1932) to give a beam of 100-500 keV protons for the first nuclear reaction produced by an accelerator. Their accelerator tube was similar to that of Figure 9B, evacuated inside, and standing about 10 feet high. In the 1950's some "Cockroft-Walton" accelerators were built with solid state selenium rectifiers instead of vacuum tubes. By placing the rectifier stack and accelerator tube in a pressure vessel at 10 atmospheres to suppress sparking, and adding another transformer-rectifier stack beams up to 4 MeV protons at 1 mA intensity have been reported (Reinhold et al. 1967). More commonly the installations are operated in air at voltages up to 1 MV, although a test facility

at up to 2.5 MV is operating without accelerator tube (Reinhold et al. 1971). At the end of the 1960's silicon rectifiers began to replace selenium because of their superior high current density and high frequency capability. The silicon rectifiers are more easily damaged by sparking, however, and so need to be carefully protected. Today many Cockroft-Walton accelerators up to about 1 MeV are used for nuclear physics in laboratories throughout the world. In addition they are used as injectors for proton and heavy ion linacs at about 750 kV.

A modified version of the Cockroft-Walton voltage multiplier, using parallel voltage feed, is shown in Figure 10. Here the rectifier stack is fed through the capacitors in parallel from a semi-circular rf electrode extending the length of the column. This arrangement allows more current with faster regulation to be supplied to the upper stages by the parallel feed, compared to the series feed of the conventional Cockroft-Walton design. The pressure vessel, usually containing N_2 and CO_2, or SF_6, suppresses sparking along the rectifier stack and acceleration tube, and allows a very compact structure. Such a pressure vessel greatly reduces the size of any D.C. accelerator of over 750 kV, although access for maintenance is more difficult. Such a system has been developed by Radiation Dynamics Inc. of New York, naming it the "dynamitron". They have built machines of 4 MV, which give beam currents up to 2 mA of hydrogen ions (Cleland et al. 1969). The voltage generator can give 10 mA of current, most of which goes into beam-induced ion and electron currents in the acceleration tube, at the high voltage

and current levels. Recently a 3 MV model of similar design has been built at Berkeley as an injector for the modified heavy ion linac, the "Super Hilac" (Spence et al. 1971). Here the voltage generator is rated at 15 mA at 50% duty factor, and uses silicon diodes at 100 kHz frequency. The beam currents will be limited by the heavy ion source and acceleration tube.

3.1.2 Electrostatic charge transfer machines.

The transfer of charge from ground potential to a high voltage dome by an insulating belt is the basis for one of the most important types of accelerators for nuclear physics. This system was pioneered in the 1930's by Robert J. Van de Graaff and co-workers, so this machine is usually called a "Van de Graaff" electrostatic generator. The status of this field was extensively reviewed by Van de Graaff et al. (1948), Herb (1959) and in Livingston et al. (1962).

The principle of the Van de Graaff accelerator is shown in Figure 11. A D.C. voltage source is applied to needle points at the grounded end of the accelerator. An insulating belt of rubberized fabric or cloth then carries the charge up to the terminal, where it is collected by points in the high voltage dome. A source of ions or electrons is placed in the high voltage dome, and a beam is accelerated down the evacuated accelerating tube. This tube is built of glass or ceramic tubes sealed to metal disk spacers which divide the potential drop uniformly along the tube by means of a resistor string, or corona discharge between surrounding corona

rings. The whole assembly is usually placed in a pressure vessel at about 10 atmospheres, allowing a compact design at the higher voltages. In the 1950's the laboratories of MIT and Los Alamos were pushing the voltage limits upwards with newly designed machines. They were built vertically to carry the large weight of the long accelerating column. They had intermediate potential shells to distribute the voltage between the terminal and the pressure vessel. Their design voltage was 12 MV, but they actually reached only 9 MV at MIT and 8 MV at Los Alamos. Development work has continued in the 1960's, especially with the introduction of the tandem system to be described in the next section, at MIT and the High Voltage Engineering Corporation (H.V.E.C.) (Trump 1967), (Chmara et al. 1971) and at other laboratories such as A.W.R.E., Aldermaston, England (Howe 1969). Work has been done on understanding high voltage breakdown phenomena, study of gas and solid insulators, and the design of better accelerating tubes. The accelerating tube, when beam is passing through it, is usually the limiting factor on the maximum voltage obtainable on the terminal. A recent improvement is the inclined field accelerating tube, which uses electric or magnetic fields transverse to the beam direction to deflect low energy electrons and ions out of the tube into the metal spacer electrodes. The transverse fields are periodically reversed so the accelerated ions of the beam deviate only slightly from the axis.

Much important development work in electrostatic accelerators has been done by R. G. Herb's group at the University of

Wisconsin and later at the National Electrostatic Corporation (N.E.C.) in Wisconsin (Herb 1971). Herb has used somewhat different techniques than those of High Voltage Engineering Corporation and the MIT group. In 1955 he built a machine using metal charge carriers in the form of staples in a rubberized fabric belt. A bakable accelerating tube was made of alumina insulating rings brazed to molybdenum disks with no organic materials. Instead of inclined field tubes for discharge suppression, Herb used decoupling sections between accelerating sections. A titanium getter-ion pump was used for a clean vacuum. The metal charge carriers later evolved into a chain of metal cylinders connected by links of an insulator such as nylon, as shown in Figure 12. This construction has a long life and minimizes dust and lint. Voltage fluctuations due to charging are very low. However, power transmission to the terminal is less than for a belt, so several chains are used. Herb has given the name "Pelletron" to this accelerator, because the charge is brought to the terminal by metal pellets. The larger versions are of the two stage type, to be described in the next section.

3.2 Multistage accelerators.

A great advance in electrostatic accelerators was made with the advent of the two-stage or "tandem" system, suggested by W. H. Bennett of Ohio State University in 1937 (Rose et al. 1970). This system will double the energy of protons or deuterons from a given amount of terminal voltage. As shown in Figure 13, negative ions are accelerated from ground potential to a positive high

voltage terminal, stripped there in a thin foil or gas canal to a positive charge, and accelerated again by an extension of the accelerating tube back to ground. A charging system is contained in one half of the accelerator. A D.C. generator with 5 MV on its terminal can produce only 5 MeV protons in the conventional single-ended, single stage configuration, Figure 11. In the two stage system H^- ions are accelerated to 5 MeV at the terminal, stripped to bare protons, and accelerated another 5 MeV to the output ground end of the accelerator giving 10 MeV total energy. Doubling the energy by this charge exchange method is much easier than building a machine capable of twice the terminal voltage. An additional advantage of the tandem over the single stage design is that the ion source is outside the accelerator, allowing it to remain pressurized for months without servicing. The tandem field has been reviewed recently by Rose et al. (1967), Wegner (1969), and Rose et al. (1970). The tandem principle can be applied to any of the D.C. accelerators of the previous section.

A tandem dynamitron voltage multiplier, built by Radiation Dynamics, Inc., has recently become operational at the Argonne National Laboratory near Chicago (Cox et al. 1971). With 4 MV on the terminal it is giving 50 μA of 8 MeV protons, with an energy spread of about 1 keV. The machine is horizontal with each half mechanically supported from its own end of the pressure vessel. Vacuum tube rectifiers are used in the voltage generator. The accelerator tube is made of sections of pyrex glass and stainless steel cemented together. SF_6 at 100 p.s.i. is used as an insulating gas. The

H^- or $^2H^-$ source can be pulsed to give output pulsed proton or deuteron beams of 1 mA intensity during the pulse of 1.3-2 nanoseconds width. This beam is used to produce pulsed neutron beams from a target, for use in neutron time-of-flight experiments. The voltage generator has operated with up to 5.7 MV on the terminal without acceleration tube, but the maximum voltage with beam is 4.0 MV at present, due to loading effects in the acceleration tube. Another 8 MeV tandem is being built for the Ruhr University in Germany with a specification of 100 μA D.C. current, and 2 mA pulsed intensity at 1 nanosecond width (P. R. Hanley 1971, private communication).

The main development and construction of tandem accelerators has been by H.V.E.C. using the Van de Graaff belt charging system (Wegner 1969). As shown in Figure 1 the tandem came into widespread use in the 1960's, with practically all units being built by H.V.E.C. With their continued development program of improving accelerating tubes, they have pushed the voltages of the FN model up to 10 MV on the terminal, and in November 1971 the MP "Emperor" model reached 14 MV on the terminal, giving 2 μA of 28 MeV protons. An illustration of an MP installation is shown in Figure 14. The injector is on the left, and a beam analyzing magnet on the right at the high energy end. The next larger model under development is the TU (Trans-Uranium), which is 81 feet long and 25 feet maximum diameter (Shaw et al. 1970). It is insulated with SF_6 gas, and rated at 16 MV with a design aim of 20 MV. It has operated at 21 MV without acceleration tube. This program has temporarily been

suspended due to lack of funding. A high current series of compact tandems, the T8 and T10 are also available. They have horizontal accelerating tubes with the voltage generator bringing charge up from below. The total length of accelerating tube is only 16 feet for 10 MV in the T10. It has produced 100 μA of protons at 8 MeV and 25 μA at 11 MeV.

A laboratory layout of the MP tandem at Yale University is shown in Figure 15. The beam balance on the "image slit" after the first bending magnet is normally used in a feedback system to regulate the terminal voltage, keeping the beam energy constant. The switching magnet directs beam to various experimental areas. It is convenient to have several independently shielded areas or "caves" so that an experiment can run in one cave, while a following experiment is set up in another cave. Various scattering or reaction chambers containing detectors are placed at the ends of the beam lines. A "multigap" spectrograph is used on one line to magnetically analyze the reaction products from a target chamber. The control room and a computer for analyzing experimental data are shown at the top of Figure 15.

The tandem accelerator is also built as a Pelletron by N.E.C. (Herb 1971). Using the techniques mentioned in the previous section, modules of 1.5 foot length and 1 MV rating are stacked up to give the desired voltage. A tandem Pelletron rated at 14 MV (28 MeV protons) is being built for the Australian National University.

The next step in pushing D.C. accelerators to higher energies is the use of 3 stages of acceleration. The principle is shown in Figure 16. A negative ion source is placed inside the negative terminal of the first stage. The negative ions are accelerated to ground potential, and then up to the positive terminal of the second stage. There they are stripped to positive ions and accelerated a third time in going back to ground potential. This system requires an additional injection stage to the 2 stage tandem. The proton or deuteron energy is the sum of the injection voltage plus twice the second stage voltage. Figure 17 shows an illustration of a laboratory using a three stage system. In this case the total energy is $5.5 + 2 \times 6 = 17.5$ MeV. Three stage systems are also in use at other laboratories such as Los Alamos and Oxford, England. At Brookhaven, New York the largest three stage system uses two MP tandems with a negative ion source in one of them. With the terminals at about 10 MV each, 4 μA of 30 MeV protons have been accelerated (Wegner 1971). This is the highest energy reached by a D.C. accelerator. The University of Washington uses a somewhat different 3-stage system with 2 model FN tandems. There a neutral atomic beam is formed by charge exchange of a positive ion beam from a source at ground potential. The neutral beam drifts to the negative terminal, where it picks up an electron in another exchange canal. It then accelerates through 3 stages as in the other systems, giving 24 MeV protons. Compared to the terminal source method, this system has the advantage of an ion source at ground potential, but the disadvantage of the lower in-

tensity from 2 charge exchanges, and more terminal pumping in the first terminal for the charge exchange canal. A three stage Pelletron machine is being installed at the University of Sao Paulo, Brazil. It produced $4 + 9 \times 2 = 22$ MeV protons in tests at N.E.C. (Herb 1971).

3.3 Ion sources and special techniques.

In order to produce the beam characteristics required for various experiments, many laboratories have developed special ion sources and devices to improve beam intensity, energy spread, and fast pulsing. Several of these will be described in this section.

Much development has taken place in ion sources (Livingston et al. 1962). The rf source was used for many years for proton and deuteron beams. Then the duoplasmatron came along with greater intensity. More recently sources for negatively charged light and heavy ions for tandems have been developed at H.V.E.C., Los Alamos, Oak Ridge and elsewhere (Rose et al. 1967). One of the most successful of the sources for negative heavy ions is that of Heidelberg (Heinicke et al. 1969). It uses a Penning discharge in a magnetic field, with a furnace for solid materials, and produces many negative ion species throughout the periodic table, such as Li, C, O, Cl, Br, U, etc.

Sources of polarized ions have been built at many laboratories in the past 10 years to replace the older scattering method of making polarized beams. They are usually too large to put inside the terminal of a single-ended machine, so negative polarized hydrogen and deuteron sources of the "Lamb-shift" type

have been developed for use with tandem accelerators. In this type of source a positive ion beam is neutralized in a cesium vapor canal. Some of the atoms are formed in the metastable 2S state. Some of these are quenched to the ground state in the following electric and magnetic field region, leaving polarized metastable atoms. Then an electron is added selectively to only the metastable atoms giving polarized negative ions. These sources have been reviewed by Haeberli (1967) and Clegg (1971). External polarized beam currents of 50-200 nanoamps have been obtained from tandem accelerators, with the highest of those intensities reported by McKibben (1971) of Los Alamos.

One of the great advantages of the D.C. accelerator is its beams of small energy spread, 1-5 keV. The energy spread is caused mainly by terminal voltage fluctuations, with a small contribution from the ion source. The terminal is normally stabilized by a feedback system from analyzing magnet image slits. For precision experiments on closely spaced levels or sharp resonances, better regulation is necessary. A system giving excellent performance is used by Duke University in North Carolina on a 4 MeV Van de Graaff (Parks et al. 1958) shown in Figure 18. They call it the "Homogenizer". In this system the main target for the experiment uses a proton beam, while an H_2^+ beam is used to regulate the terminal voltage with slits "0". This beam then passes through a 1 meter radius cylindrical analyzer to analyzer image slits "I". The differential signal from these is amplified to supply a voltage to the outer analyzer plate, bringing the beam back to the center of

the analyzer image slits. At the same time a multiple of this voltage is put on the proton target to bias it above ground potential and provide a small deceleration to the beam. The result is that energy fluctuations of the beam are compensated by voltage variations of the target. This method reduces the beam energy spread of a 2 MeV proton beam seen by the target from the normal 2 keV to only 250 eV. As a result much better high resolution data can be taken, as shown in the next section.

Another technique which is widely used in accelerators is beam pulsing. Short ion pulses of about 1 nanosecond width are useful for measuring the energy of secondary neutrons by time-of-flight and for measuring short half-lives of radioactive reaction products. One of the best pulsing systems is that in the terminal of the Oak Ridge 3 MV Van de Graaff (Moak et al. 1964) shown in Figure 19. Here a duoplasmatron ion source beam at 30 keV is chopped by moving it with pairs of electrostatic deflecting plates in two planes past an aperture. By using a frequency of 1 MHz on one pair of plates and 3 MHz on the other a Lissajous pattern is produced at the aperture. The higher frequency gives a fast axis crossing and the lower one a slower repetition rate, compared to operation with a single pair of plates. A buncher using the Klystron principle operates at 27 MHz to compress the chopped pulses in time, by decelerating the early particles and accelerating the late ones. The beam is then accelerated to 70 keV for injection into the acceleration column. The resulting beam pulses of the full energy beam are shown in Figure 20, at increasing buncher

voltage from bottom to top. With no buncher voltage (bottom) the width is 12 nanoseconds and the peak current is 1 mA. With 75% buncher drive (top) the pulse width is about 1 nanosecond, and the peak current 10 mA. For experiments requiring a lower repetition rate than is available with the terminal pulser, a lower frequency voltage is applied to a third set of deflection plates after acceleration to ground potential, to discard 1/2, 3/4, etc. of the pulses from the terminal pulser. Another method of pulse compression which has been used, is a Mobley-magnet (Mobley 1952), which sweeps the accelerated beam through various flight paths in a special magnet. But most of the pulsing systems on D.C. accelerators use methods similar to that of Moak.

At Wisconsin a polarized deuteron beam has been used with a pulsing system for a tandem, giving 3 nanoamps average beam with 2 nanoseconds pulse width (Davis et al. 1971).

3.4 High resolution experiments.

The D.C. accelerator has been known for many years for its beams of good quality, easy energy variability and small energy spread. These characteristics are very important for certain types of precision experiments. In this section some examples will be given of several high energy resolution experiments which were made possible by using special techniques with D.C. accelerators.

The first example is that of α-α scattering at 184 keV by Benn et al. (1966) using an electrostatic generator at Zurich University, Switzerland. The purpose was to measure the ground

state energy of ^{8}Be, which is formed for a short time during the interaction of the α-particles. This was done by measuring the counting rate of $^{4}He^{+}$ particles scattered at 45 degrees from an atomic He beam, as the incident energy was varied. The resonant state was seen as a small deviation in counting rate of about 4% over an interval of some 250 electron volts. To see this very small effect the beam energy spread was reduced to 75 eV by using an analyzing magnet. The beam energy was swept through a 600 eV range in 24 eV steps every 10 minutes, and the results added, to correct for long term drifts. An atomic helium beam was used as the target to reduce the Doppler energy spread (due to the random thermal velocities in a gas) to 30 eV, compared to the 230 eV of room temperature gas. The total experimental energy resolution was about 90 eV. This extremely precise experiment required good accelerator stabilization, special beam analysis, and a special target.

Another example of the importance of good energy resolution at higher energy is the elastic scattering of protons on argon by Bilpuch (1966) at Duke University, using the 2.5 MeV beam from a single stage Van de Graaff machine. For reference, Figure 21 shows the previous data in this energy region from Iowa State University, where the energy resolution was 5-10 keV (von Brentano 1967), (Barnard et al. 1961). A single resonance appears at 2.45 MeV, due to an excited state of ^{41}K. The Duke experiment was done using the energy "Homogenizer" described in Section 3.3, which gave

a beam energy resolution of about 250 eV. Figure 22 shows the complex fine structure which appears with this greatly improved resolution. What appeared to be one resonance in the Iowa data, is now shown to be 7 resonances, indicating a more complicated nuclear level structure than was shown in the older experiment. As in the Zurich experiment, special target design had to be used to keep the energy spread from target effects less than those of the accelerator beam. In this case a refrigerated windowless gas target was used to reduce the Doppler broadening. A rather high beam current of 30 μA at high resolution was available from the Van de Graaff. This was necessary to obtain good counting rates from the very thin target.

The multi-stage Van de Graaff is also capable of excellent resolution, and can of course explore the higher energy regions of 5-30 MeV, which are inaccessible to the single stage machine. One of the best examples of the fine performance of a tandem Van de Graaff is shown in Figure 23. This work was done by Van Bree and Temmer in 1968 at Rutgers University, New Jersey (G. M. Temmer 1971, private communication). The experiment was the elastic scattering of protons on carbon to study the resonance level of ^{13}N at 14.23 MeV incident energy. The large peak/valley ratio is evidence of the excellent beam energy resolution of about 1 keV. This resolution was made possible by rejecting counts when the terminal voltage of the tandem varied more than a preset amount from the central value. The use of a thin target is also important for this experiment.

These examples of high resolution experiments illustrate why the D.C. accelerator has a reputation for precise beams. These are examples of the best experiments, using special techniques to decrease beam energy spreads well below 1 keV, while average beam energy spreads at most laboratories are 1-5 keV, or $\Delta E/E$ = .01-.2%.

A special example of the space collimation that is possible with good quality negative ions is the production of "super-collimated" beams (Armstrong et al. 1969). A 4 MeV beam of negative ions from a single stage Van de Graaff at Los Alamos was directed through two collimators 1 m apart and 25 μ diameter. Any negative ions which scatter from the collimators or residual gas are stripped to positive ions and swept away in a small magnet downstream. The resultant beam was 25 μ in diameter with a divergence of only .001 degree. A measurement .5 m beyond the second aperture confirmed the 25 μ size. This method eliminates the slit scattering contribution to beam size and angular spread which would occur with positive ions.

3.5 Future developments.

There are several groups which are proposing or developing larger D.C. accelerators than have been built before. The principal groups in the U.S.A. are the companies which build large multistage electrostatic machines, High Voltage Engineering Corp. (H.V.E.C.) in Massachusetts and the National Electrostatic Corp. (N.E.C.) in Wisconsin. There is also interest in Britain in a large nuclear structure facility.

The HILAB proposal by H.V.E.C. is shown in Figure 24. This is

primarily a heavy ion facility designed to accelerate all ions up to about A = 200 to above the Coulomb barrier on uranium (Livingston 1970), (Grodzins 1970). It is a 3-stage Van de Graaff system. The negative ion sources are at ground potential in this case. The ions are accelerated to the positive high voltage terminal of the TU, stripped there to positive ions and accelerated down to ground through another stripper half way down the column. At ground potential a third stripper is used and the beam is analyzed to transmit the most abundant charge state. This beam is then accelerated through the third stage into the negative high voltage terminal of the MP tandem. There the experiments would be done with the heaviest projectiles at intensities of around 10^{11} particles/sec. For lower mass projectiles only one or two strippers would be needed. For the lower masses, A < 50, the TU alone can give sufficient energy as a tandem, so target area A can be used. This project has the disadvantage of a small experimental area inside the MP terminal, where remote control would be necessary. There are also plans at Brookhaven to do some preliminary survey experiments on high energy heavy ions using a similar system with the existing 2 MP tandems, giving somewhat lower energy than the TU + MP proposal of H.V.E.C. (Wegner 1969). H.V.E.C. has also proposed a 30 MV vertical tandem, 128 feet high, which would give 60 MeV protons (Rose et al. 1970).

The next Pelletron accelerator proposed by N.E.C. is a tandem with 20 MV guaranteed on the terminal, giving 40 MeV protons (Herb 1971). This is shown in Figure 25. The machine would be vertical

for easier mechanical support. It would be built of 20 modules, at 1 MV each, stacked up for each stage. A bending magnet below would send the beam to the experimental areas.

A study is under way at the Daresbury Nuclear Physics Laboratory in Britain for a large vertical tandem accelerator to serve as a national nuclear structure laboratory (H. R. M. Hyder 1972, private communication). It would be designed for 30 MV on the terminal, with initial operation at 20-25 MV. Its pressure vessel would be 135 feet high and 27 feet in diameter. The accelerating tubes would be divided into sections to make space for intermediate strippers, lenses, and vacuum pumps. The beam would be bent into the horizontal plane by an analyzing magnet at the bottom, and then directed into one of the beam lines radiating into three sector shaped target rooms. Space would be left for later addition of a third stage cyclotron or linac.

An interesting new idea for accelerating heavy ions to high energies with one tandem is that of the "charge-change-accelerator" of Hortig (1970). This accelerator is based on the fact that the equilibrium charge state of a heavy ion is higher after passing through a solid stripper, than after a gas stripper. An ion beam circulates back and forth through a tandem, being returned by a bending magnet at each end. A gas stripper is placed in the negative terminal and a solid stripper at each ground end. Since the charge state is greater in passing from ground to high voltage, than in the passage from high voltage to ground, the acceleration to the terminal is greater than the deceleration to

ground. Thus a net acceleration occurs for each half cycle. Hortig has done studies to follow the complicated process of the acceleration, transport, and multiple scattering of the beam, which contains many charge states of various energies. Miessner (1970) has proposed a modified version with two accelerating tubes to reduce the number of passages through the solid stripper, and a possible additional gas stripper part way down the column to reduce the deceleration. This system would make a cheap heavy ion accelerator, but needs more analysis to show its feasibility.

4. Circular accelerators

4.1 Cyclotrons

4.1.1 Classical and F. M. cyclotrons

The trend in cyclotron construction over the last 30 years is shown in Figure 1. The number of cyclotrons accelerating protons and deuterons to over 10 MeV grew in the 1940's and 1950's. The maximum energy of the larger machines was 20 MeV protons, 25 MeV deuterons, and 50 MeV α-particles. The principle of phase stability gave birth to the frequency modulated (F. M.) or synchrocyclotron just after World War II. Figure 1 shows the growth of the number of F. M. cyclotrons in the 1950's. They gave an immediate increase of proton and deuteron energy to hundreds of MeV, and produced the first mesons from accelerator beams. Tabulations of most of these cyclotrons and their characteristics can be found in several references: (Howard 1958), (Gordon et al. 1963), (Hamman et al. 1964). The classical cyclotron gave high beam intensity, up to hundreds of microamps external beam, but limited energy. The F. M. cyclotron gave much higher energies, but the intensities were low due to the low duty cycle of acceleration. Internal beams of F. M. cyclotrons were typically about 1 μA, and external beams only about .05 μA. Both classical and F. M. cyclotrons were usually of fixed energy. The sector cyclotron made possible both high intensity and high energy, which explains the rapid growth of these new cyclotrons in the 1960's, and the slow decline in the number of classical and F. M. cyclotrons. Many

of the classical cyclotrons have been converted to sector cyclotrons, adding the valuable variable energy feature at the same time. The conversion of F. M. cyclotrons to sector machines is a much larger project because of the large magnet size, but is being done or planned in a few cases. In this section a brief review of the principles of classical and F. M. cyclotrons will be given. In the following section the sector cyclotron will be described in more detail, because of its greater importance in present and future nuclear physics research.

The classical cyclotron is illustrated in Figure 26. An electromagnet provides a nearly uniform magnetic field between its poles. In the gap two hollow electrodes called "dees" are placed. These are fed with a high radiofrequency voltage, about 30-100 kV at 10-20 MHz frequency. At the center of the magnet gap is placed a source of ions, in which a stream of electrons from a hot filament ionizes gas from a feed tube, forming an arc. Modern sources are enclosed in a metal "hood" with a small opening toward the dee for beam extraction. The ions are accelerated at each crossing of the gap between the dees. During the half revolution between the gaps they are shielded from the dee-dee electric field. When they emerge into the next gap the sinewave dee voltage has reversed and they are accelerated again. As they gain energy they spiral outward in the confining magnetic field. The principle which makes the cyclotron work is that the ions take the same time for one revolution in the magnetic field, independent of

their energy. Thus their revolution frequency is constant: $\omega_p = Bq/m$, where ω_p is particle revolution frequency, B is magnetic field strength, and q/m is charge to mass ratio. Since B and q/m are nearly constant as the energy increases, ω_p is constant. The frequency of the dee voltage, ω_d, is set equal to ω_p, so that the beam particles are accelerated across the dee-dee gap near the peak of the sinewave dee voltage for many revolutions. Thus high energies can be reached in a compact machine by many passages through low voltage accelerating electrodes. When the beam approaches the full radius of the pole it is deflected out of the magnetic field by passing through a narrow channel with a high electric field across it. The beam then goes into an external beam pipe to the experimental areas. The whole dee system is placed in a vacuum box with large diffusion type vacuum pumps on it. The vertical stability of the particle orbits is produced by a decrease of the magnetic field with radius. This causes the field lines to bow outwards as shown in Figure 26. Since the magnetic force on the particles is perpendicular to the field lines, the particles above the median plane feel a downward component of force, as well as the principal inward component. Likewise the particles below the midplane feel an upward force component. Thus there is a restoring, or "focusing", force toward the median plane, trapping many particles in vertical oscillations within the dee aperture. This focusing, which fortunately existed accidentally in the first cyclotrons, gives thousands of times more beam intensity than if it were absent.

The limitation on maximum energy of the classical cyclotron

comes because the particle frequency $\omega_p = Bq/m$ gradually decreases with radius. This is due to the relativistic increase of particle mass with energy, and also by the requirement that the magnetic field must decrease with radius to give vertical focusing. So the particle slowly slips away from the peak of the accelerating sine-wave voltage as it accelerates. This usually is called "phase slip", where the phase refers to the angular position in time along the sinewave accelerating voltage wave at which the particle crosses the accelerating gap. Higher accelerating voltage gives a higher energy, but the practical problems of holding high voltages have limited classical cyclotrons to about 20 MeV protons and 50 MeV α-particles. The detailed theory and description of this classical, or fixed frequency, cyclotron can be found in many books and articles: (Cohen 1953), (Cohen 1959a), (McMillan 1959a), (Livingood 1961), and (Livingston et al. 1962).

The acceleration of heavy ion beams has been developed in several of the classical cyclotrons, as described in a review by Livingston (1970). Alvarez (1940) and Tobias accelerated C^{6+} to 50 MeV in the 37 inch cyclotron at Berkeley. This beam apparently was made by accelerating C^{2+} from the ion source part way out in radius on the third harmonic mode, $\omega_d = 3\omega_p$, stripping to C^{6+} in the residual vacuum chamber gas, and accelerating again on the first harmonic mode normally used for deuterons and α-particles, $\omega_d = \omega_p$. The beam intensity was too low for experiments however. This method of stripping from low to high charge state was developed in the 1950's in cyclotrons at Berkeley, Birmingham,

Stockholm and Saclay to provide carbon beams for physics experiments at up to 10^{11}/sec intensity and over 100 MeV energy. Cyclotrons were built in Oak Ridge and Leningrad in the 1950's to accelerate about a microamp of N^{3+} directly from the ion source to the 20 MeV energy region, 1-2 MeV/nucleon. In the late 1950's and 1960's several cyclotrons were built to accelerate the highest charge states available from the ion source, to obtain energies of around 6 MeV/nucleon which are necessary to penetrate the Coulomb barrier on heavier targets. These were at the Kurchatov Institute and Dubna in the U.S.S.R. and at Tokyo. The largest is the Dubna 310 cm model which accelerates ions up to mass 64 to 6 MeV/nucleon. It has been extensively used for the heavy element research of Flerov's group. PIG type ion sources are used in these cyclotrons to obtain high intensities of multi-charged ions (Bennett 1972a). The Dubna group under Flerov and the Berkeley hilac group of Ghiorso have been in competition for the past few years in the search for new heavy elements (Henahan 1971), (Flerov 1972). Both groups claim the discovery of elements 104 and 105, which are called kurchatovium and nielsbohrium at Dubna, and rutherfordium and hahnium at Berkeley. Research at a third laboratory is needed to resolve the controversy.

The relativistic limit of the classical cyclotron was overcome by the F. M. cyclotron. Here the frequency of the dee voltage, ω_d, is slowly reduced as the beam accelerates, to match the decrease of the particle revolution frequency, ω_p. The magnetic

field decreases with radius to give vertical focusing. The discovery of phase stability by Veksler (1945) and McMillan (1945) showed that there was a focusing action of particle phase. This means that there are oscillations of particle phase about a stable phase point. This mechanism traps the particles within a phase range of about half a cycle in a "bucket", and accelerates them without loss. Without this mechanism most of the beam would drift in phase into the decelerating half of the sinewave before reaching full energy, and be lost. F. M. cyclotrons are built with a single dee, running at about 10 kV voltage, and modulated in frequency by a large rotary capacitor or a tuning fork. The energies range from 30 MeV deuterons up to the 730 MeV proton machine at Berkeley whose magnet has a 189 inch pole diameter and weighs 4300 tons. At these high energies the magnet becomes very large and expensive. Above 1 GeV it becomes more economical to build synchrotrons, which use a beam aperture only about 1 × .5 m for weak focusing, or .1 m diameter for strong focusing machines. This reduces the magnet weight by an order of magnitude compared to F.M. cyclotrons. F.M. cyclotrons are modulated in frequency at rates of 60 cycles/sec for the larger ones to 1000 cycles/sec for the smaller machines. The beam reaches maximum energy during a short period near the low frequency end of the modulation cycle. The macroscopic duty cycle is therefore about 5%, but can be stretched to over 50% by using a small auxilliary rf electrode at large radius, which picks up the beam bucket from the main dee and spills it out slowly. With the construction of several new high current cyclotrons and a linac nearing completion in the 500-800 MeV region many of the

F. M. cyclotrons have been shut down. Improvement plans are being made at many of the remaining machines (Blosser 1969). Detailed descriptions of the principles and construction of F. M. cyclotrons can be found in (McMillan 1959a), (Livingood 1961) and (Livingston et al. 1962).

The classical and F. M. cyclotrons have been used in some laboratories to provide pulsed beams for half-life measurements or neutron time-of-flight experiments. The 90 inch cyclotron at Livermore, California, for example, used the short pulse width provided by phase slip in a classical cyclotron to give pulses a few nanoseconds wide. Wider pulse separation than the natural 5 MHz rf rate was obtained by deflecting some pulses out of the beam pipe after acceleration. F. M. cyclotrons at Columbia, New York and Harwell, U. K. have been pulsed by deflecting the whole beam from one modulation cycle vertically against a target on one of the poles. This has produced pulse widths of 2-10 nanoseconds at Harwell (Synchrocyclotron Group 1971) and 15 nanoseconds at Columbia (Rainwater 1971). Longer pulses can be obtained by pulsing the source, the dee voltage or the deflector.

Polarized beams have been produced by classical and F. M. cyclotrons. In the classical cyclotron external proton beams have been scattered on targets to give scattered polarized protons (Haeberli 1967). Elastic scattering of helium on a hydrogen target gives protons polarized nearly 100%. Polarized ion sources outside classical cyclotrons have been used to inject neutral atomic polarized beam into the center region for acceleration (Clark 1971).

Saclay injected a thermal energy atomic deuteron beam into the center region where it was ionized for acceleration. A Czechoslovakian group at Rez has injected a 40keV neutral atomic beam into the center region of a Soviet built U120 cyclotron, where it is stripped by a foil for acceleration (Bejsovec et al. 1970). The external beam intensities of the polarized beams produced by scattering and neutral beam injection are generally about 10^8 - 10^9/sec. Several F. M. cyclotrons have also used the scattering method to give polarized protons at hundreds of MeV, with intensities of about 10^7/sec. The machine at Lyon, France has accelerated polarized deuterons with an intensity of 5×10^7/sec. (Kouloumdjian 1970).

4.1.2 Operating sector cyclotrons

4.1.2.1 Principles

The high intensity of the classical cyclotron and the high energy of the F. M. cyclotron can be attained in a single machine by the use of the principle of sector focusing. The principle was first suggested by L. H. Thomas (1938) and is illustrated in Figure 27. On the cyclotron poles are placed sector-shaped pieces of iron to produce alternating strong and weak magnetic field sectors, or "hills" and "valleys". The amount of field change between hill and valley is often called "flutter". The particle orbit is no longer nearly circular, but is now scalloped, with a smaller radius, R_h, in the hill region, and a larger radius, R_v, in the valley. This is shown in Figure 27a, omitting the energy gain.

At the crossing of a valley-hill or hill-valley boundary there is a component of the velocity, v_r, in the radial direction. The magnetic force holding the particle in orbit is perpendicular to the velocity and to the magnetic field. The force due to the component v_r is shown in Figure 27b as F_v, perpendicular to the fringing field lines at the sector boundaries. This force has a component toward the median plane for particles either above or below the plane. Thus it is a restoring or "focusing" force, keeping the beam confined in the vertical direction. The force is focusing at both entrance and exit to the hill, since both v_r and the fringing direction reverse. The vertical focusing causes the particles to oscillate about the median plane at a rate of one cycle every 5-10 revolutions. This is usually expressed as a ratio of vertical to revolution frequency v_z = .1-.2. This type of focusing due to straight edged sectors is often called Thomas focusing. The great value in using sector focusing comes from the fact that the average magnetic field can now increase with radius, and its resultant vertical defocusing can be more than compensated by sector focusing. Thus the particle frequency ω_p = Bq/m can be kept constant by increasing B proportional to m, and there will be no phase slip with respect to a constant accelerating frequency, ω_d. This type of magnetic field is called "synchronous" or "isochronous". The energy will no longer be limited by phase slip to 10-20 MeV protons, but can be extended up to several hundred MeV. The unmodulated dee frequency gives 100% macroscopic duty cycle and beam currents of hundreds of microamps are obtainable,

if desired.

A later refinement of the sector design is the use of spiral sector edges. This was suggested by D. Kerst in 1955 (Symon et al. 1956) for use in the higher energy fixed field alternating gradient (FFAG) accelerators. A spiral sector pole is shown in Figure 28. The orbits have the same scalloped shape as in the straight sector design, but the pattern now rotates slowly during acceleration. The effect of the spiral is to increase the angle at which the orbit crosses the hill-valley boundary. This increases the component of velocity, v_{ll}, along the sector edge, which is responsible for vertical focusing. As indicted in Figure 28, the focusing is increased at the "blunt edge" and decreased at the "sharp edge" of the sector. The net effect is an increase in vertical focusing, because the focusing increases faster than the defocusing, with increasing spiral, and because the alternating strong and weak focusing adds an extra "alternating gradient" effect, as in quadrupole doublet lenses. The expression for the vertical restoring force due to sectors is approximately: $F^2(1 + 2 \tan^2\gamma)$, where F^2 measures the field modulation between hill and valley, or flutter, and γ is the amount of spiral, defined as the angle between the sector boundary and a radial line from the machine center. In a Thomas straight sector design, $\gamma = 0$. Most sector cyclotrons in the 50-100 MeV region use moderate spiral angles increasing to 30-50 degrees near maximum radius. This reduces the amount of flutter required, and so narrows the valley gap. The amount of power in the main magnet can then be

reduced and the isochronous field region can extend farther out in radius. The design of the Canadian cyclotron project TRIUMF uses a maximum spiral angle of 70 degrees, giving a factor of 15 increase in focusing force compared to a straight sector design with the same flutter. More detailed descriptions of the theory of sector focusing are found in Livingood (1961), Livingston et al. (1962) and Richardson (1965).

Shortly after Thomas (1938) proposed the sector cyclotron, Schiff (1938) showed that three or more strong field sectors would give radial beam stability. No use was made of the sector principle for the next decade, although it would have been valuable in extending the energy of classical cyclotrons. In 1950-1952 several 3-sector Thomas type electron model cyclotrons were built at Berkeley (Kelly et al. 1956). They accelerated electrons to $\beta = v/c = .5$, where v is the speed of the particle and c is the speed of light. This β is the same as for protons at 150 MeV. This demonstrated that the Thomas principle was practical up to at least that energy. In the 1950's interest in sector focusing grew rapidly and many cyclotrons were planned. In 1958 a 4-sector Thomas cyclotron at Delft accelerated protons to 12 MeV (Heyn et al. 1958). Also in 1958 Oak Ridge National Laboratory completed an electron model Thomas cyclotron with $\beta = .7$, corresponding to 350 MeV protons (Blosser et al. 1958). Spiral sectors came into use soon afterward, following the suggestion of Kerst. The design and planning work of laboratories throughout

the world resulted in the rapid growth in the number of operating sector cyclotrons in the 1960's, Figure 1. The status of cyclotron development has been reviewed by Khoe et al. (1967).

4.1.2.2 Example: the Berkeley 88-Inch Cyclotron

An example of a sector cyclotron in the 50-100 MeV region is the 88-Inch Cyclotron at Lawrence Berkeley Laboratory (L.R.L. 1967), shown in cross-section in Figure 29. The ion source comes in on a shaft throught the lower pole. This design feature, used in many of the newer cyclotrons, gives accurate source positioning by means of rotating plugs in the pole. Other cyclotrons use one or two shafts coming through the side of the vacuum chamber. A single dee is used here to give a simple radio frequency system, and space for deflector and probes on the other side of the vacuum tank. Some cyclotrons use two dees for greater energy gain. The cyclotron energy is varied by changing the magnetic field and the rf frequency. In the 88-Inch Cyclotron there are 17 sets of trimming coils mounted on the pole faces to shape the magnetic field to the exact isochronous radial profile required by the particle and energy being used. The isochronous field increases proportional to mass as the particle accelerates. For example, the field increases about 5% from the center to the edge when 50 MeV protons are accelerated, since the rest mass of the proton is 940 MeV. The frequency is changed in this cyclotron by moving panels in the resonator box to change the inductance of the dee stem region. On most other cyclotrons a coaxial dee stem design is used, and a movable shorting plane varies the frequency. The dee

and its stem are 1/4 of an electrical wavelength long, with maximum voltage at the accelerating gap and zero voltage at the shorted end at the back wall of the resonator box. A polarized ion source is located above the roof shielding and injects polarized protons and deuterons into the cyclotron by an axial injection system. Four diffusion pumps are located on the resonator box and the acceleration chamber.

A chart of the resonance lines of various particles which the cyclotron can accelerate is shown in Figure 30. From the resonance equation $\omega_p = Bq/m$, the magnetic field, B, is proportional to frequency, ω_p, for fixed charge/mass ratio q/m. Each line is one q/m ratio. The maximum energy of each ion species (q,m) with mass number $A > 4$ is limited by the maximum magnetic field of 17 kilogauss. Protons are limited by the maximum frequency of 16.5 MHz, ^{3}He is limited by vertical focusing, and α-particles are limited by deflector strength. For this cyclotron the constant which measures the heavy ion maximum energy, k, is 140 for particle mass $A > 4$. k is defined by the equation $E(MeV) = k\,Q^2/A$, where E is the maximum energy (at maximum magnetic field) for an ion with charge to mass ratio Q/A in proton units. Thus the maximum energy of $^{14}N^{5+}$ is $E = 140 \times 5^2/14 = 250$ MeV.

For any required heavy ion energy or energy/nucleon (top of Figure 30) there is a choice of several charge states giving that energy at different magnetic fields. The lowest charge state is nearly always used, since it is produced in greater quantity by the ion source.

The upper part of the energy range for lighter particles is on the "first harmonic" mode of operation (Figure 30). This is the usual mode in which the particle makes one revolution in one radiofrequency period: $\omega_d = \omega_p$. But it is also possible to accelerate ions on the "third harmonic" mode in which the particle takes three rf cycles to make a revolution: $\omega_d = 3\,\omega_p$. In both cases the necessary condition that the voltage reverses between gap crossings is satisfied. In the first harmonic mode it reverses once, while in the third harmonic mode it reverses three times. The existence of the third harmonic mode means that the rf frequency needs a 3 to 1 range only, to cover a 9 to 1 range in particle revolution frequency, rather than the 9 to 1 range needed if only first harmonic were used. This third harmonic region has proven very useful for heavy ion acceleration. At even lower particle frequencies the fifth harmonic mode is usable, but gives very low particle energies which are seldom used.

Other cyclotrons with two dees of widths such as 90 degrees or 140 degrees have been built, to get high energy gain per turn. These have the possibility of using the second harmonic mode, with the dees operating "push-push" (same polarity), as well as the first and third harmonic modes with the dees "push-pull" (opposite polarity). So the tuning range of the rf needs to be only 2 to 1 instead of 3 to 1 to cover the whole particle and energy range. But rf systems are more complicated for these machines.

The experimental area of the 88-Inch Cyclotron is illustrated in Figure 31. The cyclotron is enclosed in a concrete

vault with 10 foot thick walls and a 7 foot thick roof, for radiation shielding. A switching magnet sends the external beam to various caves. A high resolution beam line is formed by the analyzing magnets in Cave 3 and Cave 4. A magnetic spectrometer for analyzing reaction products is located in Cave 4C. The High Level Cave, top of Figure 31, is used for high beam intensity isotope production.

4.1.2.3 Ion sources and beam pulsing.

The ion sources used in sector cyclotrons are usually of the hooded arc type with a hot filament supplying electrons from one end through a hole about 1/8 inch diameter. The arc is confined along the magnetic field, and electrons oscillate between the filament and a reflecting anticathode at the opposite end. The arc is 3-4 inches long, and the beam is extracted half way along it by a "puller" attached to the dee, (Livingood 1961), (Livingston et al. 1962). These sources run at arc powers up to 500 watts and supply up to several milliamps of accelerated protons or deuterons, and hundreds of microamps of $^{3}He^{2+}$ and α-particles. For multiply charged heavy ions the "PIG" or Penning Ion Gauge design is best. Here the arc chamber is enlarged to 5/16 or 3/8 inch diameter and the filament is replaced by a block of tantalum or tungsten. The arc is struck between the two cold cathodes at each end by raising the voltage to about 3 kV. The cathodes then heat and emit thermionic electrons, increasing the arc current to 3-5 amps at 500-1000 volts. This provides the much greater arc powers of 2-5 kilowatts needed to produce and accelerate μA

quantities of N^{4+}, N^{5+}, etc. These ion sources were reviewed by Bennett (1972a).

Several laboratories have tested or are using unpolarized external ion sources (Clark 1971). Their advantage for negative and heavy ions is to have less charge exchange during acceleration with the source external, where the gas can be pumped away easily. More powerful heavy ion sources can be built outside the cyclotron, in the greater space available. The Cyclotron Corporation of Berkeley has built H^- cyclotrons which are injected axially from an external H^- source. They accelerate and extract up to 40 μA of H^- beam at 15 MeV (Fleischer et al. 1971). This is useful for injection into a tandem Van de Graaff to increase its energy. Work has been done at a number of other laboratories on installing external sources of the conventional type, but so far the heavy ion intensities available from a good internal PIG source are superior to those from external sources, because of transport losses at low injection energy from external source to cyclotron. Several groups are interested in external sources for ions from solid materials, to prevent coating of the cyclotron dee and deflector. The larger machines being built in the hundreds of MeV region will use external injection, as described in a later section.

There are a number of development projects on new types of high charge state heavy ion sources in various laboratories. If a source could give beams of U^{51+}, for example, they could be accelerated on the same resonance line as N^{3+} in the 88-Inch

Cyclotron (Figure 30), and in other similar cyclotrons, and reach 6 MeV/nucleon. This would be much cheaper than large linacs (Section 5.1.2) or multi-stage accelerators (Section 6). Such a source would be too large for the cyclotron center region, so it would be external with its beam being injected axially or radially. The types of source being studied include electron beam sources, spark and laser sources, and continuous plasma devices (Eninger 1971).

Sources of positive polarized protons and deuterons have become available in the past ten years. (Haeberli 1967), (Glavish 1971). These use the atomic beam system. The hydrogen molecules are dissociated into atoms by an rf discharge in a glass tube. A small hole in the tube produces a beam. The atomic beam passes through a quadrupole or sextupole magnet which acts upon the electron magnetic moment to focus one spin direction and defocus the other. In typical recent sources the beam then goes through a small rf coil in a weak magnetic field which produces rf transitions in the hydrogen atoms. The new states have 100% nuclear polarization in the following strong magnetic field, where the atoms are ionized in an electron beam. Since these sources occupy several cubic meters in volume they must be placed outside the cyclotron. The beam can be transported to the center of the cyclotron either axially or radially (Clark 1971). The axial system of the Berkeley 88-Inch Cyclotron is illustrated in Figure 29. The beam is brought down to the median plane along the pole axis at about 10 keV energy by a set of electrostatic quadrupole lenses. It is then bent into the median plane by a gridded electrostatic mirror which

is brought through the lower pole to replace the internal ion source. The first such system was operated by the University of Birmingham, England (Powell et al. 1965). A radial injection system at Saclay, France uses an electrostatic channel to focus the beam and cancel the magnetic force on a 5 keV polarized proton beam brought in from a polarized source (Beurtey et al. 1967). Modern polarized sources and injection systems using ions rather than atoms, give high external cyclotron beam intensities, 50-200 nanoamps at the 88-Inch Cyclotron, for example (H. E. Conzett 1972, private communication), compared to less than .1 nanoamp from the older scattering or atomic beam injection methods.

Pulsing of sector cyclotrons is being done by several groups. Slow pulsing in the microsecond or millisecond range can be done by pulsing the ion source arc, the dee voltage or the deflector. Usually the dee voltage is chosen, since there is already a control point in the regulator. For fast pulsing in the nanosecond range, the beam can be pulsed at the ion source, the center region or external beam deflection plates. These systems generally operate by eliminating some of the rf pulses, transmitting 1 in 5, 1 in 10, etc. The pulse width is the natural width of the rf beam microstructure, or it can be reduced by clipping off the edges of the pulses during acceleration. The University of Colorado uses a pulsed grid over the ion source exit slit to pulse proton and deuteron beams (Bentley et al. 1969). Michigan State University uses deflection electrodes inside the dee on the first half turn after the ion source to transmit 1 in 10 pulses for

acceleration (Johnson et al. 1971), Figure 32. In this case three beam defining slits can also be used after 1/2 turn, 18 turns, and 28 turns from the ion source to narrow the pulse width to .2 nanosecond (Blosser 1971a). A time spectrum of the full energy beam from this system is shown in Figure 33, with the pulsing plates on and off, showing complete suppression of the unwanted pulses.

4.1.2.4 Two stage systems.

The use of one cyclotron to accelerate the beam twice, or one cyclotron injecting into another has often been discussed by cyclotron designers. The high energy heavy ion beams of some classical cyclotrons were produced by a double cycle of acceleration (Section 4.1.1). This system could also be used in sector cyclotrons, and increased in efficiency by putting gas jets or foils at the proper positions in the acceleration region (Bennett 1972b). For example N^{2+} could be accelerated from the ion source on third harmonic mode, stripped half way out in radius to N^{3+}, stripped half a turn later to N^{6+}, and accelerated to full radius on first harmonic mode. This would give microamp quantities of high energy N^{6+} beam, which is produced in negligible amounts directly from the ion source.

A system of one cyclotron injecting into another has just been brought into operation at Dubna, U.S.S.R. (Flerov 1972). Beam from the 3 meter heavy ion cyclotron has been transported 70 meters to a 2 meter sector cyclotron where it is injected radially toward the center region. There it is stripped with a foil to a higher

charge state, which places it on a centered orbit in this cyclotron. It is then accelerated to full energy in the 2 m cyclotron. The beam intensity is 3×10^8/sec of Xe ions at 7 MeV/nucleon. This is the highest mass accelerated anywhere, to above the Coulomb barrier of uranium. Experiments are in progress on superheavy element synthesis.

4.1.2.5 Experiments.

Examples of experimental data will be shown to illustrate some of the important beam characteristics of sector cyclotrons. Many of these are work done at Berkeley, because it is most easily available to the author.

The high beam energy available from these cyclotrons made possible the experimental data shown in Figure 34, taken at the Berkeley 88-Inch Cyclotron. Here 80 MeV α-particles were used to bombard ^{26}Mg to produce the very rare unstable isotope ^{8}He, by picking up four neturons (Cerny et al. 1966). The group of counts detected at an energy of 34 MeV was identified as ^{8}He in a counter telescope. The maximum energy α-particles available from present D.C. accelerators is 40 MeV at the largest three stage facility.

The classical and F. M. cyclotrons were usually fixed energy machines. Experiments were sometimes done at various energies by using energy loss foils in the beam, but this produced a loss of resolution. The variation of energy by means of trimming coils and variable volume rf resonators came into wide use in the 1960's, and is a feature of most sector cyclotrons. An illustration of an experiment using this feature at the 88-Inch Cyclotron

is shown in Figure 35. Here an α-particle beam bombarded a helium target (Bacher et al. 1969). The cross-section, σ, is proportional to the number of counts of α's scattered into a detector at a fixed angle. The energy was varied from 30 to 70 MeV with good resolution. Several resonances of the α-α compound system can be observed, representing energy levels in ^{8}Be. The cyclotron energy changes took only 5-10 minutes for closely spaced points within a 10 MeV range. This variable energy feature has always been used on D. C. accelerators, but has become widely available on cyclotrons only in the past decade.

High energy resolution experiments have also been done at several sector cyclotrons. The classical cyclotron has traditionally been a low resolution accelerator, with external beams of several percent energy spread. The sector cyclotrons have used more careful beam centering, and better regulation of the dee voltage to give energy spreads of .2-.5% for the total external beam. For experiments requiring .01 - .02% energy spread, the beam is sent through an analyzing magnet which disperses the energies in space. An analyzing slit selects a small part of the beam to be transmitted with the required energy spread. The system developed at the Berkeley 88-Inch Cyclotron by B. G. Harvey's group (Hintz et al. 1969) is shown in Figure 36. The beam from the cyclotron is defined first at an entrance slit of width .5-2 mm, depending on the resolution required. Magnet No. 1, of 2 meter beam radius, analyzes the beam, and the analyzing slit is set to a width similar to that of the entrance slit, to select the energy spread. Magnet No. 2

can be used for further analysis, or just to clean up the beam and transmit it to the scattering chamber. Data from a test of this system using protons at 14 MeV on carbon is shown in Figure 37. The beam energy resolution was about 1 keV out of 14 MeV, or $\Delta E/E = .01\%$, using the first magnet to define the energy spread, with up to .5 μA on target. The good stability of the analyzing magnet produced stable, well defined energies. The energy was varied by making small changes in analyzing magnet current. This resolution is about equal to that of the best tandem data, Figure 23, as seen by comparing peak/valley ratio and resonance sharpness. It is a great improvement over previous cyclotron performance, and more than adequate for most experiments. By the use of such an analyzing magnet, with a cost of less than 5% that of the cyclotron, the energy resolution of any cyclotron can be improved more than a factor of 10. Similar systems are in use at the University of Michigan (Parkinson et al. 1970) and at several other sector cyclotrons.

An additional improvement in high resolution beams is the defining of the cyclotron beam during acceleration with internal slits, developed at Michigan State University by Blosser's group (1971a). Three internal slits are used to reduce the beam center spread and phase width, and obtain extraction of only one turn (e.g. no. 200) rather than the usual several turns. The energy spread of the cyclotron beam is only .04%. Only a small amount of beam is lost on the cyclotron deflector and the slits at the analyzing magnet, reducing the radioactivity induced in these ele-

ments. For this type of operation a special effort must be made to regulate the dee voltage to the same precision as the energy resolution required.

The most common type of experiment done at cyclotrons and Van de Graaffs is the study of the various reaction products from a fixed energy beam hitting a target, rather than the resonance type of experiment shown in Figures 35, 37. In these particle spectroscopy experiments the detector is as important as the beam for high resolution experiments. Solid state detectors give resolutions of $\Delta E/E = .05 - .1\%$. For better resolution a large magnet must be used, usually referred to as a magnetic spectrometer or spectrograph (Enge 1967). The complete system at Michigan State consisting of cyclotron, beam transport system, target, and the spectrograph are shown schematically in Figure 38 (Blosser et al. 1971b). The spectrograph separates the various energies coming from the target, for example an "elastic group" and an "inelastic group", and focuses them on a focal plane for detection by photographic or electronic methods. The important technique of "dispersion matching" is illustrated here (Cohen 1959b). The cyclotron beam of energy spread ΔE is transported to the target, with the energy increasing with position along the target. When the beam goes through the spectrograph the energies are brought back together at the focal plane, by matching of the spectrograph dispersion with that of the cyclotron and beam transport system. So all reaction product particles from the target which have the same difference in energy from the incoming particle are focused

to one point. This is a very useful mode of operation in which the energy resolution at the focal plane can be much better than the beam resolution, so the analyzing slits in the beam transport system can be opened to get much more beam on target than if the beam resolution had to be as good as focal plane resolution. A spectrum along the focal plane from the system at Michigan State is shown in Figure 39. This is an experiment of inelastic scattering of protons on ^{209}Bi. The peaks represent the levels of the residual ^{209}Bi nucleus. The resolution is 5 keV with an incident energy of 30 MeV, or $\Delta E/E = .17\%$. More recently a resolution of .01% has been obtained with .5 μA of beam on target (H. G. Blosser 1971, private communication). This is better resolution at the focal plane than reported by most tandem Van de Graaffs.

A spectrum from a heavy ion reaction at the Berkeley 88-Inch Cyclotron is shown in Figure 40 (D. G. Kovar 1972, private communication). This is 104 MeV O^{4+} on ^{208}Pb. The beam intensities available from the ion source are down a factor of 10-20 from the proton beams of Figures 37, 39 and quality tends to be worse. The slits in the transport system had to be opened to 2.5 mm to get sufficient beam on target. The resolution is about 100-150 keV, or $\Delta E/E = .1\%$, with .1-.3 μA on target. This is about twice as good resolution as with solid state detectors on heavy ions. Dispersion matching is used here to improve the beam intensity and resolution. It is not clear exactly why the resolution is worse with heavy ions than with light ions, with narrow slits in both cases.

4.2 Other circular accelerators

Several other types of circular accelerators for protons and electrons have been used in nuclear structure research. Their principles of operation are described fully in Livingood (1961) and Livingston et al. (1962), and will not be set forth in this section.

Proton synchrotrons have energies of 1 GeV and above. Several have been used for proton inelastic scattering, or in searches for exotic nuclei formed when the high energy beam breaks a target nucleus apart. At the 3 GeV "Saturne" machine at Saclay, France a high resolution spectrometer system has been built for inelastic scattering studies at resolutions of 100 keV out of 1 GeV, or $\Delta E/E = 10^{-4}$. In the first experiments they have obtained 160 keV at 1 GeV.

The most common circular electron accelerator is the betatron, an induction accelerator. These have accelerated electrons to energies as high as 300 MeV at the University of Illinois. Most are used as sources of medical X-rays up to 30 MeV, but a few have been used in nuclear research at 20-300 MeV. Presently they are being superceded by high intensity electron linacs for pulsed neutron work, or by the more economical electron synchrotrons in the energy region of 100 MeV to several GeV. The microton is also used in a few laboratories to accelerate electrons to 10-30 MeV. The principal type of electron accelerator now being constructed or planned for nuclear physics up to 1 GeV is the electron

linac. These will be described in Section 5.

4.3 Future sector cyclotrons.

The sector cyclotron has been so successful that a number of laboratories are building new machines. Some of these are similar to those now operating, and some are new designs at higher energies. This section will describe some of the new machines now under construction or planned in the energy range over 100 MeV.

The first example is that of the rebuilding of the Columbia University F.M. cyclotron (Rainwater 1971). This will be the first F.M. cyclotron with sector focusing. The advantage of sectors is that the magnetic field can rise with radius to reduce the frequency swing and allow a fast F.M. rate of 300 Hz. This high rate along with a higher dee voltage will greatly increase the beam current from 1 μA to 10-40 μA. The addition of auxilliary coils and sector iron in the magnet gap will increase the energy from 380 MeV to 550 MeV. A median plane plan view of the new machine is shown in Figure 41. The dee comes in from the rotating capacitors on the right. A unique feature of this design is the mounting of one set of iron sectors on the dee at rf potential, to increase the flutter. The cyclotron was shutdown in September 1970 and the conversion was expected to take about a year. This project can be compared with the conversion project at CERN for the 600 MeV F.M. cyclotron (MSC Staff 1971). In the CERN project a new fast cycling rf system will be installed, 500 Hz, at higher dee voltage. No sectors, will be used. The beam current is

expected to increase from the present 1 μA to 10 μA or more. There are studies at Dubna also on adding sector focusing to the F.M. cyclotron there (Glazov et al. 1967).

A sector cyclotron for 580 MeV protons is being built near Zurich, Switzerland by the Swiss Institute for Nuclear Research, "SIN" (Willax 1971). A plan view of the laboratory is shown in Figure 42. The main 8 sector cyclotron has separate magnets for each hill, and no iron in the valleys. The spiral angle reaches 33 degrees at maximum radius. This separated sector design leaves space in the valleys for rf resonators, injection, and extraction. The injector is a 70 MeV sector cyclotron. The current output will be up to 100 μA. The main cyclotron will be for fixed energy protons, but the injector cyclotron will be a multi-particle, variable energy machine which will be used separately part of the time for lower energy work. The installation of the accelerators should be complete at the end of 1973. The experimental program of this "meson factory", will include nuclear structure studies with the high intensity proton beam, as well as experiments with the π and μ-meson beams.

Another cyclotron in the same energy range is the 500 MeV proton machine being built at Vancouver, B.C., Canada (Warren 1971). This "meson workshop" is called "TRIUMF", meaning "Tri-University Meson Facility". TRIUMF will accelerate negative hydrogen ions, H^-, which will be injected from a 300 keV external source down the axis of the upper pole. The advantage of the H^- ions is that they can be easily extracted from the cyclotron by a simple stripping

foil. In fact several beams can be extracted simultaneously by proper positioning of several foils. The H^- acceleration sets an upper limit on maximum magnetic field in the hills of 5.8 kilogauss, to avoid excessive break-up of the ions due to electric dissociation at high energies. This leads to a large outer orbit diameter of 52 feet, compared to 30 feet for the Zurich cyclotron. The maximum spiral angle will be 70 degrees. The vacuum must be kept below 10^{-7} torr to keep the charge exchange during acceleration below 4%. The maximum beam currents are expected to be 100 μA at 500 MeV and 400 μA at 450 MeV. These limits are set by the induced radioactivity from spill beam produced by electric dissociation and gas stripping. Construction should be complete at the end of 1973.

Another separated sector cyclotron like that of Zurich is being built at the University of Indiana (Rickey et al.1969, 1971) This is a multiparticle, variable energy 4 sector Thomas cyclotron. Protons will reach 200 MeV, and heavier ions will have k = 280 in the equation $E = k\ Q^2/A$. An illustration of the system is shown in Figure 43. The pre-injector will provide D.C. acceleration up to 500 keV for protons. The beam then goes into an injector cyclotron, where it is accelerated to 15 MeV, in the proton case. It then goes to the main cyclotron to accelerate to 200 MeV, for protons. The injector cyclotron is a 1/3 scale model of the main cyclotron, so many of the same construction techniques can be used for both. The novel "dee" design is shown in cross-section in Figure 44. The dees are triangular in plane view, and

occupy two opposite valleys. Secondary dees can be placed inside the primary dees, to operate on the second harmonic of the main dee frequency. This has the effect of "flat-topping" the sine-wave accelerating voltage, as shown in Figure 45. All the beam within a 45 degree phase interval will now receive the same energy gain within .1%. With the normal sine-wave, only a 5 degree phase width has this uniformity. This feature will be valuable for producing beams with large microscopic duty factor, and high intensity beams of high resolution. The TRIUMF group is also planning this type of operation, with a first and third harmonic on the same dee. The Indiana cyclotron is a versatile design for light and heavy ions, and is part of several proposals for multi-stage heavy ion accelerators. The cyclotron should be complete in 1973.

At Dubna there is a proposal to convert the 3.1 m heavy ion classical cyclotron to a 4 m sector machine for higher energy heavy ions (Shelaev et al. 1971). This would be the largest single heavy ion cyclotron, with k = 625, compared to 250 for the present 3.1 m, and 240 for the Indiana cyclotron under construction. The intensities would be 10^{11}/sec at 6 MeV/nucleon up to xenon. This intensity is much higher than the present two stage cyclotron system gives. But the particle and energy performance is similar, and a shutdown period would be required for the conversion, so it is not clear at present whether Dubna will build the 4 m cyclotron or an ERA (Section 5.1.2) for its next heavy ion accelerator.

A study has been made at the University of California at Los Angeles (UCLA) of a 2-stage heavy ion cyclotron, in which the two stages are stacked above each other with stripping between stages (Wright et al. 1971). The design and size are similar to Indiana, except that there are two accelerating chambers 15 inches apart vertically, with separate rf systems, and an "interpole" iron slab between them. The final energy would be 200 MeV for protons and at least 9 MeV/nucleon up to uranium. This is a variation of an idea of Dzhelepov et al. (1968) who suggested reinjecting heavy ions after stripping into the same cyclotron for a second cycle of acceleration. The UCLA design has separate magnetic field trimming for the two cycles to avoid the phase slip of the Dzhelepov system.

5. Linear accelerators

5.1 Positive ion linacs

5.1.1 Operating machines.

The principles of linear accelerators have been frequently described (Livingood 1961), (Livingston et al. 1962), (Lapostolle et al. 1970). Only a brief summary will be given here. The earliest form of linear accelerator was built by Wideröe (1928). An illustration of this design is shown in Figure 46, in a configuration used by Sloan and Lawrence (1931). The ions are injected by a small D.C. accelerator. The main accelerator consists of a series of "drift tubes" connected to a source of rf voltage. The polarity alternates from tube to tube, as shown. When the first drift tube has a negative polarity, beam entering the accelerator is accelerated. The length of the first drift tube is made such that the voltage will reverse while the beam drifts through it. When the beam enters the gap between the first and second drift tubes the polarities are plus-minus, as shown, and it receives another acceleration. The beam drifts through the second tube in another half cycle of rf and is accelerated at the next gap. The drift tubes increase in length proportional to beam velocity. They are similar in function to the dees of a cyclotron, shielding the beam from the electric field during a half cycle of the rf. In fact it was an illustration in Wideröe's original article which gave Lawrence the idea for the cyclotron, in which the linac trajectories were wrapped around in a magnet, and the same electrodes were used

many times. The early linacs accelerated only heavy ions, because only low frequency power sources up to 10 MHz were available. A proton linac would have been very long at low frequencies, since the protons accelerate very rapidly. It is shown in a more detailed analysis that there is phase stability of the beam if it crosses the gap while the voltage is increasing. This is because the later particles get more acceleration, for example, and catch up with the earlier particles. However this crossing time gives transverse defocusing to the beam, which must be overcome to prevent beam loss. The early remedy was the installation of grid wires on the entrance to each drift tube to produce an electric field at each gap which converged toward the axis. This caused some beam loss. Modern linacs use magnetic quadrupole lenses inside the drift tubes.

For higher energy beams of protons in the 10 MeV region, higher frequencies are needed to keep the drift tube lengths short. A better structure for these frequencies is the "Alvarez" design shown in Figure 47, developed at Berkeley in 1946 (Alvarez 1946), (Alvarez et al. 1955). The long electrical lines of Wideröe's design are replaced by a standing electromagnetic wave in a cylindrical cavity. The TM_{010} (transverse magnetic field) mode is chosen because it has maximum electric field along the axis, with the magnetic field in a circular pattern around the axis. Here the drift tubes are used to shield the beam from the electric field while the field is directed backwards toward the ion source. The beam crosses the gap between tubes when the electric field is forward in the accelerating direction. The first proton linac of

Alvarez accelerated protons to 32 MeV in a length of 40 feet. The frequency was 202 MHz, set by the tank diameter of 39 inches. A photo of the first 10 MeV tank of the 50 MeV proton linac at the Rutherford Laboratory in England is shown in Figure 48. The beam travels from right to left through the drift tubes supported on stems from the tank wall.

The duty cycle of proton linacs is typically about 1% because of the large rf power required. The energy can only be varied in large steps of about 20 MeV, by turning off whole tanks. Ion sources for proton linacs have been of the rf or duoplasmatron type, similar to those for Van de Graaffs, since both types of accelerator are injected by D.C. sources. A buncher is usually used between the source and the first tank, to compress the D.C. beam into rf bunches which arrive at the right time for acceleration by the linac rf system. A polarized proton source was put into a large Cockroft-Walton terminal at the Rutherford Laboratory linac. Beam pulsing can be done easily at proton linacs, since the source is external.

Linear accelerators can be thought of as divided into cells one drift tube long. The accelerating electric field in the gap is at the center of the cell, and the center of the drift tube is at the cell boundary. In Figure 49 are shown several operating modes of linacs. The mode of operation is classified by the difference in phase of the electric field from one cell to the next at one instant of time. In the Wideröe design, Figure 46, the electric field reverses from one gap to the next,

so it goes through half a cycle, or π radians. This is the "π mode" of operation. In the Alvarez linac, Figure 47, the electric field is the same from one gap to the next, so it operates in the 2π mode. In Section 5.1.2 we will discuss a linac which uses the $\pi/2$ mode.

Some proton linacs were used for nuclear physics starting in the late 1940's, Figure 1. Following the 32 MeV proton machine at Berkeley were the 68 MeV proton linac at Minnesota, the 50 MeV linac at the Rutherford Laboratory, and others in Poland and the U.S.S.R. These machines did much important work, but most have been shut down since the advent of the sector cyclotron and tandem Van de Graaff, which have multiparticle capability and 100% macroscopic duty cycle. Today most proton linacs are used as injectors for synchrotrons, where the requirement is for high current, low duty cycle, and fixed energy.

The Wideröe and Alvarez designs have also been used for modern heavy ion linacs, "hilacs" (Livingston 1970). Twin hilacs were completed at Berkeley and Yale University in 1957-58 (Hubbard et al. 1961). These were Alvarez type machines for accelerating heavy ions up to ^{40}Ar to 10 MeV/nucleon. This energy was chosen to be over the Coulomb barrier on heavy elements. Other hilacs were built for the same ion and energy region at Kharkov, U.S.S.R. and Manchester, England. In the Berkeley and Yale linacs there were 2 tanks. A 500 kV Cockroft-Walton accelerator injected beam into the 15 foot long "prestripper" tank, which accelerated the ions to 1 MeV/nucleon. A stripping foil or gas jet was placed between

tanks to increase the average charge state. This gave a higher rate of energy gain in the "post-stripper" tank, making a shorter machine possible. The post-stripper was 90 feet long. The Manchester hilac used a Wideröe linac for the prestripper region and an Alvarez design for the post-stripper. Several years ago the Berkeley hilac macroscopic duty cycle was increased up to 50% for the lighter ions. This hilac was shut down in early 1971 for conversion to the "Superhilac", which will be discussed in the next section.

The experimental program at the hilacs includes heavy element synthesis, Coulomb excitation, and in-beam atomic spectroscopy. The new elements of atomic number 102-105 have been produced at the Berkeley hilac.

5.1.2 Future machines

There are several positive ion linacs under construction for nuclear physics at present. For protons there is the meson factory at Los Alamos, New Mexico. For heavy ions there are the Superhilac at Berkeley, the Unilac and TALIX in Germany. Hilacs were reviewed by Main (1971a). Studies are also being made on new types of ion linacs.

The Los Alamos Meson Physics Facility "LAMPF", will have an energy of 800 MeV protons and an average beam current of 1 mA (Knapp 1971). The macroscopic duty cycle will be 6%, extendable to 12% later. The accelerator is shown in Figure 50. A 750 kV Cockroft-Walton injects protons into the first linac section.

This is an Alvarez type, modified by adding side posts which convert it from 2π mode to $\pi/2$ mode operation for greater stability. Here the beam is accelerated to 100 MeV. At this energy the drift tubes become long and inefficient, so the structure must be changed. A new structure was developed at Los Alamos to accelerate the protons from 100 to 800 MeV, and is shown in Figure 51. This is called the side-coupled cavity structure, and is very efficient, stable during beam loading, and not sensitive to errors in construction (Knapp et al. 1968). The $\pi/2$ mode is used, where four cavities make one reversal of the rf along the accelerator length. Every second cavity is not excited and so is placed to the side, since it doesn't contribute to beam acceleration. This shortens the length of the accelerator. Many separate tanks are used, with focusing magnets between them. They are connected by bridge couplers, where power is fed in from klystron amplifiers. The length of the whole accelerator is over 1/2 mile. One unique feature of LAMPF is that both protons and H^- beams will be accelerated simultaneously on opposite phases of the rf cycle. These beams are then separated in a magnet after acceleration. The high intensity 900 μA proton beam will be used for meson production while the 100 μA H^- beam can be used for nucleon experiments. The first 800 MeV beam is scheduled for July 1972, with experiments due to start in late 1972.

The experimental program of this high intensity "meson factory" will include π and μ-meson research, and high resolution proton spectroscopy (Rosen 1969). The intensity of 1 mA at 800 MeV

is 10 times more than the cyclotrons under construction at Zurich and Vancouver, and 1000 times more than the usual F.M. cyclotron internal beam. So meson production will be increased by those factors, and very low cross-section experiments can be done which were not possible before. The high resolution proton spectrometer magnet is shown in Figure 52 (Zeidman 1971). The beam radius is 3.5 meter, with bending in the vertical plane. The resolution will be extremely good: 30 keV in 800 MeV or $\Delta E/E = 4 \times 10^{-5}$. This will make possible the resolution of individual energy levels of many nuclei. Dispersion matching (Section 4.1.2.5) will be used, so an incident beam with 1% energy spread can be used on target.

The next heavy ion linac due to come on is the Superhilac at Berkeley (Main 1971b). The old hilac is being modified to make possible the acceleration of all masses to an energy of 8.5 MeV/nucleon (Figure 4). A new 2.5 MV dynamitron type pressurized injector has been built to give adequate injection velocity to the low Q/A (.05) of uranium ions available from the ion source (Spence et al. 1971). The modification is being made at minimum cost, so the rf amplifier system and its power supplies are retained. Two Alvarez sections separated by a stripper will again be used. The last part of the post-stripper tank will be divided into separately excited cavities, so that the energy will be continuously variable from 2.5-8.5 MeV/nucleon by turning off, or reducing the power in some of the cavities. The duty cycle will be 30% for the heaviest particles, and up to 80% for the light ions. The old hilac was shut down in early 1971 to start the conversion. The Superhilac is

expected to start operation in 1972. It will be the first accelerator to give heavy ion beams of all masses with energies over the Coulomb barrier for all targets.

Another hilac under construction is the UNILAC near Darmstadt, Germany (Blasche et al. 1970), (Blann 1971). This is being built by the Gesellschaft für Schwerionenforschung (GSI), with the design being done in Heidelberg. UNILAC is shown in Figure 53. The injection D.C. accelerators will be Cockroft-Waltons at 300 kV in air, for rapid source access. Four ion sources will be available: two Cockroft-Waltons will each feed a PIG or a duoplasmatron type source (Krupp 1972). Three types of linac structure will be used in UNILAC. A Wideröe prestripper stage will accelerate the ions to 1.4 MeV/nucleon. After stripping, an Alvarez stage will accelerate the beam to 4.5 MeV/nucleon. Then any of a series of 20 single gap cavities can be separately excited to provide variable energy. Maximum energy is 8.5 MeV/nucleon for a gas stripper, and 10 MeV/nucleon for foil stripping for the heavier ions, and higher energies for lighter ions (Figure 4). This very versatile machine is due to operate in 1974.

Studies of a helix wave guide structure have been made at several laboratories. The group at Frankfurt, Germany proposed a heavy ion design, "Helac" (Klein et al. 1970), as an alternative design to UNILAC. Another application would be a helix section added to a tandem. The GSI has recently approved a Frankfurt proposal to add 14 helix sections, occupying 22 m of length, to the Heidelberg tandem Van de Graaff. This will accelerate mass 80 ions

to 5.5 MeV/nucleon, and will be called "TALIX" (Klein et al. 1971).

There is development work underway for superconducting ion linacs at Stanford University, California. A group is studying reentrant cavity design and beam dynamics for application to a heavy ion linac or a booster linac added to a tandem Van de Graaff (Glavish 1972). The techniques for using superconducting niobium will be based on the extensive Stanford experience with cavities for electron linacs (Section 5.2.2). Karlsruhe and Frankfurt are testing superconducting helices for use in proton and heavy ion linacs (Klein et al. 1972). Studies are also being done at Caltech, California on superconducting helical waveguides for a hilac (Sierk et al. 1972). The advantages of a superconducting hilac are 100% duty cycle, high energy gain/length giving a compact machine, and lower operating cost. The fabrication techniques for the cavities are still being developed at present, so it is not clear yet whether the above advantages outweigh the possible construction and reliability problems which might be present with a superconducting design (Sierk et al. 1972), (Panel 1972).

Studies for an entirely different type of compact linac, the electron ring accelerator (ERA), are underway in Russia, Germany, Italy, and the U.S.A. The ERA might be used for either heavy ions at 10 MeV/nucleon or high energy protons in the region of 100 GeV. A heavy ion ERA might operate as described by Peterson (1972). An electron beam of about 1000 amps is accelerated to 3-6 MeV during a short pulse of 20-30 nanoseconds. This beam is injected into a "compressor", which is a cyclotron-

type magnetic field formed by a coil system. Here a ring forms which is compressed in diameter by a factor of 10 as the magnetic field is increased. The ring is now about 3 cm in major radius and 1 mm in minor radius. A puff of gas is introduced and begins to be ionized and trapped by the electron ring. After a millisecond U^{23+} would be the main charge state in the case of uranium injection. Then the magnetic field coils on one end would be reduced slightly in strength, and the electron ring would move axially toward the weaker field, pulling the ions with it at field strengths of 60 MV/meter. In less than 2 m of length an energy of 10 MeV/nucleon would be obtained for uranium. At Dubna α-particles have been accelerated to 29 MeV with this method. The ERA has great promise as a heavy ion accelerator because of its compactness, but has very short pulses of 10^{-10} sec. with possible repetition rates of several hundred Hz. Also more development work is needed for understanding various beam instabilities, and injecting heavier ions.

Another new principle for accelerating heavy ions is that of using very high intensity linear electron beams at several MeV energy (Graybill 1972). The electron intensities are about 30,000 amps with a pulse width of 50 nanoseconds. In this device the pulsed electron beam drifts through a chamber filled with a gas of the desired ion species at a pressure of about 100 μ. The electron beam ionizes some of the gas and accelerates it to energies of several MeV/charge. For example nitrogen in charge states 4, 5, 6 has been accelerated to 17-24 MeV. The apparatus

is very compact in this design, but the beam pulse is short, about 10 nanoseconds, and more development is necessary to obtain higher energies of heavy ions.

5.2 Electron linacs

5.2.1 Operating machines

Detailed discussions of the principles of electron linacs are given in several references (Livingood 1961), (Livingston et al. 1962) and (Lapostolle et al. 1970). Only a brief description will be given here. Some early electron linacs used standing wave cavities, but most modern machines use the traveling wave principle illustrated in Figure 54. Here the electron bunches ride on the crests of microwaves traveling down a waveguide. The guide is loaded with disks or "irises" to adjust the wave velocity to be equal to the speed of light, since the electrons reach approximately that speed soon after injection. The structure can also be thought of as a series to TM_{010} mode cavities, like that used in the Alvarez linac, with holes in the ends for the beam and for coupling from one cavity to the next. The cavity size is much smaller than that of a proton linac. The 300 foot long 1 GeV Stanford Mark III linac for example has an accelerating tube 8 cm inside diameter, with iris apertures 2 cm in diameter. The frequency is 2800 MHz. Injection is from an 80 keV electron gun, giving electrons with half the speed of light. A buncher is used to increase the linac acceptance of the D.C. beam. Power is fed in every 10 feet by klystron amplifiers. The duty cycle of elec-

tron linacs is usually about .1% because of the large rf power required. Today most electron linacs are based on the Stanford work, and they are offered commercially by several companies. Many of these linacs in the 10-20 MeV region are used to make high energy X-rays for medical sterilization and therapy work.

The electron linacs used for nuclear physics include some high energy machines such as the Stanford Mark III which do electron scattering to study nuclear sizes and shapes. This work is also done at multi-GeV electron synchrotrons. The other class of linacs are those in the 20-100 MeV region which make the low macroscopic duty factor even shorter by producing short pulses for neutron time-of-flight experiments. Monoenergetic photon beams are also used in experiments by accelerating positrons, which decay in flight. A photo of the 140 MeV machine at Oak Ridge National Laboratory,"ORELA", is shown in Figure 55 (Pering et al. 1969). The accelerator is 75 feet long. The klystron amplifiers, located in an adjacent room, feed power to the linac by rectangular wave guides. The laboratory at Oak Ridge is shown in Figure 56. Its main purpose is to measure neturon cross-sections, by the time-of-flight method. Eleven neutron flight paths radiate from the tantalum target. They have lengths of 15 to 250 feet. The beam can be pulsed as short as 2 nanoseconds for good neutron energy resolution. Another electron linac facility is at Lawrence Livermore Laboratory, California. Here a 100 MeV linac has recently been installed (Fultz et al. 1971a). It is being used for neutron physics and photonuclear reactions. An above

ground photo shows several of the neutron beam tubes, including one 250 m in length, Figure 57.

Some examples of data taken at these facilities will illustrate the types of experiments being done. In Figure 58 is shown data from a photoneutron experiment at Livermore (Fultz et al. 1971b). Here positrons were accelerated in the linac from a target part way along the accelerator. They annihilated in a thin Be target, producing monoenergetic photons (γ-rays). The energy could be varied from 10-28 MeV. The target was ^{26}Mg. Neutrons from (γ, n), (γ, pn) and (γ, 2n) reactions emerging in all directions were counted to calculate the total cross-section. The energy resolution was 200-300 keV.

Another example of data is shown in Figure 59. This is an energy spectrum of the neutrons transmitted through a target of ^{243}Am taken at Oak Ridge (J. A. Harvey 1972, private communication). The time-of-flight method was used on an 18 m flight path. Pulses from the linac were 20 ns wide. Over 100 resonances are seen between 60 and 200 eV. The .3% energy resolution gives an absolute resolution of less than 1 eV. This good absolute resolution is very valuable in studies of the closely spaced energy levels of heavy nuclei.

Recently there has been much interest in increasing the macroscopic duty cycle of electron linacs to make coincidence experiments possible. At Saclay a 500 MeV linac was completed in 1969, which has a duty cycle up to 2% (Leboutet et al. 1969), (Aune et al. 1971). The average current can be up to 600 μA.

Experiments are being done on electron scattering, photonuclear reactions, and π production.

5.2.2 Future machines.

Several electron linacs are now under construction in the energy range 100-2000 MeV, with emphasis on high duty factor. One is the high duty factor MIT linac. Another is the first superconducting linac, at Stanford.

The MIT linac will have a duty factor of 2% at 400 MeV and 6% at 200 MeV (Bertozzi et al. 1967), similar to that of the Saclay project. The energy spread will be ±.2%. A special feature of experimental equipment will be a high resolution spectrometer magnet for electron scattering. This will use dispersion matching (Section 4.1.2.5) to obtain $\Delta E/E = 2 \times 10^{-4}$ on the focal plane, even though the beam resolution on the target is .5%. The facility is just coming into operation.

A very interesting new project is the construction at Stanford of a superconducting electron linac designed for 100% duty cycle at 2 GeV (Schwettman et al. 1967), (Suelzle 1971). The accelerator is shown in Figure 60. The main waveguide length is 160 m. The design energy gradient of 13 MeV/m will then give 2 GeV energy. In addition to its value for coincidence experiments, the 100% duty cycle makes possible the precise regulation of the rf level, giving a beam energy resolution of 10^{-4}. The superconducting cavities will have "quality factor", Q, of about 10^{11}. This means that the rf power will go mostly into beam loading. The beam current will be 100 μA, requiring 200 kW of rf

power at 2 GeV. The cavity structure will look like a disk loaded waveguide, but will be operated as a standing wave linac. The material is niobium operated at 1.8° K. Each of the 24 sections will be contained in a 20 foot long dewar of liquid helium, surrounded by a liquid nitrogen cooled vacuum jacket. The liquid helium line runs along the 500 foot accelerator length to supply the dewars, and helium gas returns to the 300 watt refrigerator. A number of new techniques for niobium cavity fabrication, liquid helium handling, and rf cavity voltage stabilization have been developed for the construction of this impressive accelerator. At present the injector and the first 20 foot tank are complete, and under test. Present techniques have produced cavities with energy gradients of 16-26 MeV/m in models at 8000 MHz (X band). But the larger L-band cavities, 1300 MHz, to be used in the accelerator have so far averaged only about 3 MeV/m, a factor of 4 below the design value. Work is continuing on developing a better cavity fabrication process. The remaining sections of the accelerator will be built during the next 2 years. It will be very interesting to watch the completion of this linac and weigh its attractive duty cycle and resolution against the operational and maintenance problems which may arise in its cryogenic system. Development work on superconducting cavities is underway at other laboratories also.

An interesting application of the superconducting linac is the proposal by the University of Illinois for its use as the accelerating element in a microtron (Allen et al. 1970). This would

be a 30 MeV linac of the Stanford type, with magnets at each end to recycle the beam through it in the microtron configuration. The final energy would be 600 MeV. This system would have 100% duty factor like the Stanford design, but would use a much smaller cryogenic system. The linac portion is under construction and beam has been accelerated to 1 MeV (Hanson 1971). The energy gradient is limited at present to 1 MeV/foot by field emission, and more work on cavity processing is planned.

A proposal has been made by Iowa State University for a 50 MeV normal conducting linac, using the design of the Los Alamos 25 MeV electron prototype model for LAMPF (Baglin 1971). The duty cycle would be 12% at 50 MeV and 20% at 25 MeV. This would be a versatile machine for nuclear physics, with a much larger duty cycle than any other linac except for the Los Alamos model and the Stanford project.

6. Two stage hybrid accelerators

6.1 Present machines

In several laboratories, two different kinds of accelerators are combined to give accelerating systems which have advantages in cost or size compared to a single larger accelerator. We have already seen the advantages of two or three stages of acceleration with the electrostatic accelerator. In linacs there are always at least the two stages consisting of D.C. injector and linac tank. And in cyclotrons, Dubna has effectively combined two cyclotrons with stripping between them. It is particularly in the heavy ion field that several stages are useful, with stripping between stages. In this section we shall mention two types of hybrid accelerator now operating, the cyclograaff and the Orsay linac-cyclotron project.

The cyclograaff consists of a negative ion cyclotron injecting into a tandem Van de Graaff. The advantage here is that a relatively inexpensive cyclotron can add 15 MeV of proton energy to a tandem of 12-15 MeV, making a total of 27-30 MeV. The energy resolution will be determined by the cyclotron, which is .1-.3% or 15-40 keV. The two cyclograaffs now operating are at Duke University (Purser et al. 1971b), and at Lawrence Livermore Laboratory. A drawing of the Livermore facility is shown in Figure 61. The 15 MeV injector cyclotrons for both laboratories were built by the Cyclotron Corporation of Berkeley (Fleischer et al. 1971). The Duke group has found that by stabilizing the cyclotron power supplies and using internal slits the cyclotron

beam energy spread can be reduced to 15 keV. They have also taken resonance curves by fast tandem voltage changes, showing the value of easy energy change inherent in this type of facility.

At Orsay, France heavy ion beams have been radially injected from a linac into a cyclotron in project "Alice" (Cabrespine et al. 1971). This type of two-stage heavy ion system was suggested 20 years ago by Tobias (1952). The system is shown in Figure 62. Heavy ions from a PIG source are injected from a 140 kV D.C. accelerator. The linac is of the Wideröe or Sloan-Lawrence type, which produces 1.1 MeV/nucleon. The beam is then injected into the cyclotron, where a stripper foil increases the charge state from Ar^{5+} to Ar^{12+}, for example, and places it on a centered orbit in the cyclotron. The cyclotron is a variable energy sector type with k = 70. Normal acceleration and extraction take place in the cyclotron. The latest performance reported is .6 nA of Kr^{24+} at 500 MeV (Bieth et al. 1972). Heavy ion reaction studies are in progress with this beam.

6.2 Future machines

Proposed hybrid accelerators are primarily intended to accelerate heavy ions to energies of 6-10 MeV/nucleon. There are many ways of producing these beams. One can use two stages of the same type of accelerator, as in the multi-stage electrostatic accelerators like HILAB, or two cyclotrons at Dubna, or two stage linacs like the superhilac or UNILAC. Or one can combine accelerators of different types in a hybrid system like the Orsay

Alice project. Many proposals have come forward in the past several years, and have been summarized by Martin (1971a), Livingston (1970), Livingston et al. (1971), Purser (1971a), Blann (1971) and others.

A typical hybrid system proposal is that from Argonne National Laboratory, U.S.A., called the Midwest Tandem Cyclotron, "MTC" (Khoe et al. 1971), (Morrison 1970). It is shown schematically in Figure 63. As shown on the right it is a TU tandem injecting into a six sector ring cyclotron. The energies and particles range from 350 MeV protons to 10 MeV/nucleon uranium. As shown at the left of Figure 63 the tandem and cyclotron can be used independently by adding a small injector cyclotron. This would be a versatile facility for heavy and light ions. Other similar proposals include APACHE from Oak Ridge (Martin et al. 1971b), (Zucker 1970), the TANDETRON from Rochester University (Purser 1970), a Michigan State University design including 600 MeV protons (Blosser et al. 1971c) and others from Brookhaven and Los Alamos. There is also interest in Europe at the Bohr Institute. With the current budget limitations in the U.S.A. the prospects are that possibly one of these many proposals will be approved for construction in the next few years, just as one meson factory at Los Alamos was approved out of many proposals several years ago.

7. Summary

To summarize the descriptions given in the text, the principal types of accelerators for nuclear physics in the energy range up to 1000 MeV are listed in Table I. The beam characteristics are listed for each one, for purposes of comparison. The table illustrates the wide variety of particles, energies and beam resolution and timing which are available for experiments today.

In Table II the main new types of accelerators under construction are listed. These will be higher energy light and heavy ion machines, high intensity proton accelerators for meson and nucleon studies, and high duty cycle electron linacs.

Further in the future are other proposals of the type in Table II and also many tandem-cyclotron designs. Development work is underway on new techniques such as applying super-conductivity to ion linacs, and the electron ring principle for a compact heavy ion or high energy proton accelerator. If the work on high charge state heavy ion sources is successful it would give many existing cyclotrons a capability equal to the more elaborate two-stage proposals.

It is hoped that this survey of nuclear physics accelerators has been of value to readers working in other fields, by presenting the present status and future prospects for the various types of accelerators. Only a brief description could be given of each type, so the list of references will be useful for those wishing more information.

Table I. Principal Operating Accelerators for Nuclear Physics, 0-1000 MeV.

Accelerator	Maximum energy (MeV)	Variable energy	External Beam (μA)	External Beam ΔE	External Beam Emittance (mm-mr)	Best Analyzed Beam (μA)	Best Analyzed Beam $\frac{\Delta E}{E}$(%)	Time Structure Macro D.F.(%)	Time Structure Micro D.F.(%)	Time Structure Shortest Pulse	Polarized p,d (nA)	Heavy Ions largest A at 5 MeV/A
D.C. Accelerators												
Single-ended	.1-9p .1-9α	Yes	1-15,000	.25-5keV at 2 MeV	10-15	10-30	.01%	100	100	.8ns	15	^{1}H
Tandem	8-30p 8-32α	Yes	1-100	1-5 keV	1-10	1-10	.01%	100	100	.7ns	50-200	^{16}O
Cyclotrons												
Classical	5-22p 20-45α	Usually No	10-300	1-3%				100	1		.03-.07	^{64}Zn
F.M.	50-730p 50-900α	No	.01-.1	.1-5%				1-80	10-100	2ns	.002-.03	^{4}He
Sector	3-100p 20-160α	Usually Yes	1-200	.02-.5%	5-50	.5	.01%	100	5	.2ns	50-200	^{40}Ar
Dubna 2 stage	7/A	Yes	10^{9}/sec					100				^{136}Xe
Linacs												
Heavy Ion	10/A	Limited	1-50	2-4%				.1-3	10			^{40}Ar
Electron	20-20,000	Yes	1-1000	.2-30%	10-.1			.01-6	1	2ns		
2 Stage Hybrid												
Cyclograaff	27-30	Yes	2	15-50keV				100	5			
Orsay	5/A	Yes	10^{8}/sec	.8%				30	5			^{84}Kr

Table II. New Types of Accelerators For Nuclear Physics Under Construction, 0-1000 MeV.

	Location	Estimated Completion	- EXTERNAL BEAM - Max. Energy (MeV)	Variable Energy	Intensity (μA)	Macro. D.F.(%)	$\frac{\Delta E}{E}$(%)	Comments
D.C. Machines								
A.N.U.	Australia	1972	28p Other ions	Yes	5-10	100	.01	Tandem Pelletron
HILAB	U.S.A.	Indef.	$\geq 7/A$ $A \leq 200$	Yes	.1-10	100	.03	TU+MP tandems, heavy ions
Cyclotrons								
F.M.								
CERN	Switz.	1972	600p	No	10-20	≤ 80	.1-.5	Conversion: New rf, center region.
Columbia	U.S.A.	1972	550p	No	10-40	≤ 50		Conversion: 3 sectors, new rf and center region.
Sector								
Indiana	U.S.A.	1973	200p Other ions	Yes	10	100	.01-.2	D.C. injector+2 cyclotrons, sep. sector.
Vancouver	Canada	1973	500p	Yes	100	100	.05-.2	H^- accel., multiple external beams.
Zurich	Switz.	1974	585p	No	100	100	.3	2 cyclotrons, sep. sector final stage.
Linacs								
Ion								
Los Alamos	U.S.A.	1972	800p	Yes	1000	6-12	1	Alvarez + side coupled, simul. H^+ and H^- beams.
Super-Hilac	U.S.A.	1972	8.5/A All A	Yes	.1-100	30-80	.6	Alvarez, 2.5 MV inj., heavy ions.
UNILAC	Germany	1974	$\geq 7/A$ All A	Yes	.1-100	>25	.02-10	Wideröe+Alvarez+cavities, heavy ions.
Electron								
M.I.T.	U.S.A.	1972	400e	Yes	300	2-6	.4	High D.F., similar to Saclay.
Stanford	U.S.A.	1974	2000e	Yes	100	100	.01	First superconducting, 100% D.F.
Hybrid								
TALIX	Germany		5.5/A $A \leq 81$	Yes	1-10	100	.1-1	MP + helix, heavy ions

Acknowledgements

The author wishes to thank B. G. Harvey of Lawrence Berkeley Laboratory for encouragement in writing this paper. He also wishes to acknowledge valuable help in obtaining information by discussions and printed material from the following people: B. G. Harvey, J. Cerny, H. E. Conzett, D. G. Kovar, F. D. Becchetti, and F. B. Selph of Lawrence Berkeley Laboratory; B. L. Berman, S. C. Fultz and D. R. Rawles of Lawrence Livermore Laboratory; A. D. Bacher of Indiana University; D. A. Bromley of Yale University; W. Haeberli of the University of Wisconsin; J. L. McKibben, L. Rosen and K. H. Harper of Los Alamos Scientific Laboratory; H. G. Blosser of Michigan State University; C. D. Moak and J. A. Harvey of Oak Ridge National Laboratory; F. Chmara and P. H. Rose of High Voltage Engineering Corp.; J. C. Hardy of Chalk River Nuclear Laboratories; P. R. Hanley of Radiation Dynamics, Inc.; G. M. Temmer of Rutgers University; K. Battleson of National Electrostatics Corp.; L. R. Suelzle and H. F. Glavish of Stanford University High Energy Physics Laboratory; H. R. M. Hyder, University of Oxford.

The author also wishes to acknowledge the kind cooperation in supplying material for figures of: Figure 11 -- United States Atomic Energy Commission Office of Information Services; Figures 13, 14, 16, 17, 24 -- High Voltage Engineering Corp.; Figure 15 -- D. A. Bromley, Yale University; Figures 19, 20 -- C. D. Moak, Oak Ridge National Laboratory; Figure 23 -- G. M. Temmer, Rutgers University; Figure 35 -- A. D. Bacher, Indiana

University; Figures 38, 39 -- H. G. Blosser, Michigan State University; Figure 40 -- D. G. Kovar, Lawrence Berkeley Laboratory; Figure 48 -- Rutherford High Energy Laboratory; Figure 49, 50, 51, 52 -- Los Alamos Scientific Laboratory; Figure 54 -- Stanford Linear Accelerator Center; Figures 55, 56, 59 -- J. A. Harvey, Oak Ridge National Laboratory; Figures 57, 58 -- B. L. Berman, Lawrence Livermore Laboratory; Figure 61 -- Lawrence Livermore Laboratory; Figure 43 -- M. E. Rickey, Indiana University; Figures 12, 25 -- National Electrostatics Corp.; Figure 42 -- the SIN group at Zurich.

Thanks are also due to the Lawrence Berkeley Laboratory Graphic Arts group for excellent work on the figures, L. Bell for drafting work on some of the figures, Vertis Ellis and the Nuclear Chemistry Department for typing.

Footnotes and References

Allen J. S. et al. 1970 Particle Accelerators 1, 239-245.

Alvarez L. W. 1940 Phys. Rev. 58, 192-193.

Alvarez L. W. 1946 Phys. Rev. 70, 799-800.

Alvarez L. W. et al. 1955 Rev. Sci. Instr. 26, 111-133.

Armstrong D. D. and Wegner H. E. 1969 Bull. Am. Phys. Soc. 14, 532.

Aune B. et al. 1971 IEEE Trans. Nucl. Sci. NS-18, 3, 561-563.

Bacher A. D. et al. 1969 Bull. Am. Phys. Soc. 14, 1218.

Baglin J. E. E. 1971 IEEE Trans. Nucl. Sci. NS-18, 3, 572-574.

Banford A. P. 1966 The Transport of Charged Particle Beams (London: Spon Ltd.) 229 pgs.

Barnard A. C. L. and Kim C. C. 1961 Nucl. Phys. 28, 428-437.

Barton H. A. et al. 1932 Phys. Rev. 42, 901.

Bejšovec V. et al. 1970 Nucl. Instr. and Meth. 87, 229-236.

Benn J. et al. 1966 Phys. Letters 20, 43-45.

Bennett J. R. J. 1972a IEEE Trans. Nucl. Sci. NS-19, 2, 48-66.

Bennett J. R. J. 1972b Particle Accelerators 3, 43-48.

Bentley R. et al. 1969 Bull. Am. Phys. Soc. 14, 1244.

Bertozzi W. et al. 1967 IEEE Trans. Nucl. Sci. NS-14,3, 191-196.

Beurtey R. and Durand J. M. 1967 Nucl. Instr. and Meth. 57, 313-320.

Bieth C. et al. 1972 IEEE Trans. Nucl. Sci. NS-19, 2, 93-100.

Bilpuch E. G. 1966 in Proc. Conf. on Isobaric Spin in Nuclear Physics (New York: Academic Press) 235-267.

Blann M. 1971 Nucl. Instr. and Meth. 97, 1-17.

Blasche K. et al. 1970 in N.R.H.I. pp. 518-539.

Blewett M. H. 1967 Ann. Rev. Nucl. Sci. 17, 427-468.

Blosser H. G. et al. 1958 Rev. Sci. Instr. 29, 819-834.

Blosser H. G. 1969 IEEE Trans. Nucl. Sci. NS-16,3, 405-414.

Blosser H. G. 1971a in Oxford Cycl. Conf., 257-273.

Blosser H. G. et al. 1971b Nucl. Instr. and Meth. 91, 61-65.

Blosser H. et al. 1971c in Oxford Cycl. Conf. pp. 50-57.

Burrill E. A. 1965 IEEE Trans. Nucl. Sci. NS-12, 3, 235-241.

Cabrespine A. and Lefort M. 1971 Nucl. Instr. and Meth. 97, 29-40.

Cerny J. et al. 1966 Phys. Rev. Letters 16, 469-473.

Chmara F. and Charpentier R. 1971 IEEE Trans. Nucl. Sci. NS-18, 3, 123-125.

Chodorow M. et al. 1955 Rev. Sci. Instr. 26, 134-204.

Clark D. J. 1971 in Oxford Cycl. Conf., 583-601.

Clegg T. B. 1971 Brookhaven National Laboratory Report, N.Y., U.S.A. BNL 50310, 223-230.

Cleland M.R. et al. 1969 IEEE Trans. Nucl. Sci. NS-16, 3, 113-116.

Cockroft J. D. and Walton E. T. S. 1932 Proc. Roy. Soc. A136, 619-630; A137, 229-242.

Cohen B. L. 1953 Rev. Sci. Instr. 24, 589-601.

Cohen B. L. 1959a in Handbuch der Physik (Berlin: Springer-Verlag) 105-169.

Cohen B. L. 1959b Rev. Sci. Instr. 30, 415-418.

Conzett H. E. 1966a IEEE Trans. Nucl. Sci. NS-13, 4, 313-317.

Conzett H. E. and Harvey B. G. 1966b Nucleonics 24, 2, 48-57.

Courant E. D., Livingston M. S. and Snyder H. S. 1952 Phys. Rev. 88, 1190-1196.

Cox S. A. and Hanley P. R. 1971 IEEE Trans. Nucl. Sci. NS-18, 3, 108-112.

Davis J. C. et al. 1971 Bull. Am. Phys. Soc. 16, 582.

Dzhelepov V. P. et al. 1968 Atomnaya Energiya 24, 323-326.

Enge H. A. 1967 Physics Today 20, 7, 65-75.

Eninger J. E. 1971 Nucl. Instr. and Meth. 97, 19-27.

Fleischer A. A. et al. 1971 in Oxford Cycl. Conf. pp. 658-665.

Flerov G. N. 1972 IEEE Trans. Nucl. Sci. NS-19, 2, 9-15.

Fultz S. C. et al. 1971a IEEE Trans. Nucl. Sci. NS-18, 3, 533-537.

Fultz S. C. et al. 1971b Phys. Rev. C, 4, 149-165.

Ginzton E. L. et al. 1948 Rev. Sci. Instr. 19, 89-108.

Glavish H. F. 1971 Brookhaven National Laboratory Report, N.Y. U.S.A. BNL 50310, 207-222.

Glavish H. F. 1972 IEEE Trans. Nucl. Sci. NS-19, 2, 307-308.

Glazov A. A. et al. 1967 in Proc. Sixth International Conf. High Energy Accelerators. Cambridge, Mass., U.S.A. Cambridge Electron Accel. Rept. CEAL-2000. pp. 303-314.

Gordon H. S. and Behman G. A. 1963 in American Institute of Physics Handbook (London: McGraw-Hill) 8:168-222.

Graybill S. E. 1972 IEEE Trans. Nucl. Sci. NS-19, 2, 292-296.

Griffiths R. J. et al. 1966 Nucl. Instr. and Meth. 40, 181-191.

Grodzins L. 1970 in N.R.H.I. pp. 572-582.

Haeberli W. 1967 Ann. Rev. Nucl. Sci. 17, 373-426.

Hamman D. J. and Veazie W. H. Jr. 1964 (Columbus, Ohio, U.S.A.: Battelle Memorial Institute) REIC Rept. No. 31, Pt. II, 204 pgs.

Hanson A. D. 1971 IEEE Trans. Nucl. Sci. NS-18, 3, 149-152.

Harvey B. G. 1969 Introduction to Nuclear Physics and Chemistry (New Jersey: Prentice-Hall). 463 pgs.

Heinicke E. and Baumann H. 1969 Nucl. Instr. and Meth. 74, 229-232.

Henahan J. F. 1971 Chem. and Eng. News 49, 3, 26-30.

Herb R. G. 1959 in Handbuch der Physik (Berlin: Springer-Verlag) 64-104.

Herb R. G. 1971 IEEE Trans. Nucl. Sci. NS-18, 3, 71-75.

Heyn F. A. and Khoe K. T. 1958 Rev. Sci. Instr. 29, 662.

Hintz R. E. et al. 1969 Nucl. Instr. and Meth. 72, 61-71.

Hortig G. 1970 in N.R.H.I. 568-571.

Howard F. T. 1958 ORNL 2644 Oak Ridge National Laboratory, U.S.A. 311 pgs.

Howard F. T. 1967 Oak Ridge National Laboratory Report ORNL-AIC-1. pp 31-36.

Howard F. T. 1969 Isochronous Cyclotrons - 1969. Oak Ridge National Laboratory Report ORNL-AIC-2. 54 pgs.

Howe F. A. 1969 IEEE Trans. Nucl. Sci. NS-16, 3, 98-99.

Hubbard E. L. et al. 1961 Rev. Sci. Instr. 32, 621-634.

Johnson W. P. et al. 1971 in Oxford Cycl. Conf., 325-332.

Kelly E. L. et al. 1956 Rev. Sci. Instr. 27, 493-503.

Kernan W. J. 1968 Accelerators (Oak Ridge, Tenn., U.S.A.: USAEC Div. of Tech. Info.) 57 pgs.

Kerst D. W. 1941 Phys. Rev. 60, 47-53.

Khoe T. K. and Livingood J. J. 1967 IEEE Trans. Nucl. Sci. NS-14, 3, 23-28.

Khoe T. K. et al. 1971 in Oxford Cycl. Conf., 30-40.

Klein H. et al. 1970 in N.R.H.I. pp. 540-556.

Klein H. et al. 1971 Nucl. Instr. and Meth. 97, 41-49.

Klein H. and Kuntze M. 1972 IEEE Trans. Nucl. Sci. NS-19, 2, 304-306.

Knapp E. A. et al. 1968 Rev. Sci. Instr. 39, 979-991.

Knapp E. A. 1971 IEEE Trans. Nucl. Sci. NS-18, 3, 508-512.

Kouloumdjian J. et al. 1970 Nucl. Instr. and Meth. 79, 192-196.

Krupp H. 1972 IEEE Trans. Nucl. Sci. NS-19, 2, 69-73.

Lapostolle P. M. and Septier A. L. (Eds.) 1970 Linear Accelerators (Amsterdam: North-Holland) 1204 pgs.

Lauritsen T. and Adjzenberg-Selove F. 1966 Nucl. Phys. 78, 37.

Lawrence E. O. et al. 1932 Phys. Rev. 42, 150-151.

Leboutet H. et al. 1969 IEEE Trans. Nucl. Sci. NS-16, 3, 299-303.

Livingood J. J. 1961 Principles of Cyclic Particle Accelerators (Princeton, N. J., U.S.A.: D. Van Nostrand Co., Inc.) 392 pgs.

Livingston M. S. 1959 Physics Today 12, 10, 18-23.

Livingston M. S. and Blewett J. P. 1962 Particle Accelerators (New York: McGraw-Hill). 666 pgs.

Livingston M. S. 1966 The Development of High Energy Accelerators (New York: Dover). 317 pgs.

Livingston R. S. 1970 Part. Accel. 1, 51-77.

Livingston R. S. and Martin J. A. 1971 Part. Accel. 2, 189-202.

L.R.L. 1967 88-Inch Sector-Focused Cyclotron, Pub. No. 54, 10 M, July 1967, Lawrence Radiation Laboratory, Berkeley, Calif., U.S.A. 48 pgs.

Main R. M. 1971a IEEE Trans. Nucl. Sci. NS-18, 3, 1131-1136.

Main R. M. 1971b Nucl. Instr. Meth. 97, 51-64.

Marmier P. and Sheldon E. 1969 Physics of Nuclei and Particles Vol. I (New York: Academic Press) 809 pgs.

Martin J. A. 1971a in Oxford Cycl Conf., 3-12.

Martin J. A. et al. 1971b in Oxford Cycl. Conf. pp. 41-49.

McKibben J. L. et al. 1971 in Polarization Phenomena in Nuclear Reactions Eds. H. H. Barschall and W. Haeberli (Madison, Wisconsin, U.S.A.: Univ. of Wisc. Press) pp. 828-831.

McMillan E. M. 1945 Phys. Rev. 68, 143-144.

McMillan E. M. 1959a in Experimental Nuclear Physics, III. Ed. E. Segrè. (New York: John Wiley and Sons) pgs. 639-785.

McMillan E. M. 1959b Physics Today 12, 10, 24-34.

Miessner H. 1970 in N.R.H.I. pp. 627-629.

Moak C. D. et al. 1964 Rev. Sci. Instr. 35, 672-679.

Mobley R. C. 1952 Phys. Rev. 88, 360-361.

Morrison G. C. 1970 in N.R.H.I. pp. 601-614.

MSC Staff 1971 in Oxford Cycl. Conf. pp. 719-727.

Nuclear Data 1970 Nuclear Data, Current Sheets B4, 640.

Panel 1972 Panel discussion. IEEE Trans. Nucl. Sci. NS-19, 2, 312-313.

Parkinson W. C. and Bardwick J. 1970 Nucl. Instr. and Meth. 78, 245-254.

Parks P. B. et al. 1958 Rev. Sci. Instr. 29, 834-839.

Pering N. C. and Lewis T. A. 1969 IEEE Trans. Nucl. Sci. NS-16, 3, 316-320.

Peterson J. M. 1972 IEEE Trans. Nucl. Sci. NS-19, 2, 276-279.

Powell W. B. and Reece B. L. 1965 Nucl. Instr. and Meth. 32, 325-332.

Purser K. H. 1970 in N.R.H.I. pp. 615-622.

Purser, K. H. 1971a IEEE Trans. Nucl. Sci. NS-18, 3, 1121-1130.

Purser F. O. et al. 1971b in Oxford Cycl. Conf., 13-23.

Rainwater J. 1971 IEEE Trans. Nucl. Sci. NS-18, 3, 262-267.

Ratner B. S. 1964 Accelerators of Charged Particles (New York: The MacMillan Co.) 120 pgs.

Reinhold G. and Bill J. 1967 IEEE Trans. Nucl. Sci. NS-14, 3, 145-150.

Reinhold et al. 1971 IEEE Trans. Nucl. Sci. NS-18, 3, 92-93.

Richardson J. R. 1965 Prog. Nucl. Tech. and Instr. 1, 1-101.

Rickey M. E. et al. 1969 IEEE Trans. Nucl. Sci. NS-16, 3, 397-404.

Rickey M. E. and Sampson M. B. 1971 Nucl. Instr. and Meth. 97, 65-70.

Rose P. H. and Galejs A. 1967 Prog. Nucl. Tech. and Instr. 2, 3-116.

Rose P. H. and Wittbower A. B. 1970 Sci. Amer. 223, 2, 24-33.

Rosen L. 1966 Physics Today 19, 12, 21-36.

Rosen L. 1969 Science J. 5A, 1, 39-45.

Rutherford E. 1927 Proc. Roy. Soc. 117, 300.

Schiff L. I. 1938 Phys. Rev. 54, 1114-1115.

Schwettman H. A. et al. 1967 IEEE Trans. Nucl. Sci. NS-14, 3, 336-344.

Seaborg G. T. 1968 Ann. Rev. Nucl. Sci. 18, 53-152.

Shaw J. et al. 1970 in N.R.H.I. pp. 623-626.

Shelaev I. A. et al. 1971 Nucl. Instr. Meth. 93, 557-561.

Sierk A. J. and Tombrello T. A. 1972 IEEE Trans. Nucl. Sci. NS-19, 2, 309-311.

SIN 1970 Swiss Institute for Nuclear Research, Zurich, Switzerland. Progress Report 1970, 123 pgs.

Singh P. P. et al. 1965 Nuclear Physics 65, 577-601.

Sloan D. H. and Lawrence E. O. 1931 Phys. Rev. 38, 2021-2032.

Spence D. A. et al. 1971 IEEE Trans. Nucl. Sci. NS-18, 3, 97-101.

Suelzle, L. R. 1971 IEEE Trans. Nucl. Sci. NS-18, 3, 146-148.

Symon K. R. et al. 1956 Phys. Rev. 103, 1837-1859.

Synchrocyclotron Group 1971 in Oxford Cycl. Conf. pp. 673-674.

Thomas L. H. 1938 Phys. Rev. 54, 580-588.

Tobias C. A. 1952 Phys. Rev. 85, 764.

Trump J. G. 1967 IEEE Trans. Nucl. Sci. NS-14, 3, 113-121.

Tuve M. A. et al. 1935 Phys. Rev. 48, 315-337.

Van de Graaff R. J. 1931 Phys. Rev. 38, 1919-1920.

Van de Graaff R. J. et al. 1948 Rep. Prog. Phys. 11, 1-18.

Veksler V. 1945 J. of Phys., U.S.S.R. 9, 153-158.

von Brentano P. 1967 in International Nuclear Physics Conf., Sept. 1966. Ed. R. L. Becker. (New York and London: Academic Press) p. 208.

Walter R. L. 1970 in Polarization Phenomena in Nuclear Reactions (Madison, Wisc.: Univ. of Wisc. Press) 317-349.

Warren J. B. 1971 IEEE Trans. Nucl. Sci. NS-18, 3, 272-276.

Wegner H. E. 1969 IEEE Trans. Nucl. Sci. NS-16, 3, 81-89.

Wegner H. E. 1971 IEEE Trans. Nucl. Sci. NS-18, 3, 68-70.

Wideröe R. 1928 Archiv für Elektrotechnik 21, 387-406.

Willax H. A. 1971 in Oxford Cycl. Conf., 58-72.

Wilson R. R. and Levinger J. S. 1964 Ann. Rev. Nucl. Sci. 14, 135-174.

Wright B. T. et al. 1971 IEEE Trans. Nucl. Sci. NS-18, 3, 277-281.

Zeidman B. 1971 Los Alamos Scientific Laboratory Report LA-4773-MS, Pt. 1, pp. 1-45.

Zucker A. 1970 in N.R.H.I. pp. 583-600.

Notes on References

"Oxford Cycl. Conf." -- Fifth International Cyclotron Conference Ed. R. W. McIlroy (London: Butterworths) Oxford, England. Sept. 1969.

"N.R.H.I." -- Nuclear Reactions Induced by Heavy Ions. Eds. R. Bock and W. R. Hering (Amsterdam: North-Holland).

†Work performed under the auspices of the U. S. Atomic Energy Commission.

Figure Captions

Fig. 1. Number of operating proton and deuteron accelerators for nuclear physics during the past 30 years, 10-1000 MeV, world-wide.

Fig. 2. Energy levels of the ^{7}Li nucleus. Energies are in MeV at left side (Lauritsen et al. 1966).

Fig. 3. Energy levels of the ^{238}U nucleus. Energies are in MeV at right side. (Nuclear Data 1970).

Fig. 4. Energy per nucleon plotted against projectile mass number for present and future accelerators. Dotted curves, CB, give Coulomb barriers for an ion on uranium (Z=92), and on itself ($Z_1=Z_2$). (Purser 1971a).

Fig. 5. The yield of γ-rays in the $^{27}Al(p,\gamma)^{28}Si$ reaction for proton energies of 4-11 MeV for various averaging intervals. (Singh et al. 1965)

Fig. 6. Source of beam of particles, and phase plot representation of source. Z-axis is beam line direction and X-axis is a transverse direction.

Fig. 7. Illustration of the transport of a beam from a source to an image with two focusing lenses. Typical ray trajectories are shown above, and phase plots below.

Fig. 8. Beam rays at target and detector, showing effect of beam divergence on angular spread at detector.

Fig. 9. Cockroft-Walton voltage multiplier (A), and evacuated beam accelerating tube (B).

Fig. 10. Shunt-fed Cockroft-Walton accelerator, or "dynamitron". Both evacuated beam tube and rectifier system are inside pressure vessel for good high voltage insulation.

Fig. 11. Single stage Van de Graaff accelerator in pressure vessel. (Kernan 1968).

Fig. 12. Interior of Pelletron electrostatic accelerator showing charging chain and column structure.

Fig. 13. Two stage tandem Van de Graaff accelerator principle.

Fig. 14. Two stage tandem Van de Graaff installation. H.V.E.C. MP model.

Fig. 15. Two stage tandem Van de Graaff laboratory at Yale University.

Fig. 16. Three stage tandem electrostatic accelerator principle.

Fig. 17. Three stage tandem electrostatic accelerator laboratory at the University of Texas.

Fig. 18. "Homogenizer" at Duke University Van de Graaff using electrostatic analyzer for generating target bias voltage. Energy spreads on target are reduced to 250 eV (Parks et al. 1958).

Fig. 19. Beam pulsing system at Oak Ridge National Laboratory Van de Graaff. (Moak et al. 1964).

Fig. 20. Beam pulses produced by pulsing system of Fig. 19. Increasing buncher drive from bottom totop. Pulse width at top is 1 ns. (Moak et al. 1964).

Fig. 21. Excitation curve of p-^{40}Ar elastic scattering taken at the Iowa State University Van de Graaff with an energy resolution of about 5 keV. (von Brentano 1967) Compare with Fig. 22.

Fig. 22. Excitation curve of p-^{40}Ar elastic scattering taken at the Duke University Van de Graaff with an energy resolution of 250 eV. (Bilpuch 1966) Compare with Fig. 21.

Fig. 23. Excitation curve over resonance of p-^{12}C elastic scattering taken at the Rutgers University tandem Van de Graaff by Van Bree and Temmer. Compare with Fig. 37.

Fig. 24. HILAB proposal for producing high energy heavy ions by coupling a TU with an MP tandem Van de Graaff. Experiments with high mass projectiles would be done inside MP terminal.

Fig. 25. Two stage tandem Pelletron with 20 MV on terminal (40 MeV protons) proposed by the National Electrostatics Corp. of Wisconsin.

Fig. 26. Classical cyclotron schematic drawing. Vacuum chamber would enclose dees and beam.

Fig. 27. Sector cyclotron magnetic structure. Origin of Thomas axial focusing is illustrated.

Fig. 28. Spiral sector cyclotron pole. Velocity components which provide axial focusing are shown.

Fig. 29. Berkeley 88-Inch Cyclotron in cross-section.

Fig. 30. Resonance chart of magnetic field vs. particle frequency for Berkeley 88-Inch Cyclotron.

Fig. 31. Cyclotron and experimental area of Berkeley 88-Inch Cyclotron.

Fig. 32. Beam pulsing system in center region of Michigan State University Cyclotron. 9 out of 10 pulses can be suppressed by deflection electrodes. (Johnson et al. 1971).

Fig. 33. Time structure of γ-rays from protons hitting a target at the Michigan State cyclotron. Beam was pulsed by a pulsing system (Fig. 32) and defined by a slit system. γ-ray pulse widths indicate proton widths of .2 ns. (Johnson et al. 1971).

Fig. 34. Experimental data showing ^{8}He counts in an experiment at the Berkeley 88-Inch Cyclotron. The high bombarding α-particle energy of 80 MeV and a special counter telescope made the experiment possible. (Cerny et al. 1966).

Fig. 35. α-α scattering excitation curve taken at the Berkeley 88-Inch Cyclotron, illustrating the variable energy capability of the modern sector cyclotron.

Fig. 36. High resolution beam analyzing system at the Berkeley 88-Inch Cyclotron. (Hintz et al. 1969).

Fig. 37. Excitation curve over resonance of p-^{12}C elastic scattering at 14.23 MeV, taken at Berkeley 88-Inch Cyclotron with system of Fig. 36. (Hintz et al. 1969) Compare with Fig. 23.

Fig. 38. Michigan State University cyclotron, transport system and magnetic spectrograph shown schematically. The principle of dispersion matching at the spectrograph is shown. (Blosser et al. 1971b).

Fig. 39. Inelastic scattering experiment, p-^{209}Bi, at Michigan State University Cyclotron, using system of Fig. 38. (Blosser et al. 1971b).

Fig. 40. Heavy ion reaction experiment, ^{208}Pb (^{16}O,^{17}O)^{207}Pb, at Berkeley 88-Inch Cyclotron, using beam analyzing and spectrometer magnets of Fig. 31.

Fig. 41. Columbia University cyclotron combining sectors with F.M., now under construction for 550 MeV protons. It is a conversion of an older machine. (Rainwater 1971).

Fig. 42. New laboratory of the SIN separated sector cyclotron being built near Zurich, Switzerland for 585 MeV protons. Injector cyclotron is at lower left and main cyclotron at lower right. (SIN 1970).

Fig. 43. The new separated sector cyclotron now under construction at the University of Indiana for 200 MeV protons and other particles.

Fig. 44. The dee system in a valley of the new Indiana cyclotron. (Rickey et al. 1969).

Fig. 45. The rf wave shape on the Indiana dee system. The 1st and 2nd harmonic superimposed gives much better "flat-topping" than the 1st harmonic alone. (Rickey et al. 1969).

Fig. 46. The principle of the Wideröe or Sloan-Lawrence type of positive ion linear accelerator.

Fig. 47. The principle of the Alvarez type of positive ion linear accelerator.

Fig. 48. The first tank of the proton linear accelerator at the Rutherford High Energy Laboratory, England.

Fig. 49. Some common modes of operation of linear accelerators. Electric field directions are shown.

Fig. 50. High intensity 800 MeV proton linac meson factory, LAMPF, under construction at Los Alamos Scientific Laboratory.

Fig. 51. New side-coupled cavity structure used for the last stage of LAMPF.

Fig. 52. The High Resolution Spectrometer system, for 30 keV proton resolution at 800 MeV, at LAMPF.

Fig. 53. The UNILAC heavy ion linear accelerator now under construction by GSI near Darmstadt, Germany. (Livingston 1970).

Fig. 54. The principle of the traveling wave electron linac, with its disc-loaded wave guide accelerating tube.

Fig. 55. The 140 MeV electron linac at Oak Ridge National Laboratory, "ORELA".

Fig. 56. The ORELA electron linac laboratory. The linac is in the center, and experimental area to the left.

Fig. 57. Above ground view of the 100 MeV electron linac facility at the Lawrence Livermore Laboratory, California, showing neutron time-of-flight beam tubes.

Fig. 58. Excitation curve of neutrons produced by photons bombarding ^{26}Mg at the Livermore electron linac.

Fig. 59. Spectrum of neutrons transmitted through an ^{243}Am target, taken by time-of-flight measurement at the ORELA electron linac.

Fig. 60. The 2 GeV superconducting electron linac under construction at the Stanford University High Energy Physics Laboratory. (Suelzle 1971).

Fig. 61. The Cyclograaff facility now operating at the Lawrence Livermore Laboratory.

Fig. 62. The "ALICE" heavy ion project recently completed at Orsay, France. The linac at upper left injects beam into the sector cyclotron, below. Inset at lower left shows typical injection orbits in cyclotron median plane, where charge changes in a stripping foil. (Purser 1971a).

Fig. 63. Two stage hybrid heavy ion accelerator system of tandem Van de Graaff injecting beam into separated sector cyclotron, proposed by Argonne National Laboratory. (Khoe et al. 1971).

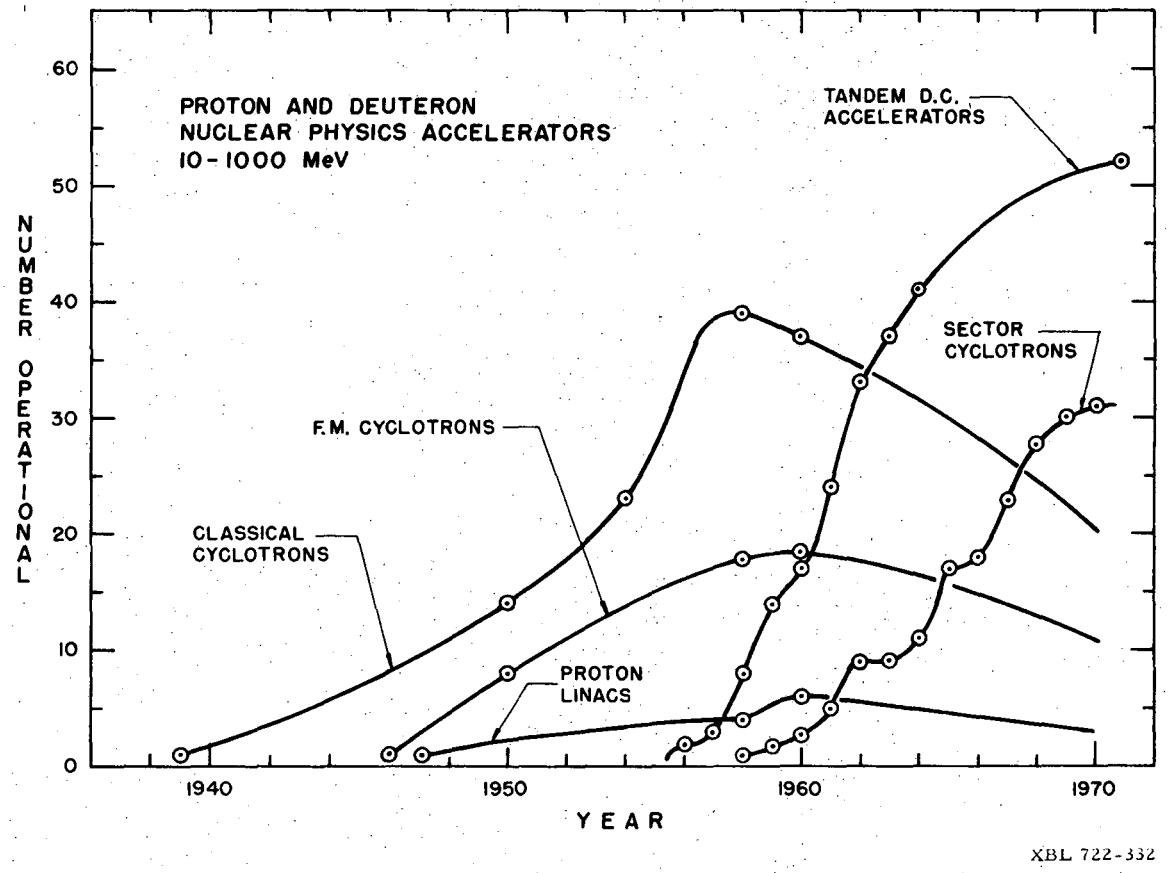
PROTON AND DEUTERON
NUCLEAR PHYSICS ACCELERATORS
10-1000 MeV
TANDEM D.C.
ACCELERATORS
SECTOR
CYCLOTRONS
F.M. CYCLOTRONS
CLASSICAL
CYCLOTRONS
PROTON
LINACS
NUMBER OPERATIONAL
0
10
20
30
40
50
60
1940
1950
1960
1970
YEAR
XBL 722-332

Fig. 1

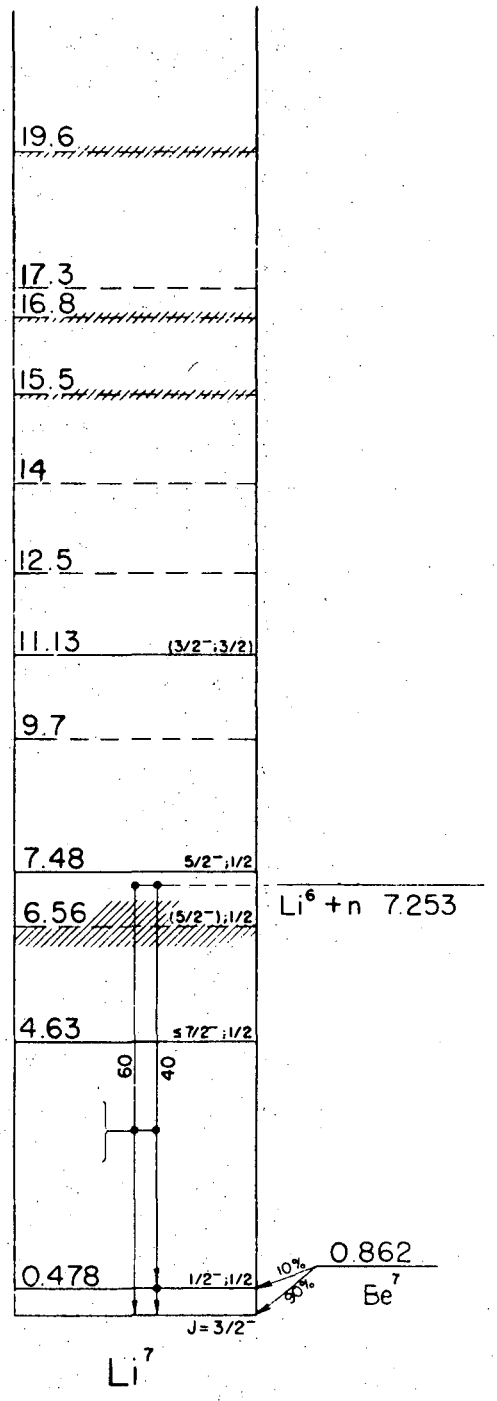

XBL 723-467

Fig. 2

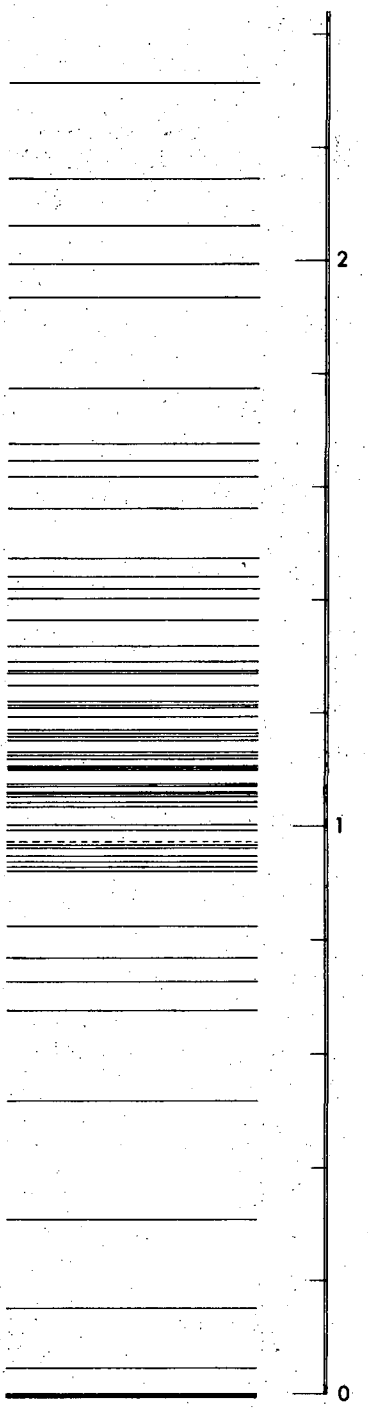

XBL 723-468A

Fig. 3

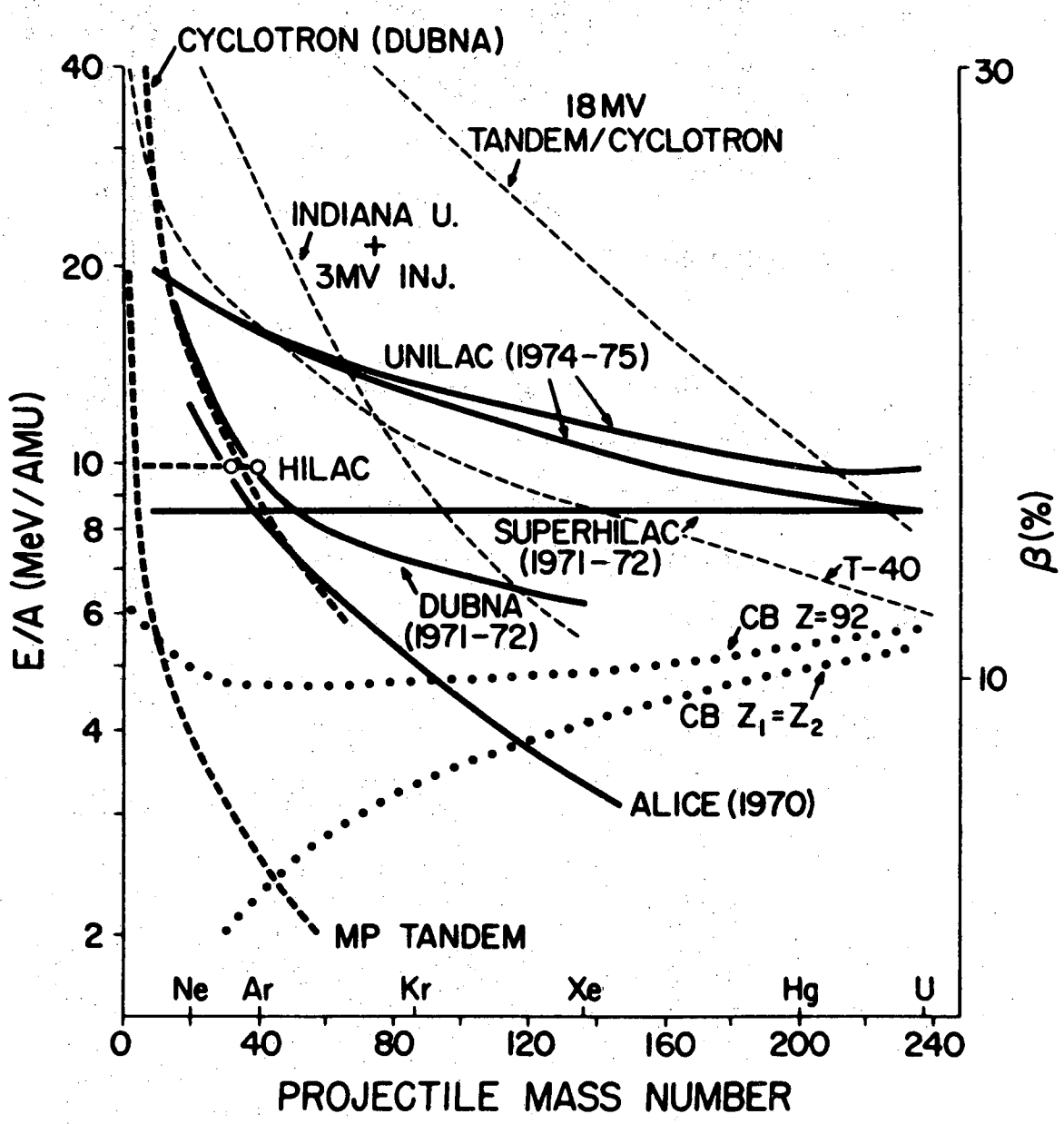

XBL 723-466

Fig. 4

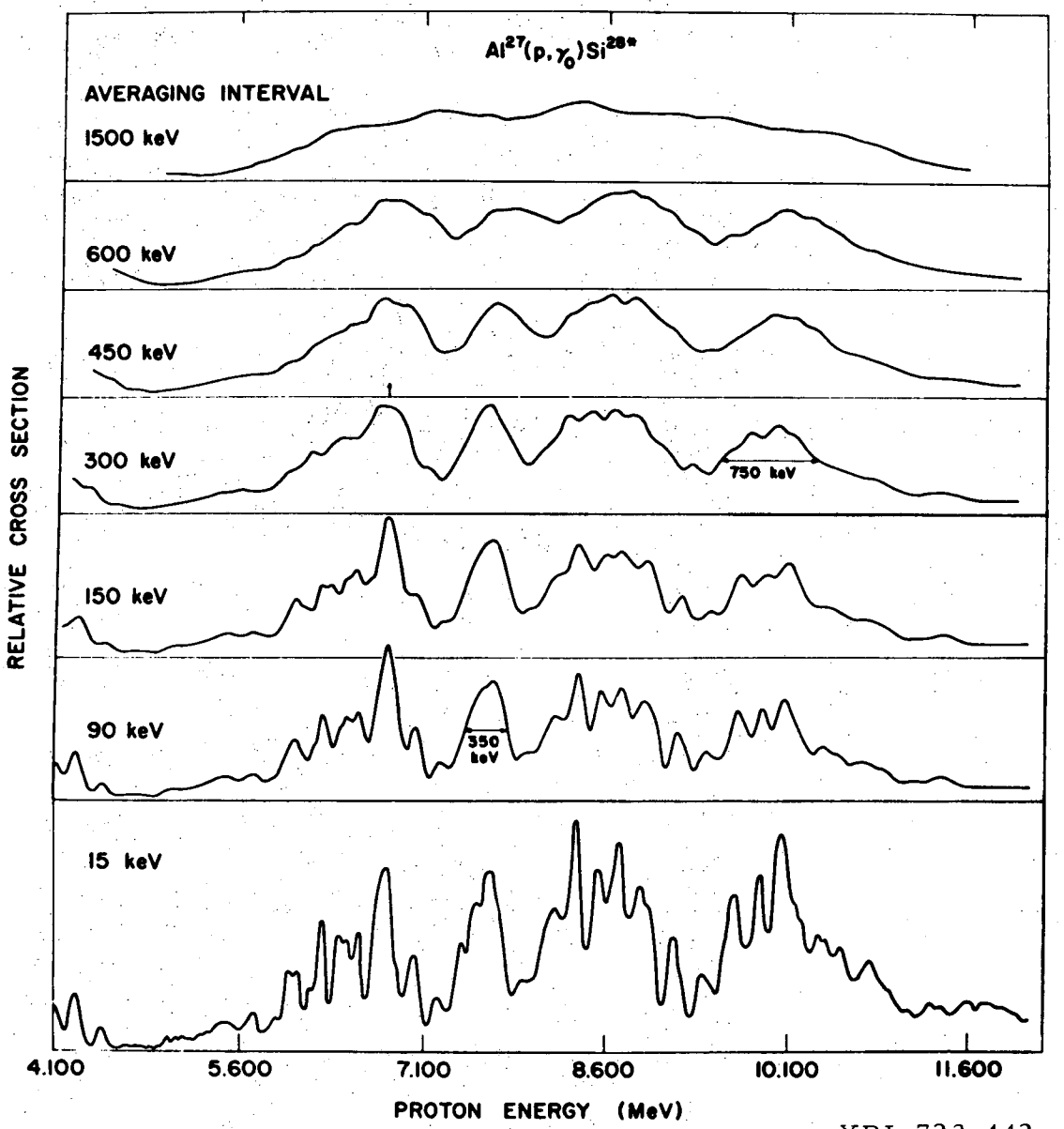

XBL 723-442

Fig. 5

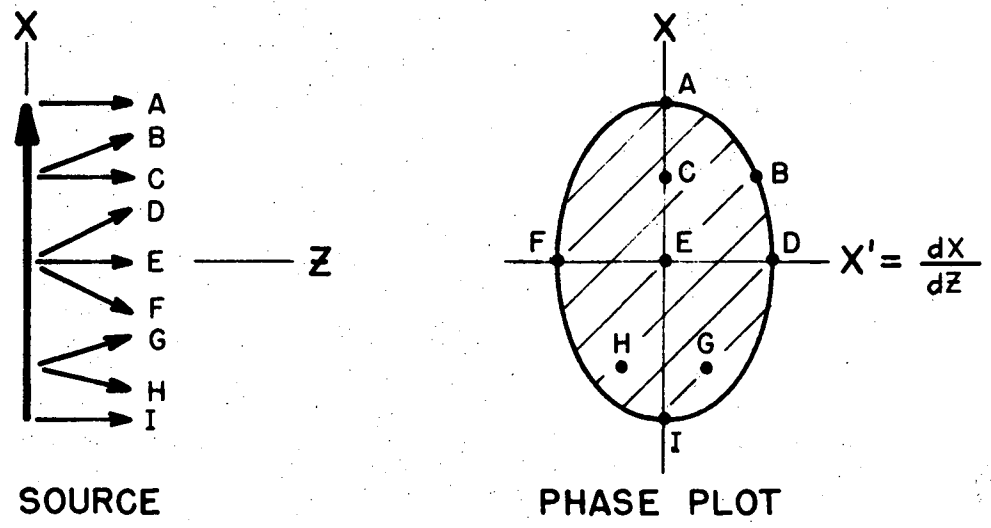

XBL 722-334

Fig. 6

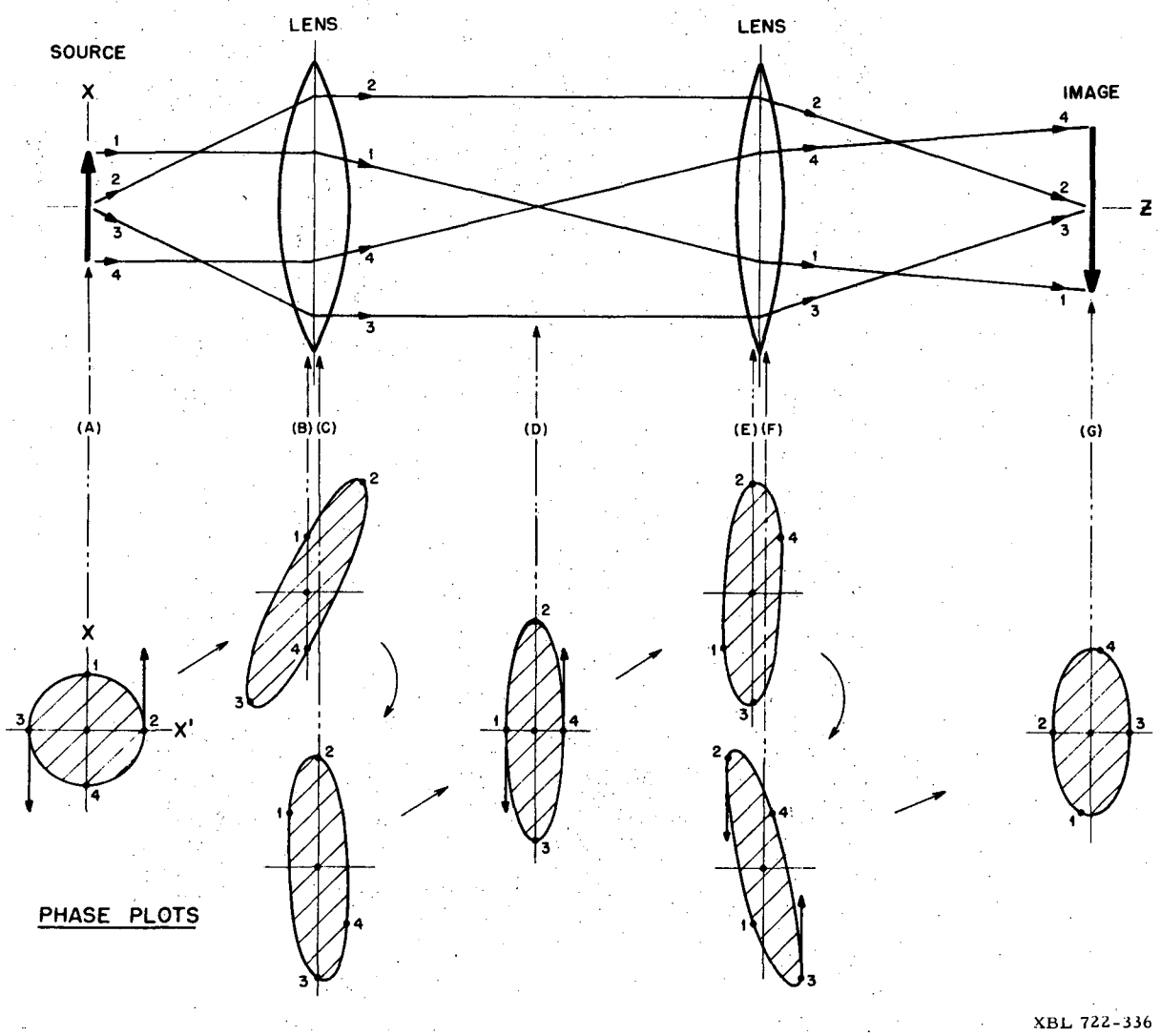

Fig. 7

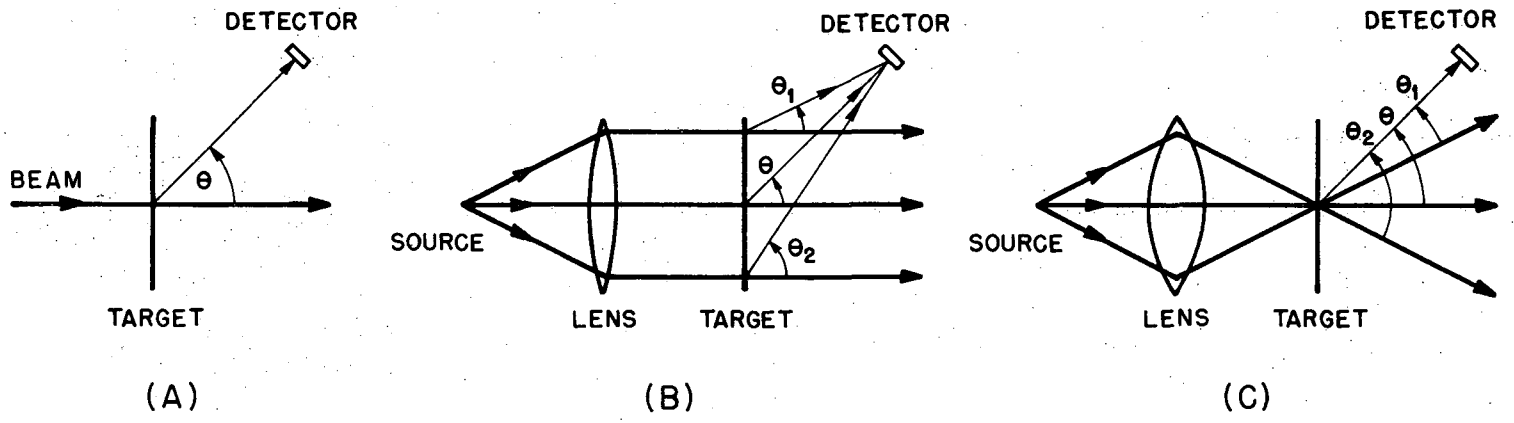

XBL 722-335

Fig. 8

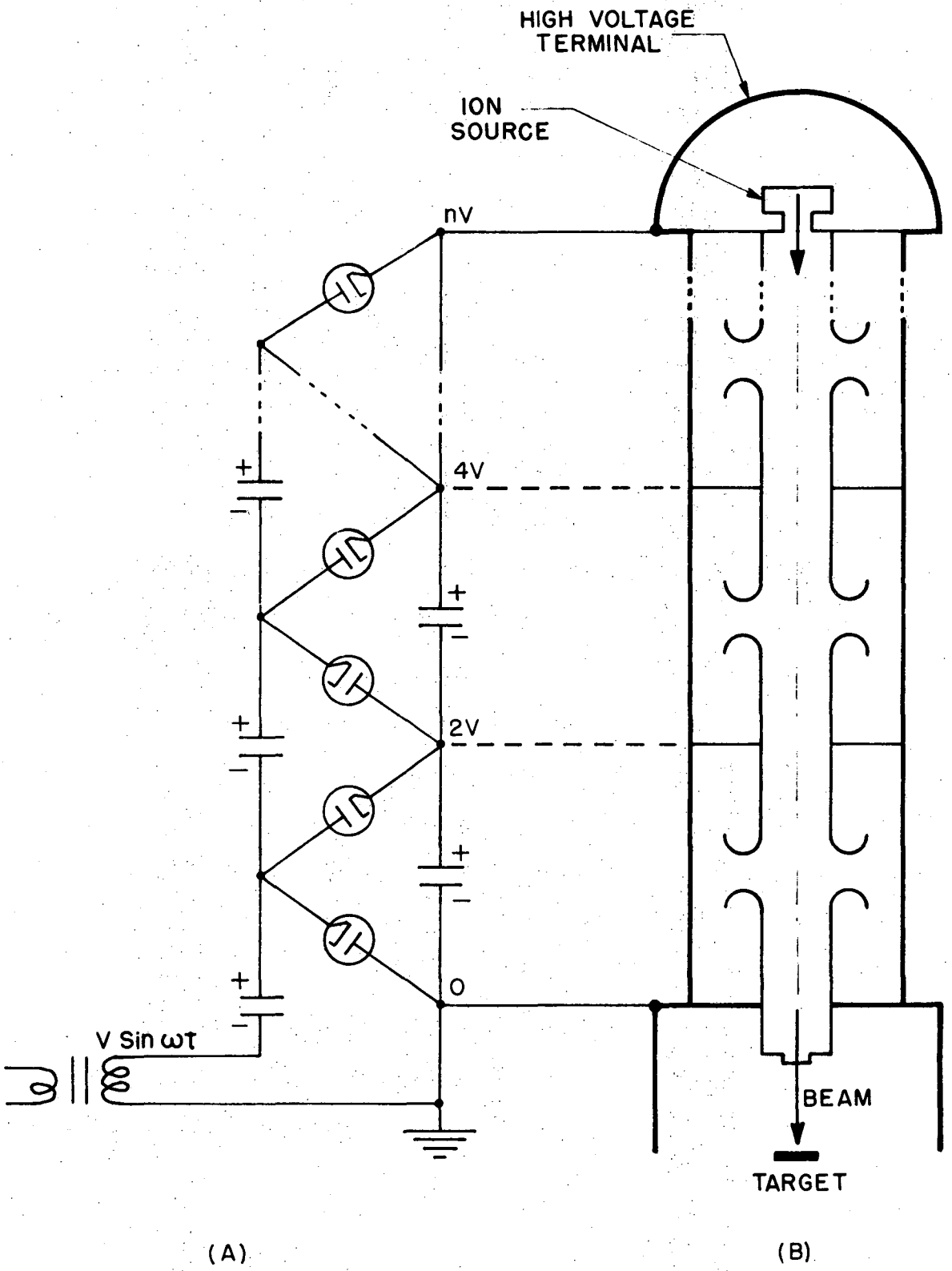

XBL 722-346

Fig. 9

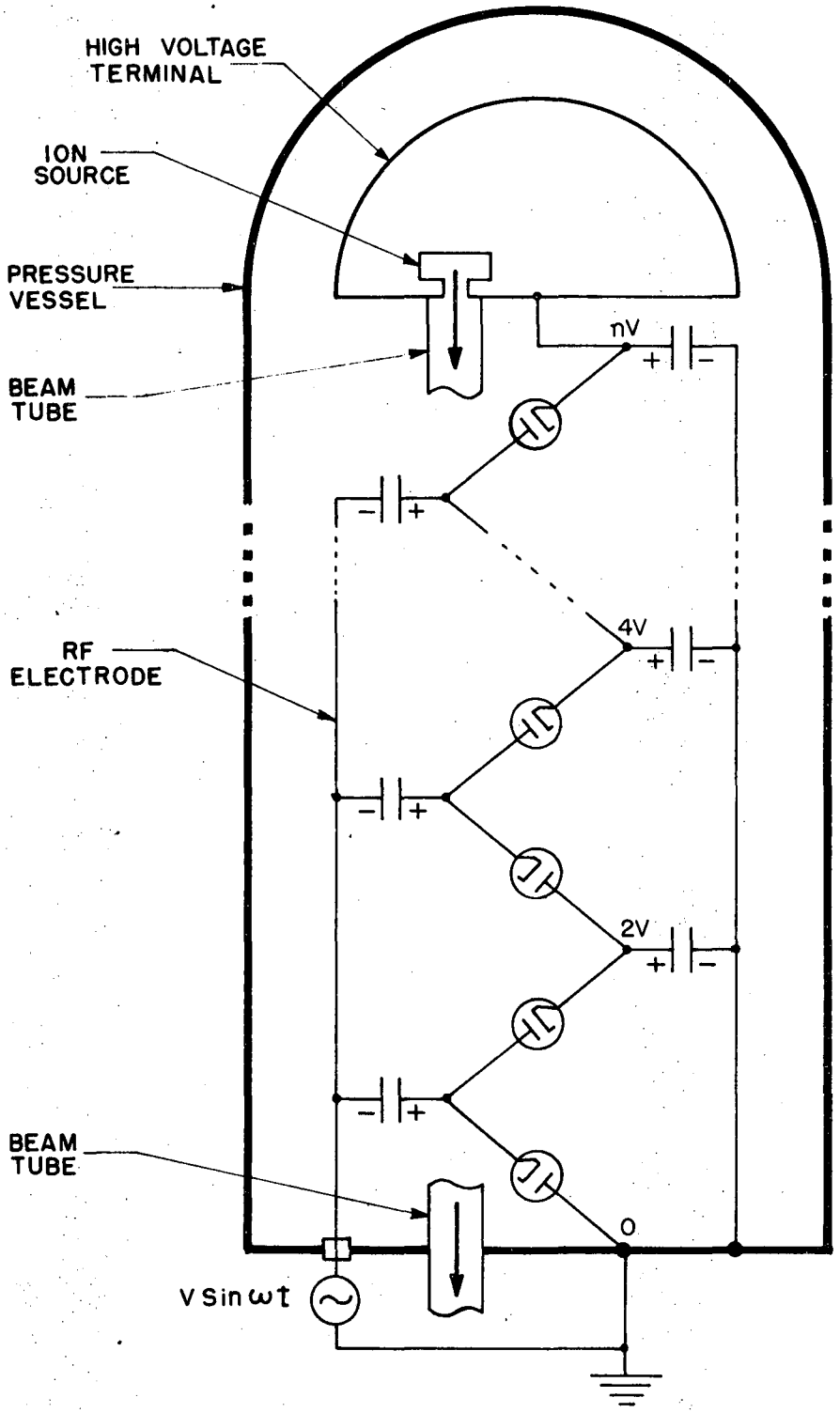

XBL 722-347

Fig. 10

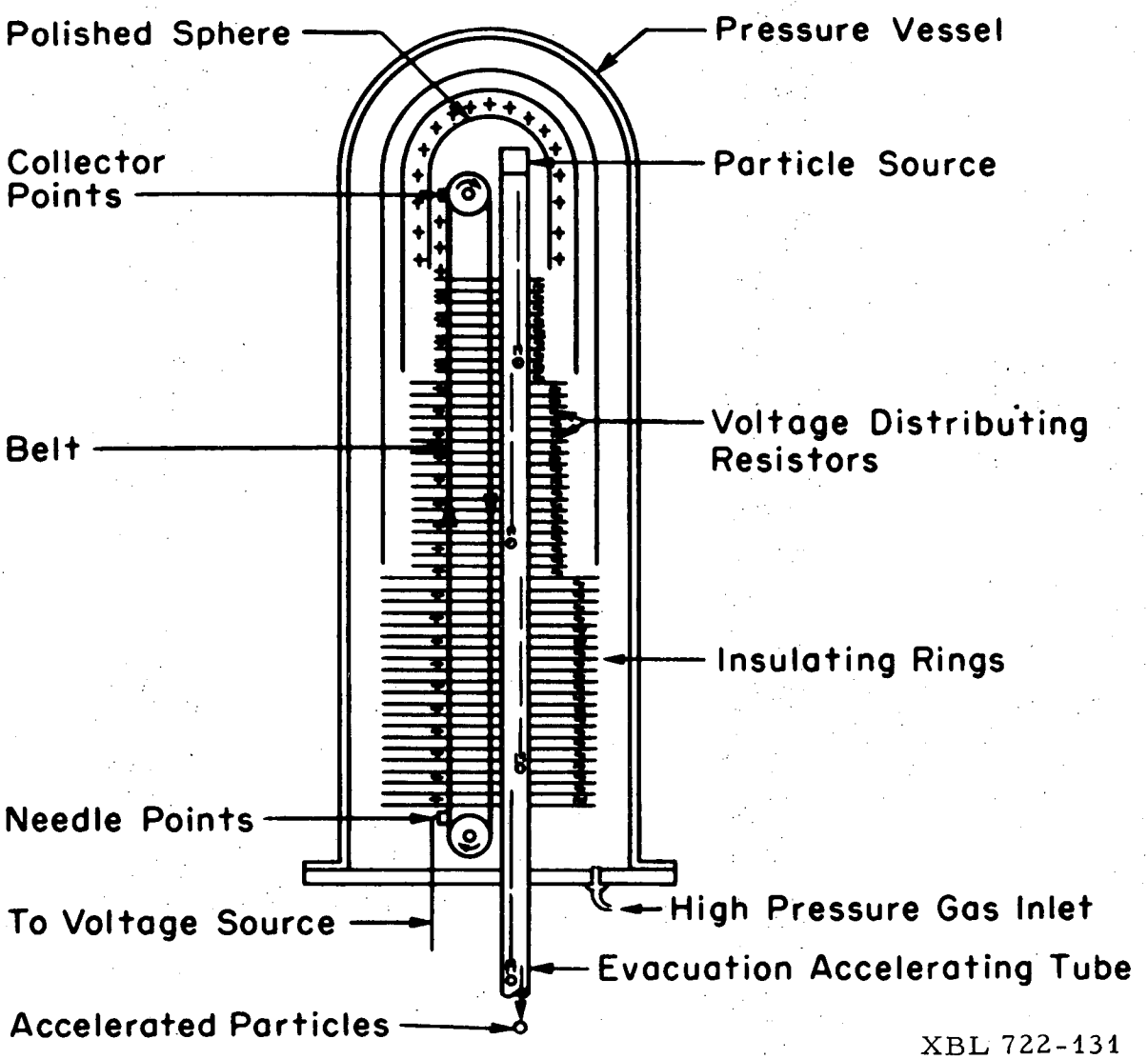
Polished Sphere
Pressure Vessel
Collector Points
Particle Source
Belt
Voltage Distributing Resistors
Insulating Rings
Needle Points
To Voltage Source
High Pressure Gas Inlet
Evacuation Accelerating Tube
Accelerated Particles
XBL 722-131

Fig. 11

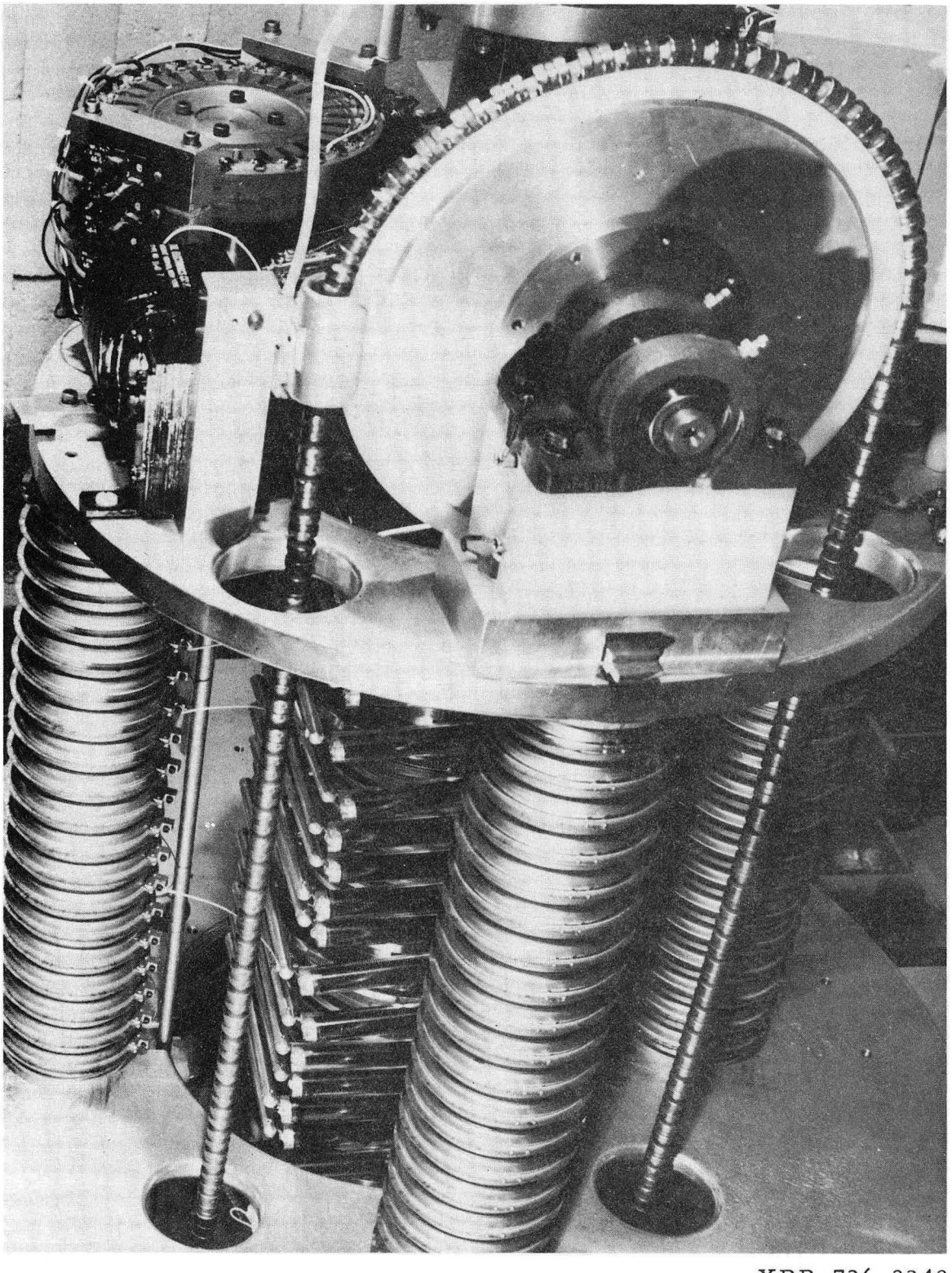

XBB-726-3243

Fig. 12

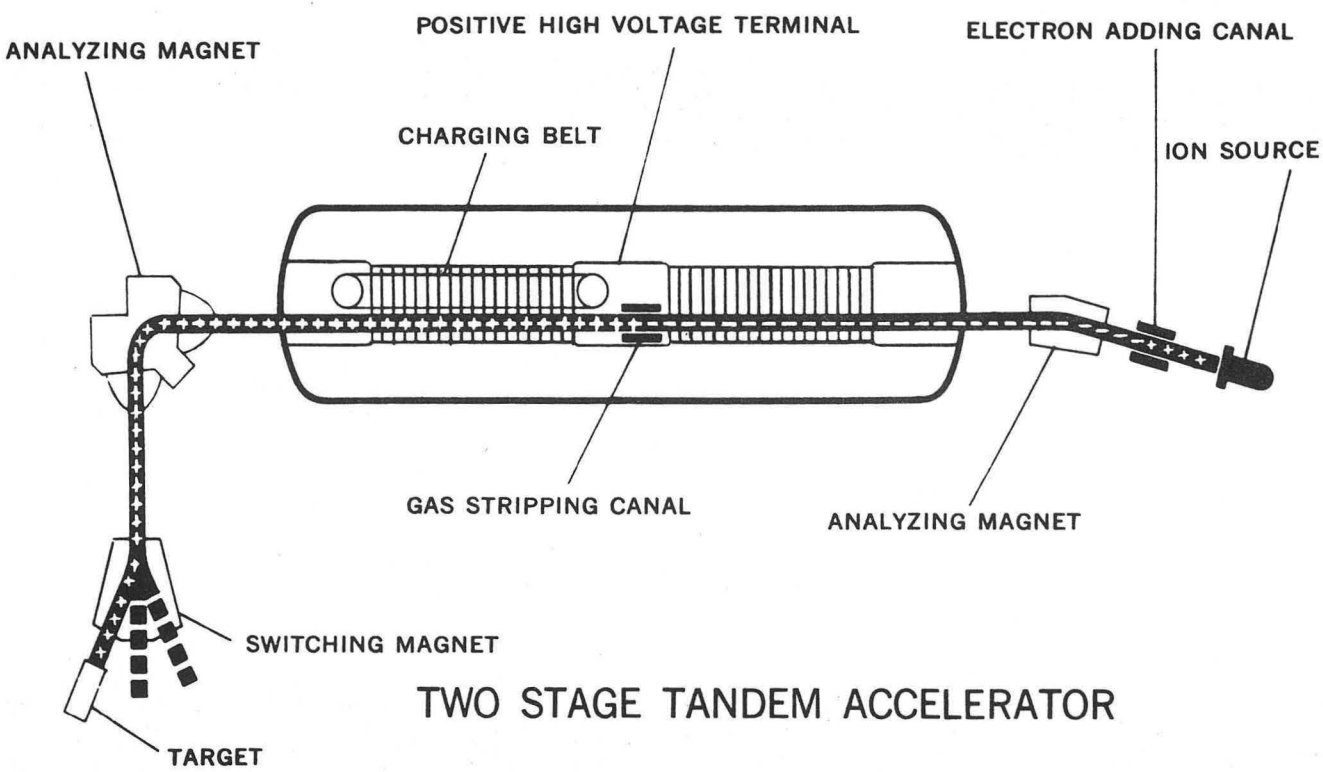

TWO STAGE TANDEM ACCELERATOR

XBL 722-132

Fig. 13

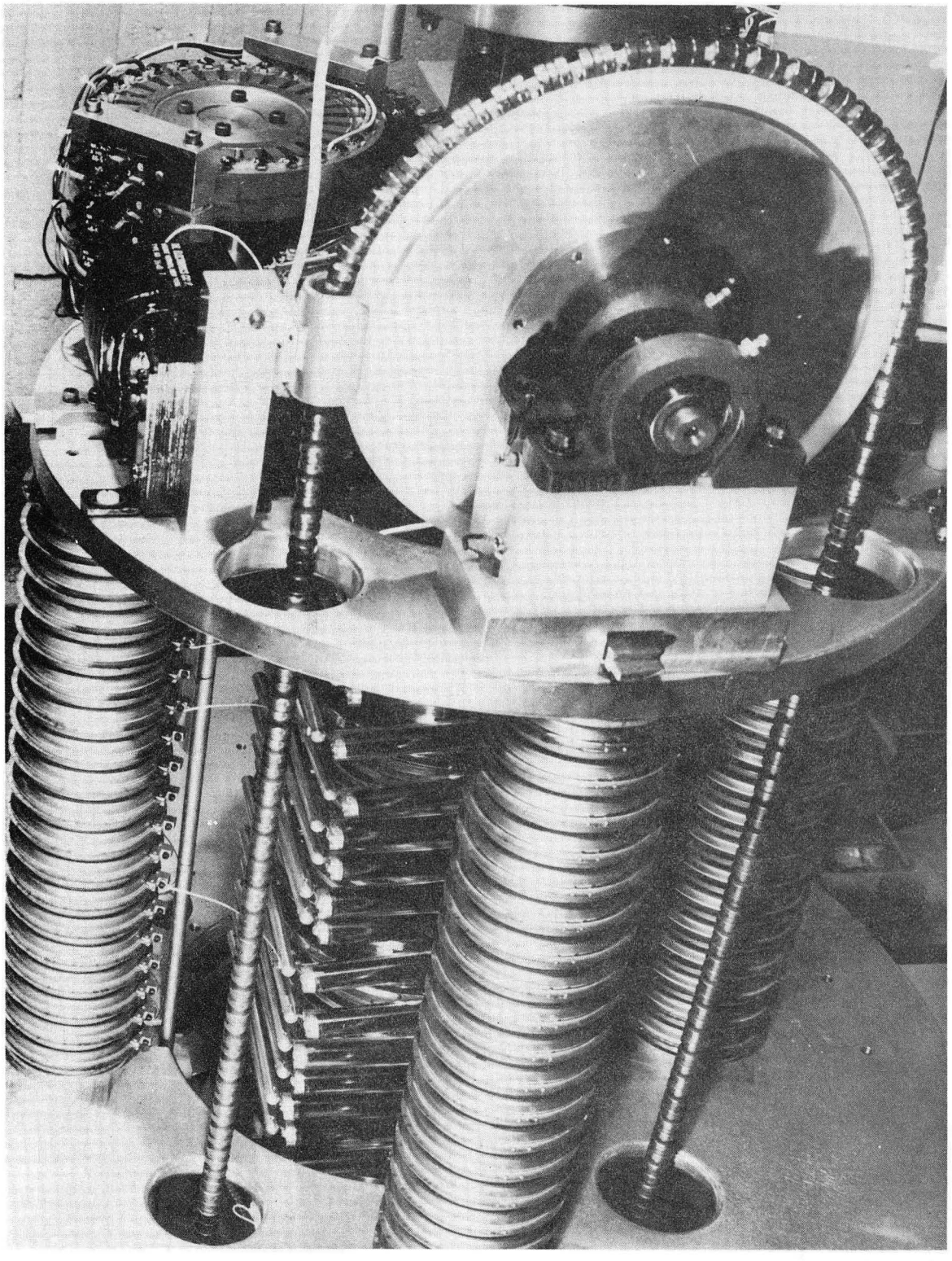

XBB-726-3243

Fig. 12

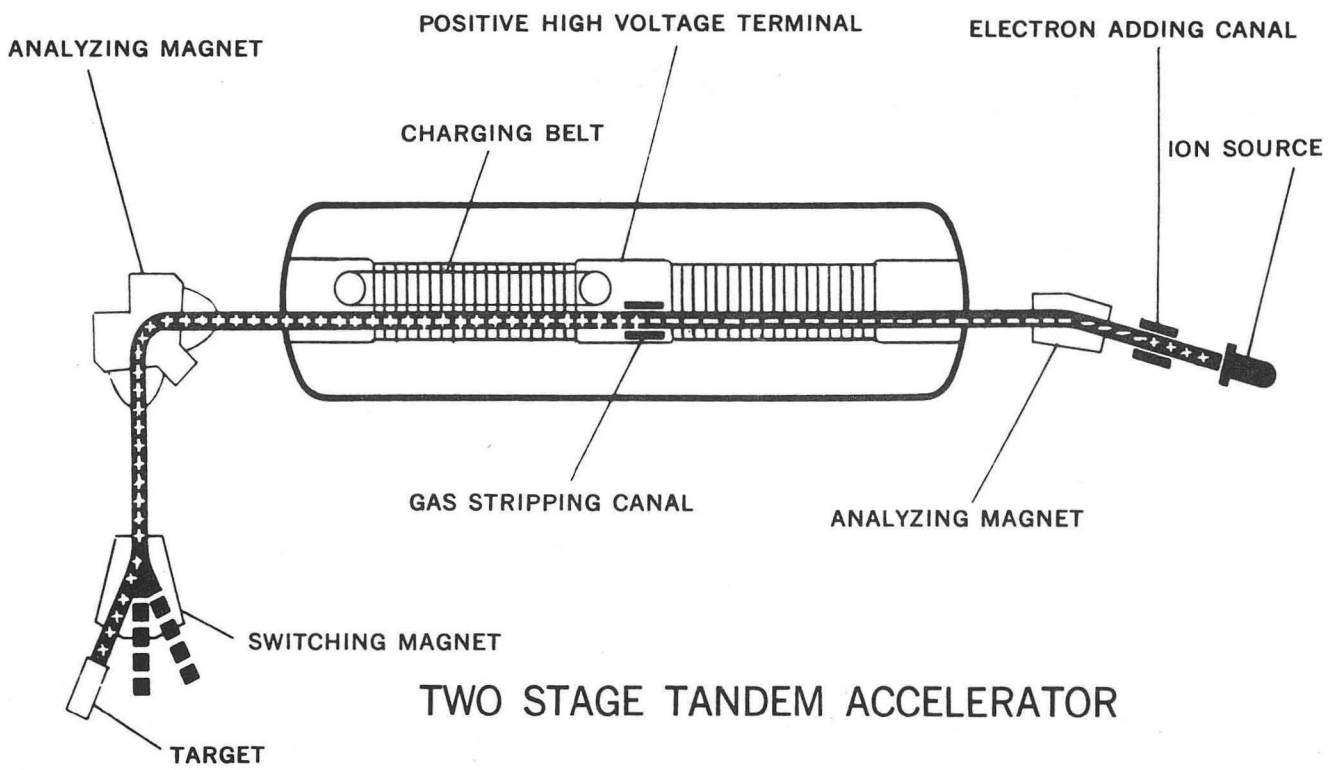

TWO STAGE TANDEM ACCELERATOR

XBL 722-132

Fig. 13

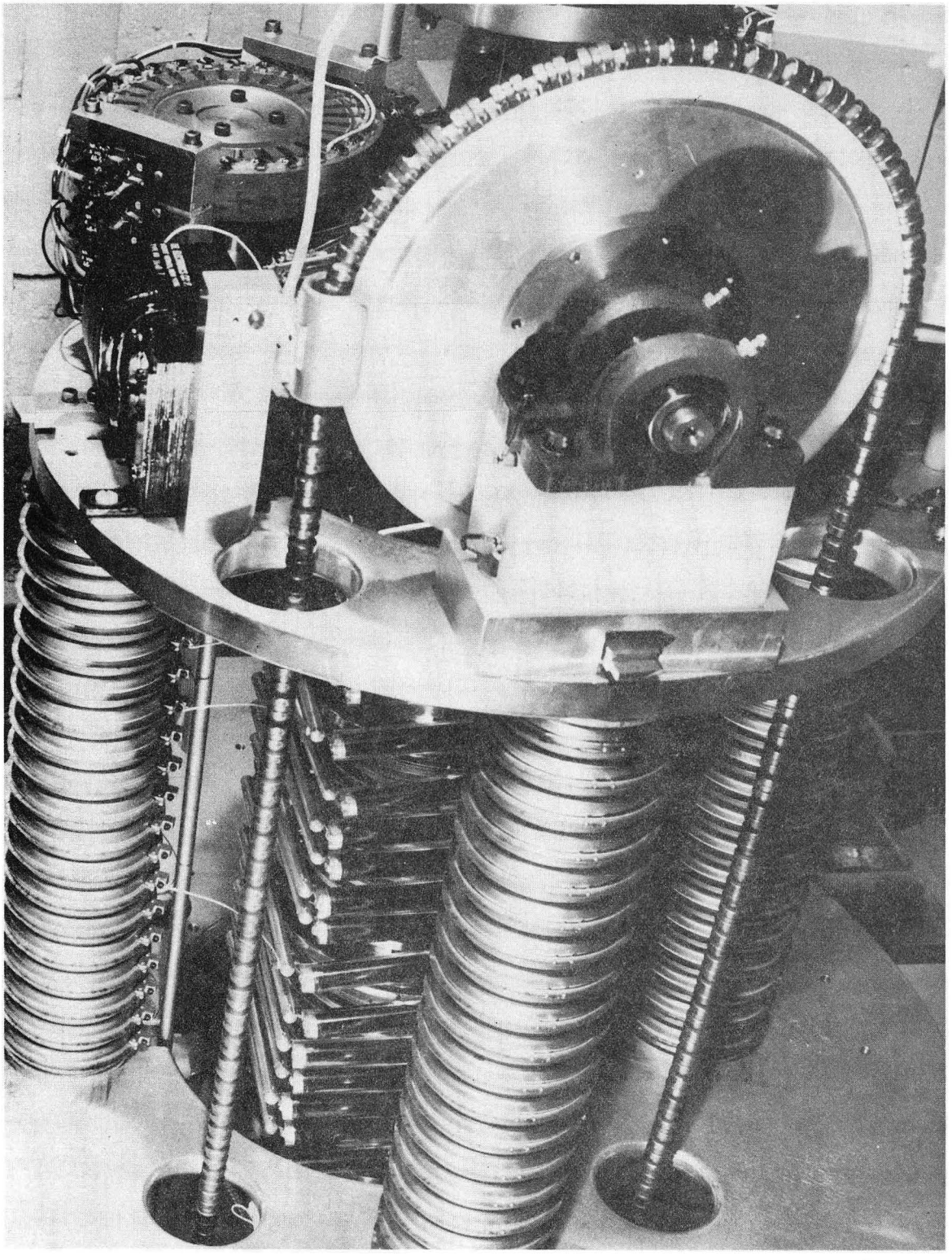

XBB-726-3243

Fig. 12

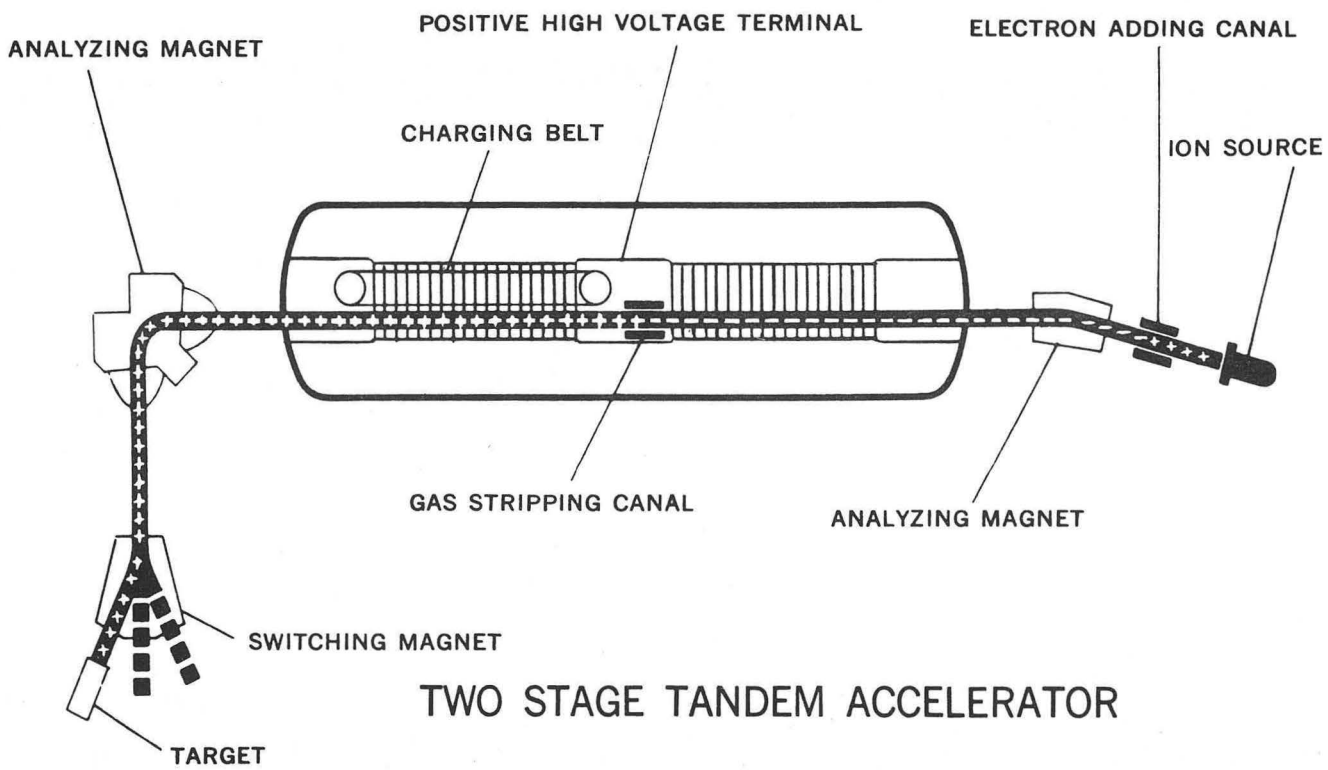

TWO STAGE TANDEM ACCELERATOR

XBL 722-132

Fig. 13

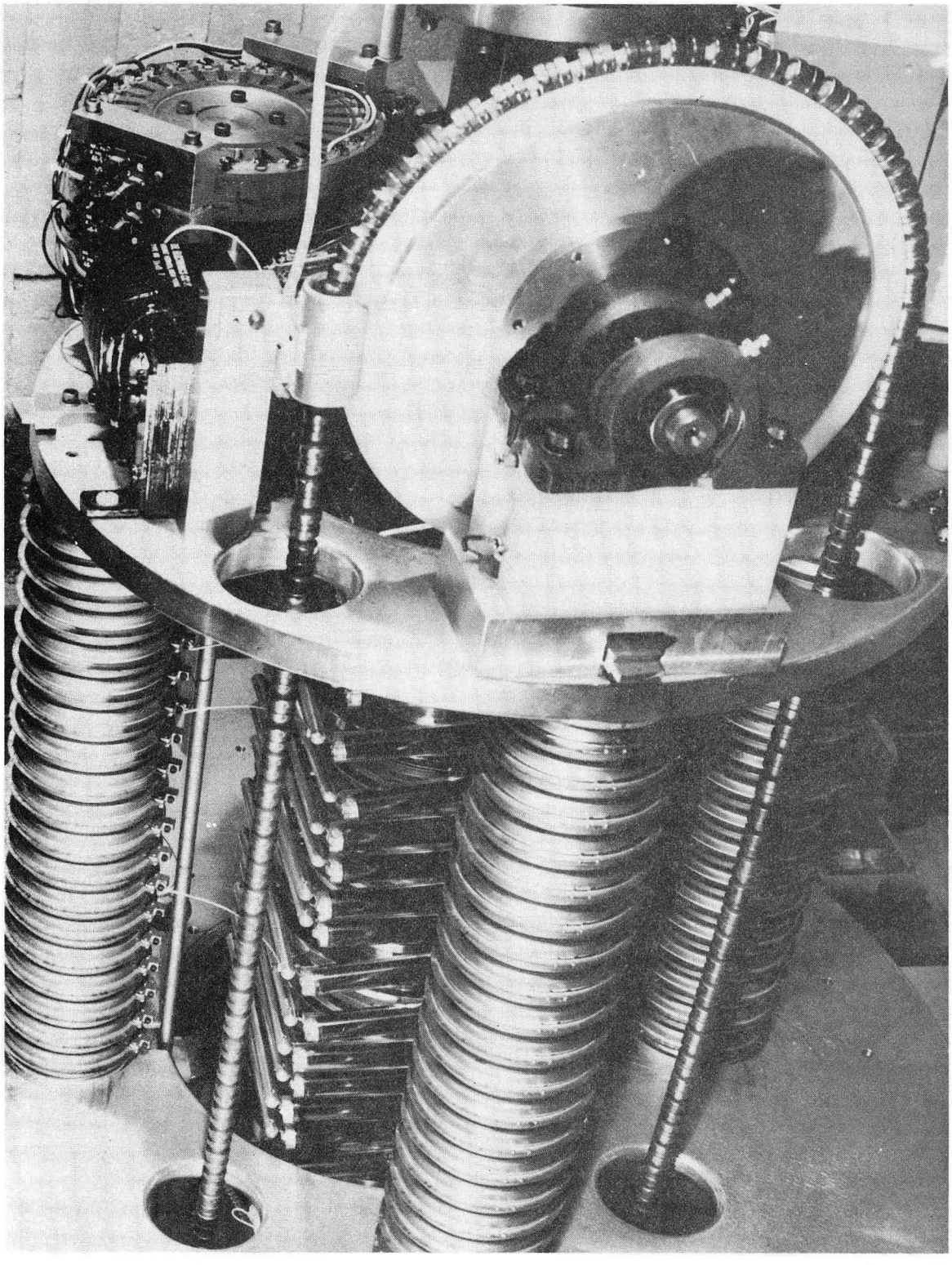

XBB-726-3243

Fig. 12

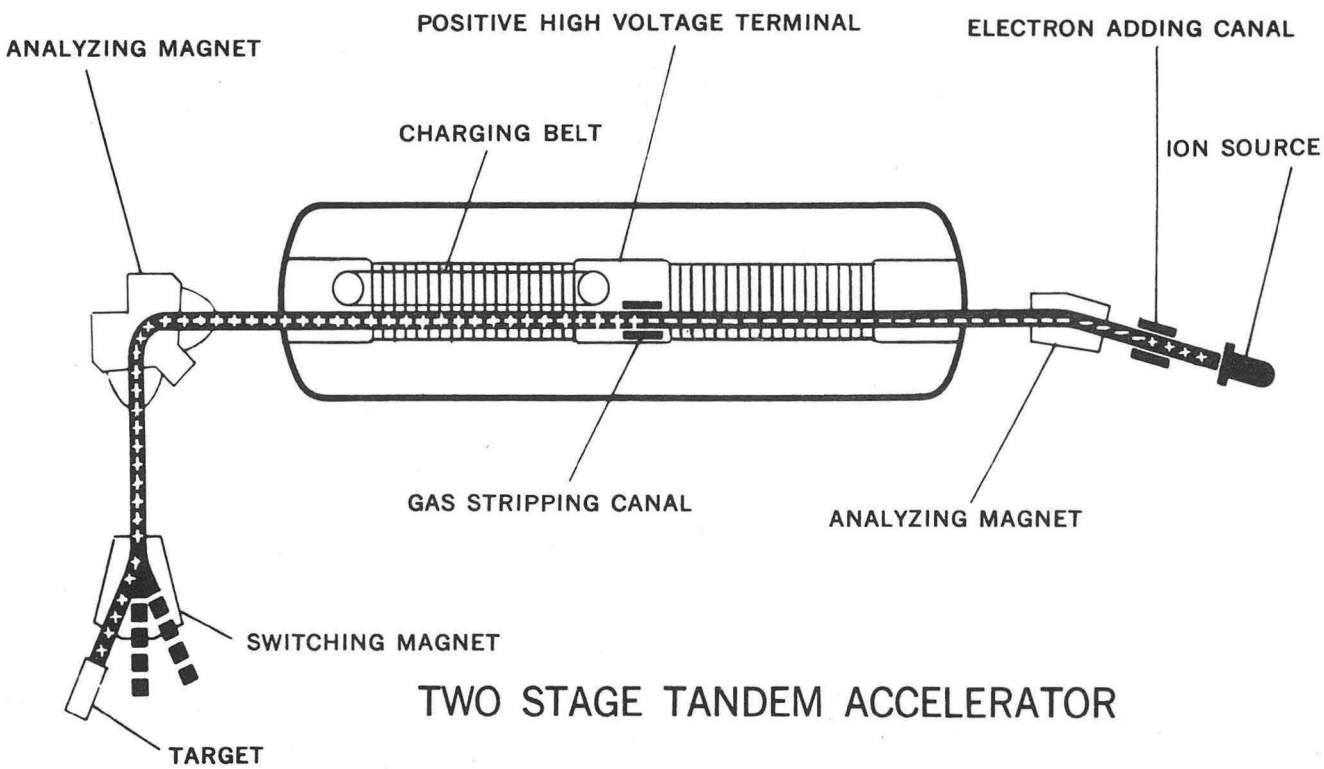

TWO STAGE TANDEM ACCELERATOR

XBL 722-132

Fig. 13

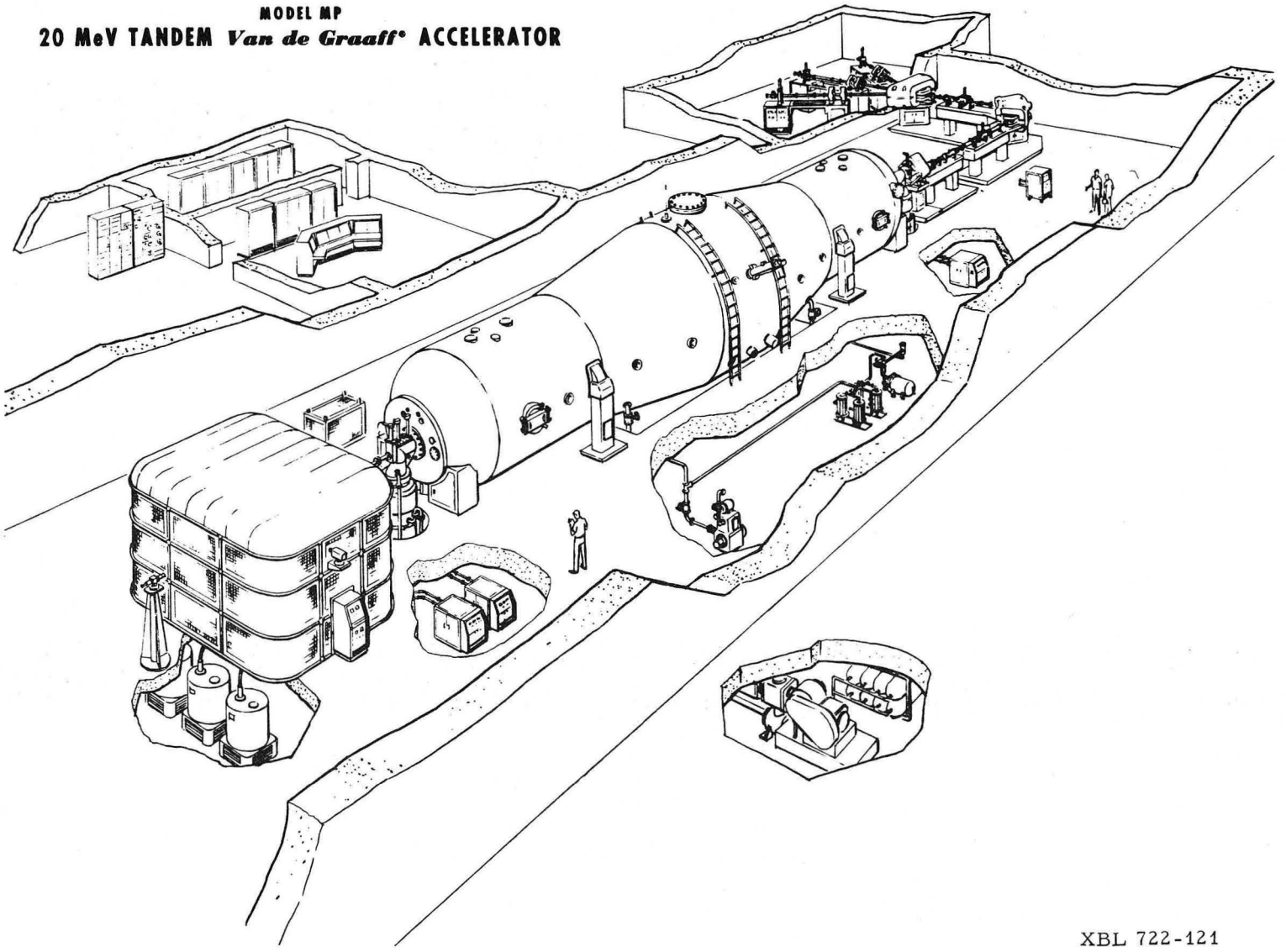

XBL 722-121

Fig. 14

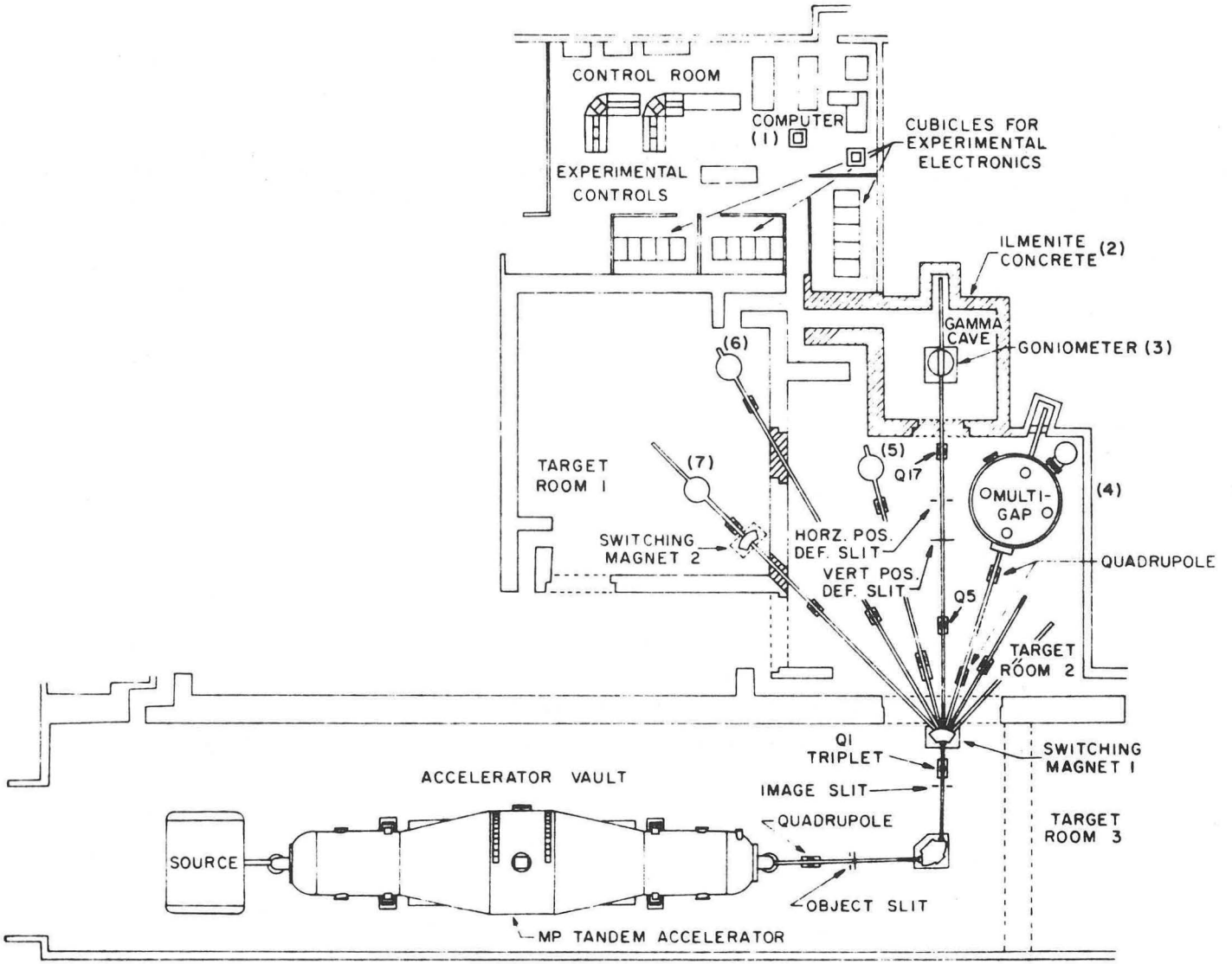

YALE WRIGHT NUCLEAR STRUCTURE LABORATORY FACILITY LAYOUT

XBL 722-129

Fig. 15

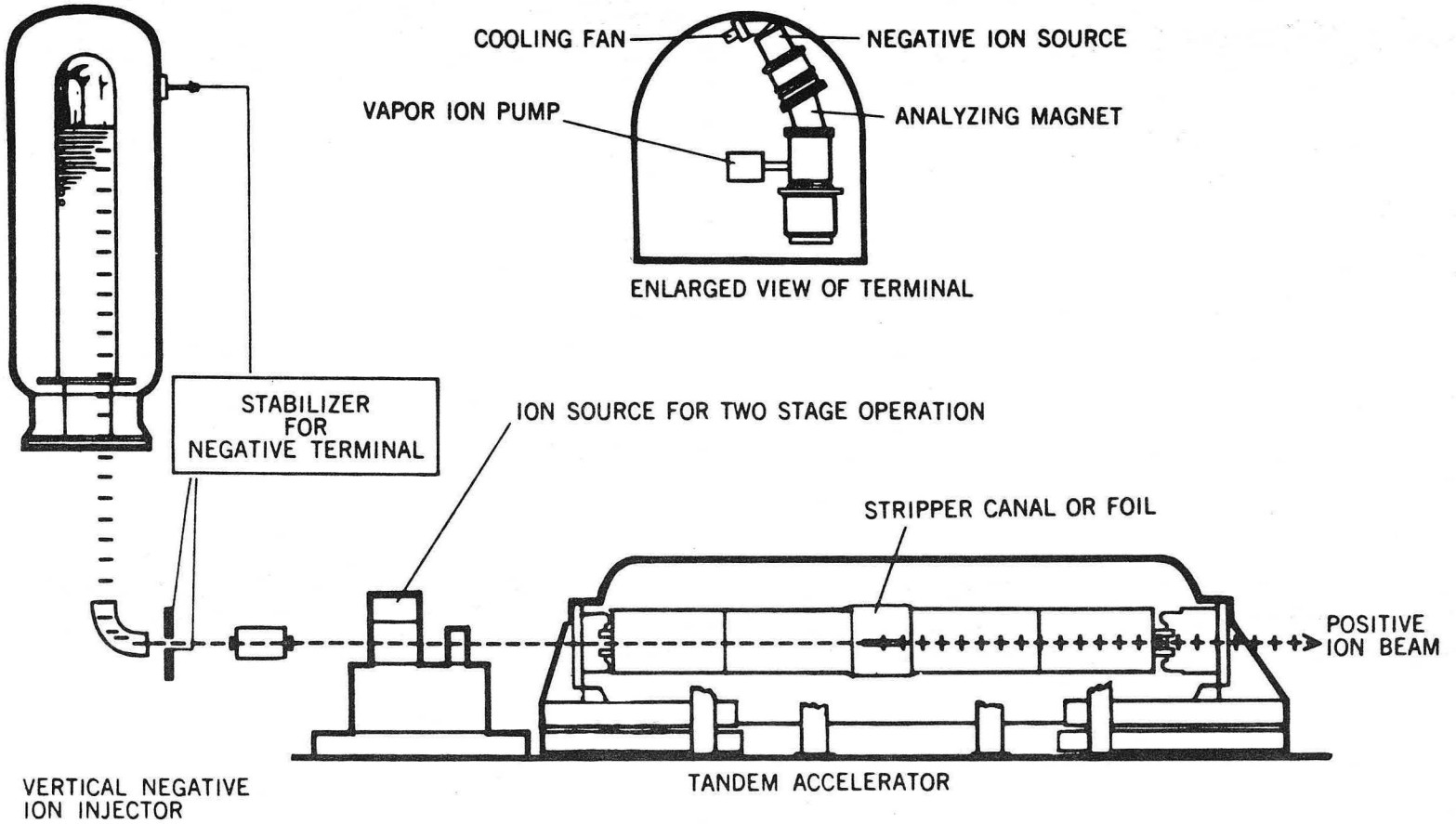
COOLING FAN
NEGATIVE ION SOURCE
VAPOR ION PUMP
ANALYZING MAGNET
ENLARGED VIEW OF TERMINAL
STABILIZER FOR NEGATIVE TERMINAL
ION SOURCE FOR TWO STAGE OPERATION
STRIPPER CANAL OR FOIL
POSITIVE ION BEAM
VERTICAL NEGATIVE ION INJECTOR
TANDEM ACCELERATOR
XBL 722-133

Fig. 16

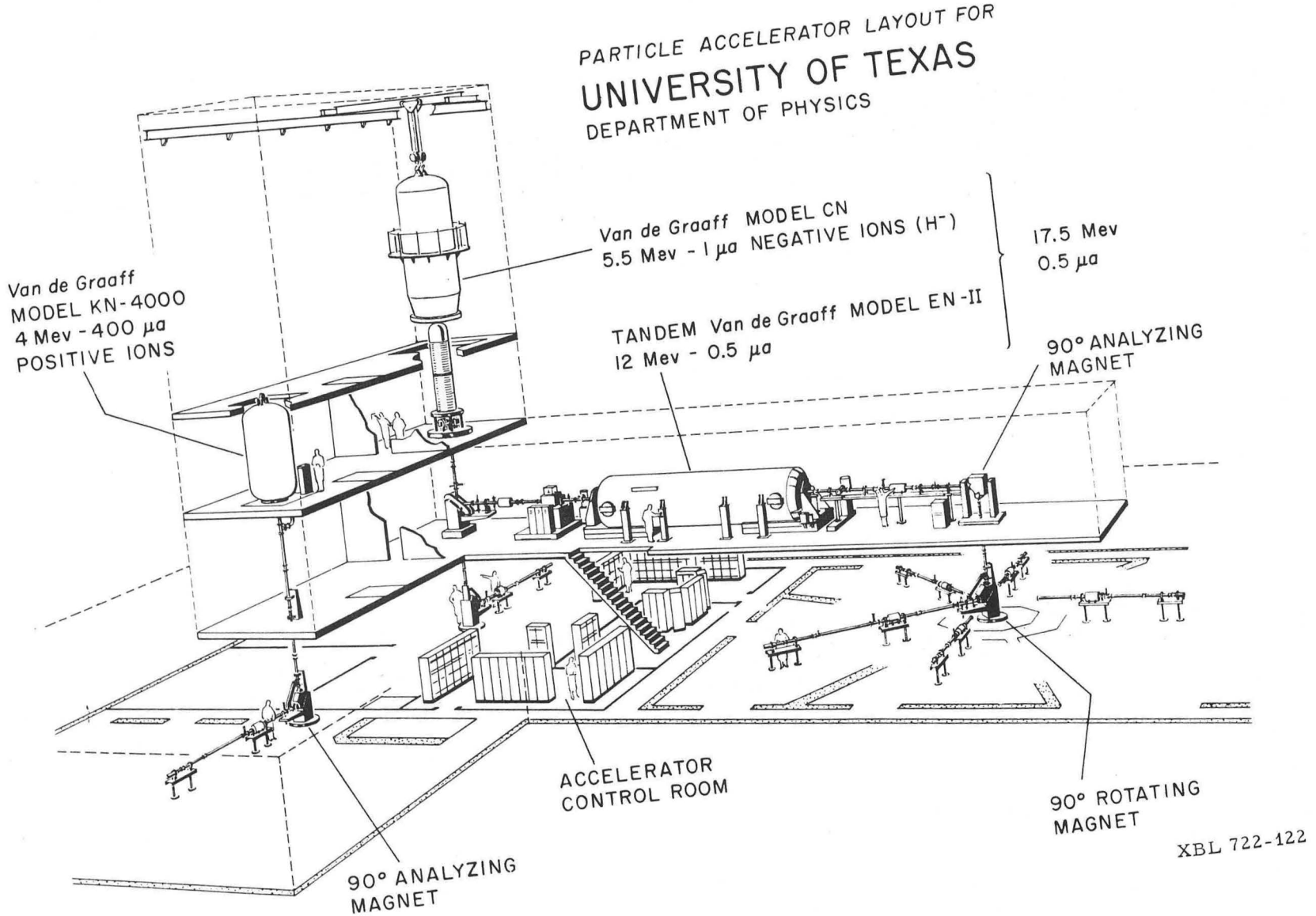
PARTICLE ACCELERATOR LAYOUT FOR
UNIVERSITY OF TEXAS
DEPARTMENT OF PHYSICS
Van de Graaff
MODEL KN-4000
4 Mev - 400 μa
POSITIVE IONS
Van de Graaff MODEL CN
5.5 Mev - 1 μa NEGATIVE IONS (H⁻)
TANDEM Van de Graaff MODEL EN-II
12 Mev - 0.5 μa
17.5 Mev
0.5 μa
90° ANALYZING
MAGNET
ACCELERATOR
CONTROL ROOM
90° ROTATING
MAGNET
90° ANALYZING
MAGNET
XBL 722-122

Fig. 17

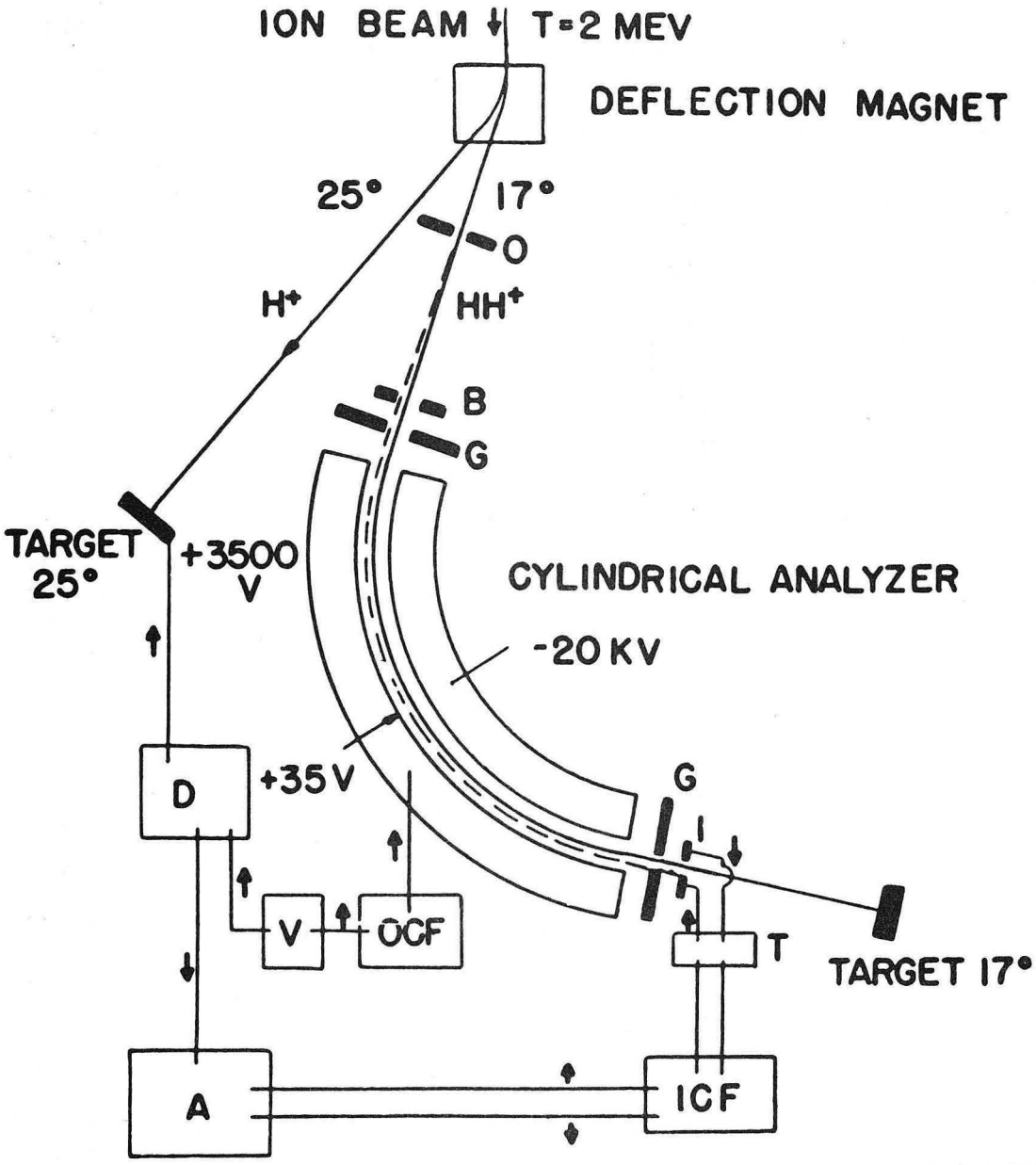

XBL 723-462

Fig. 18

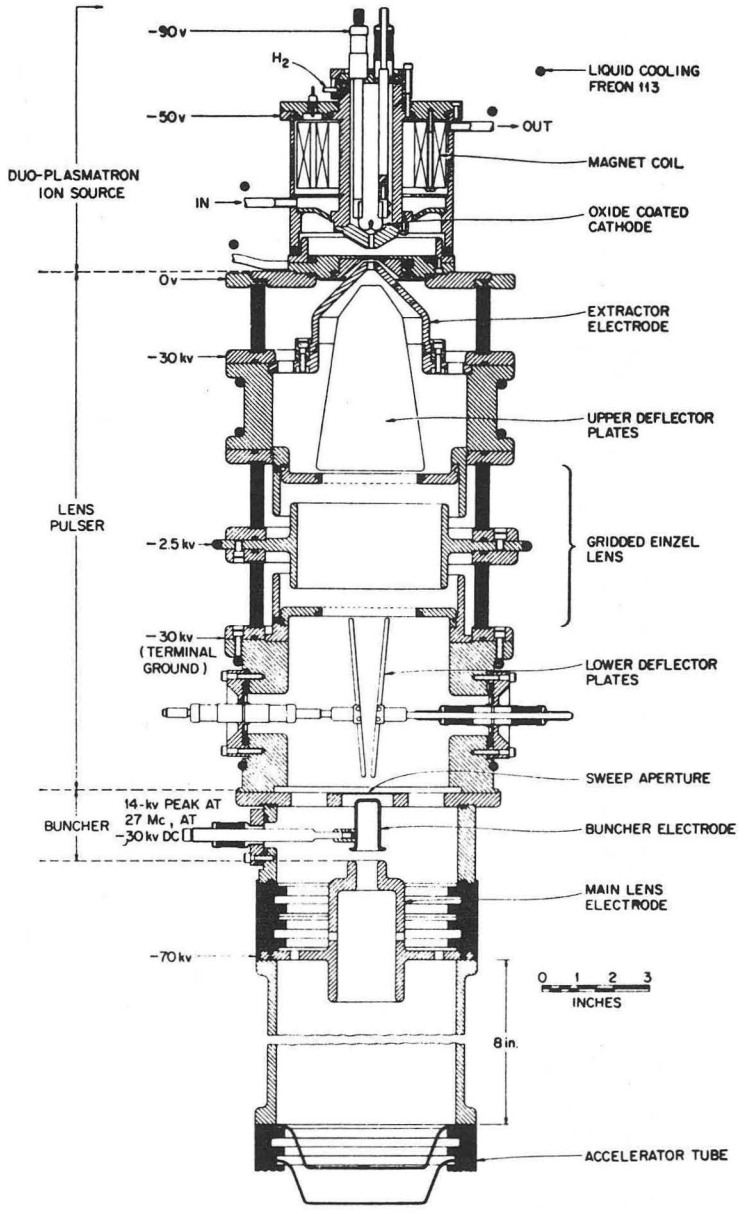

XBL 722-130

Fig. 19

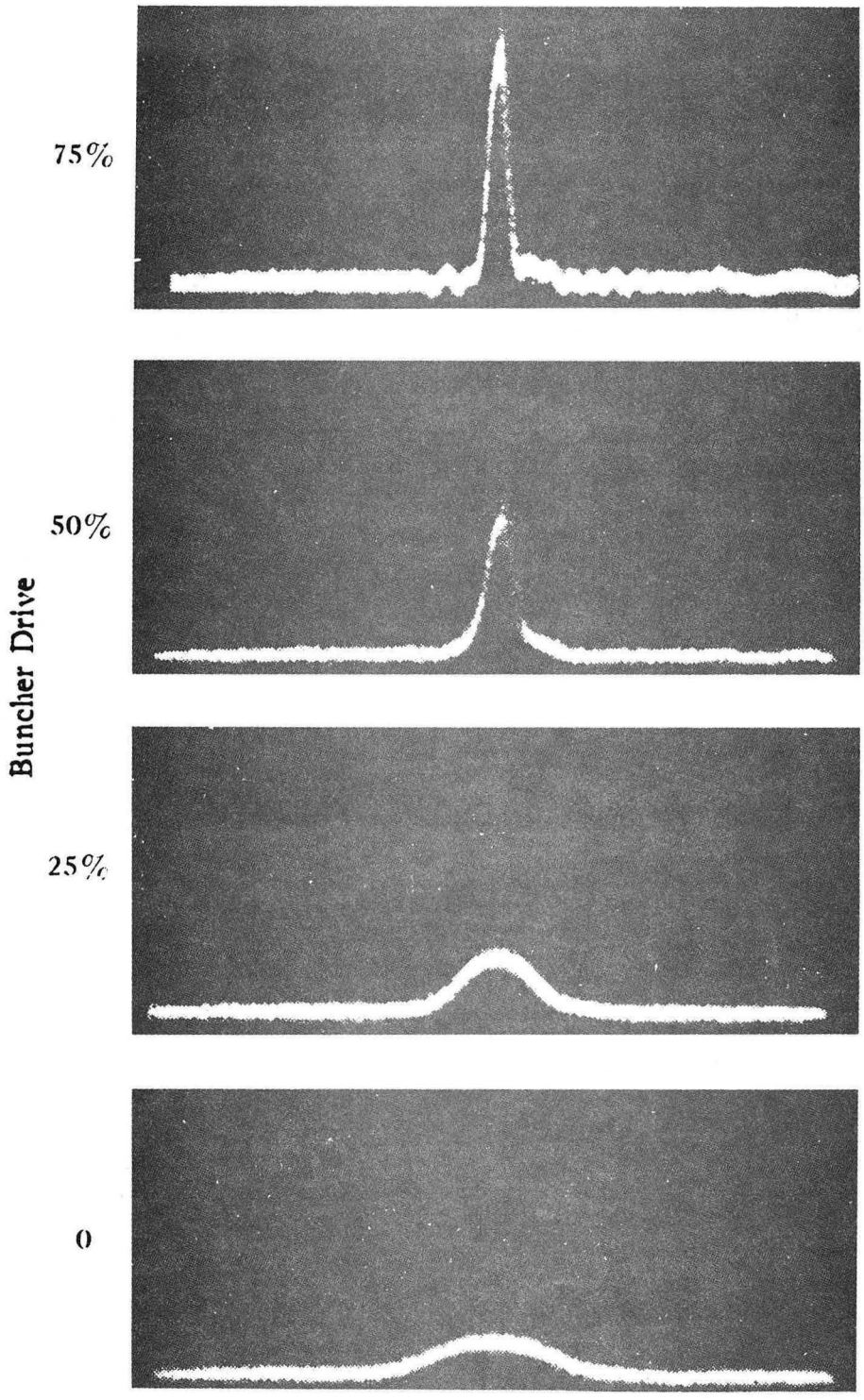

Sweep speed: 5nsec/cm

Fig. 20

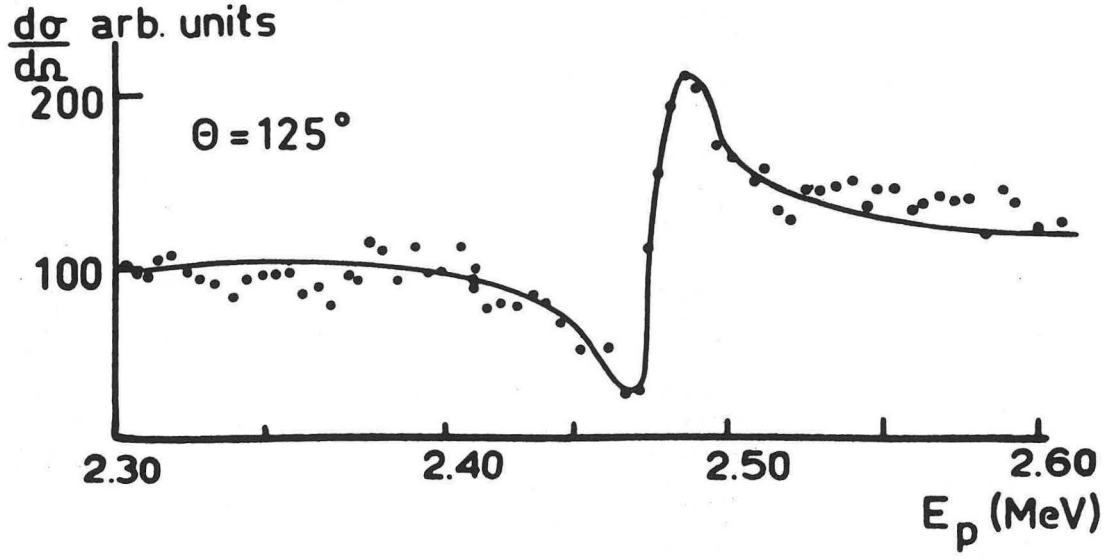

XBL 723-464

Fig. 21

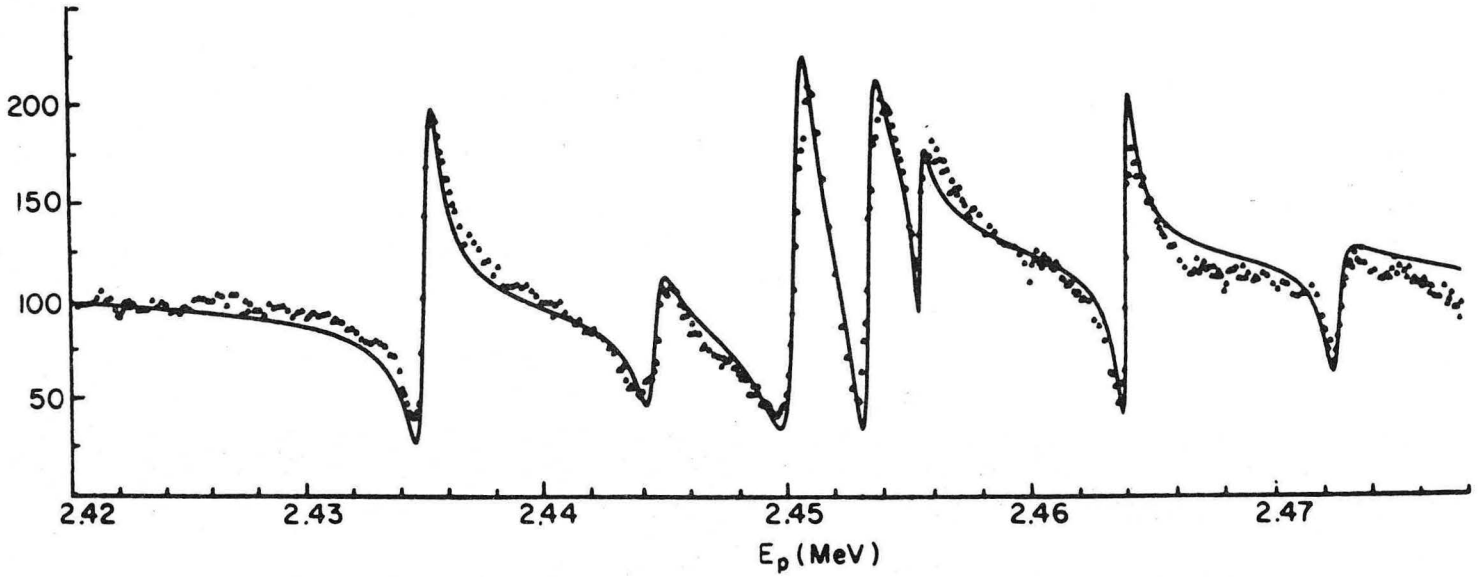

XBL 723-461

Fig. 22

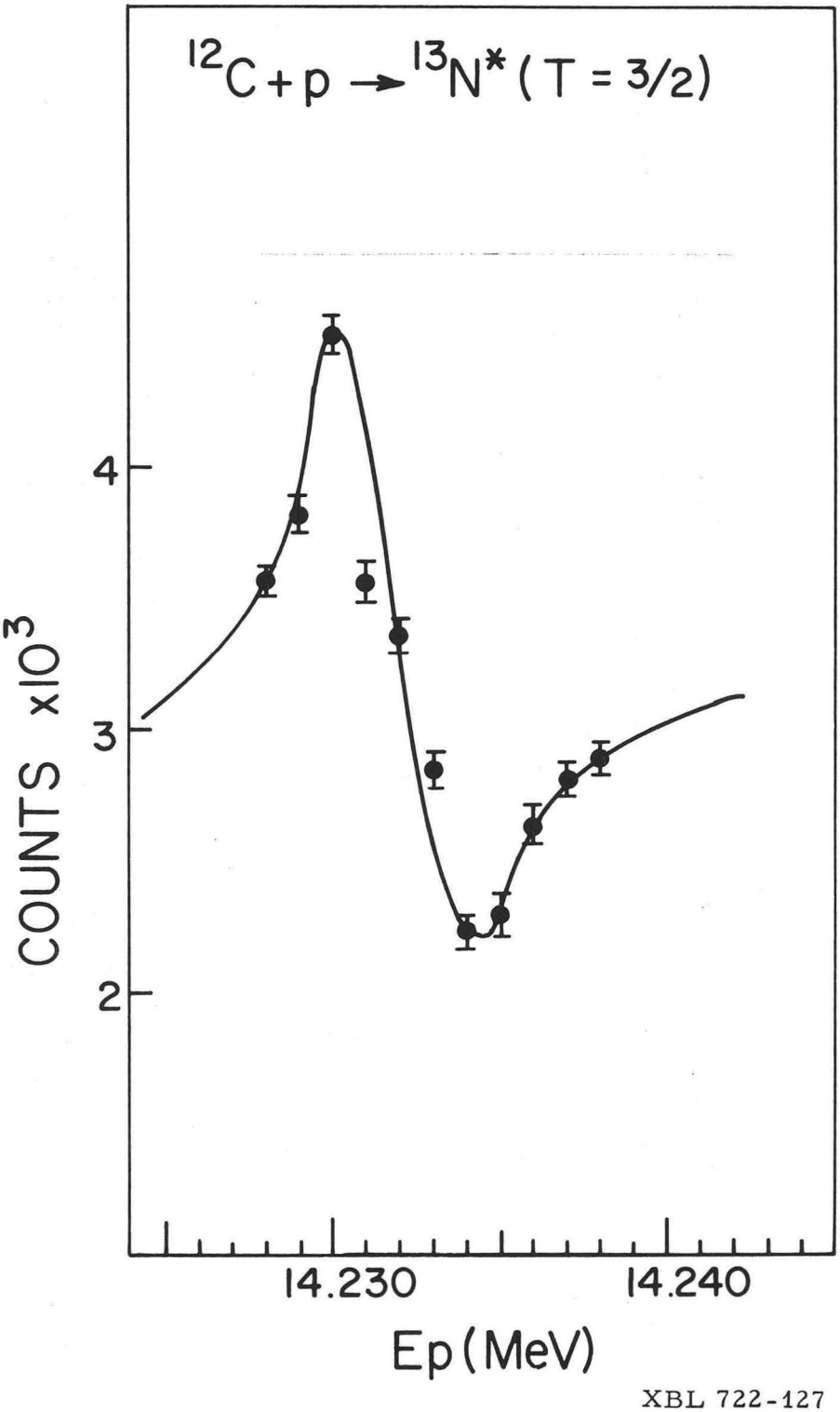
$^{12}C + p \rightarrow {}^{13}N^*\ (T = 3/2)$
COUNTS x10^3
4
3
2
14.230
14.240
Ep (MeV)
XBL 722-127

Fig. 23

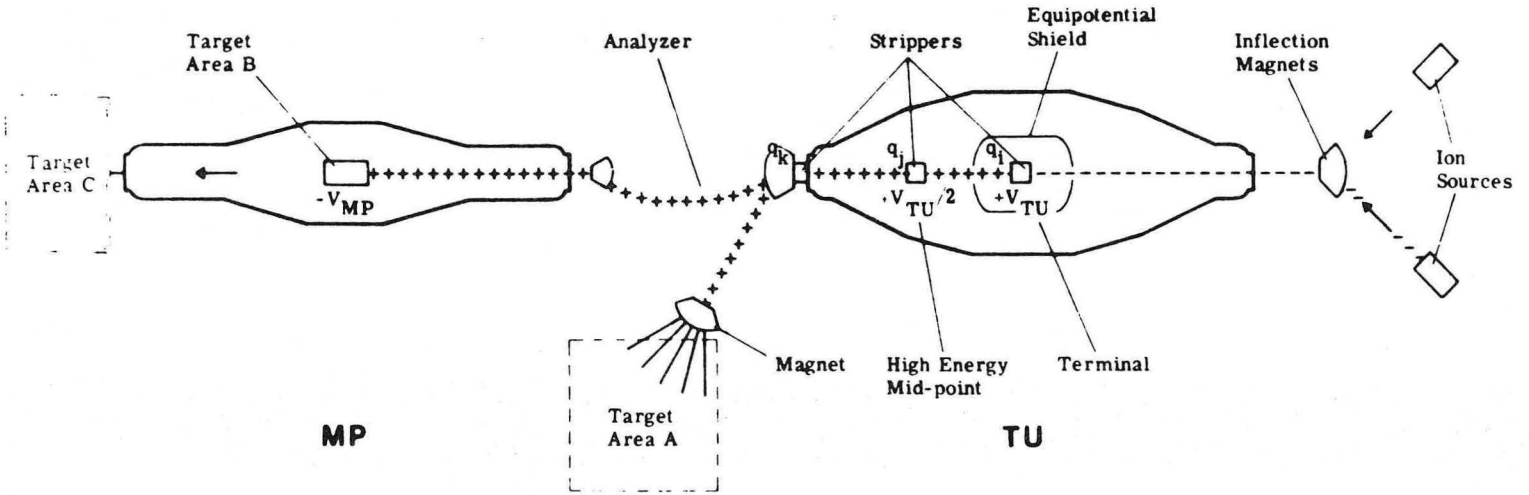

XBL 722-325

Fig. 24

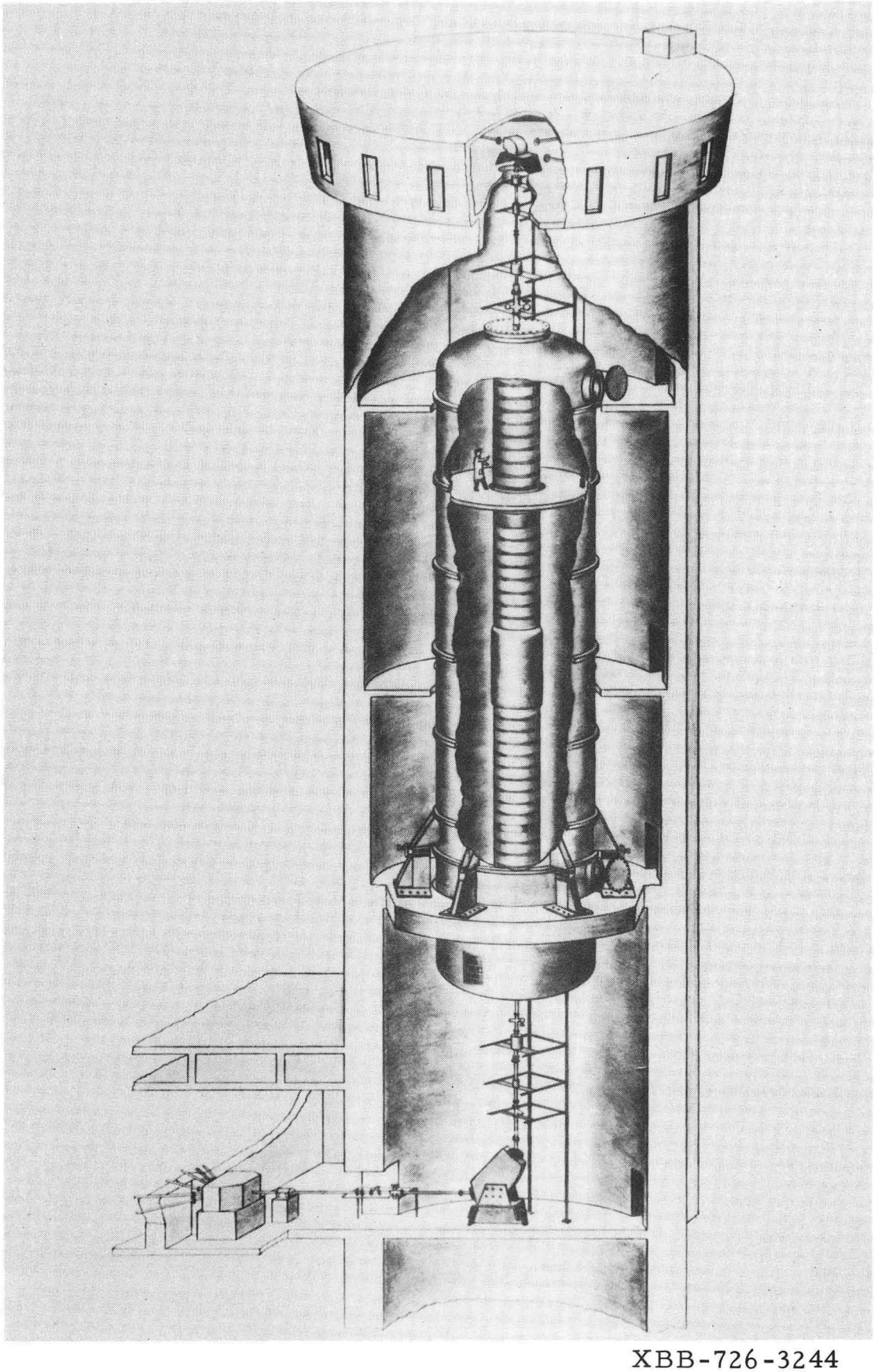

XBB-726-3244

Fig. 25

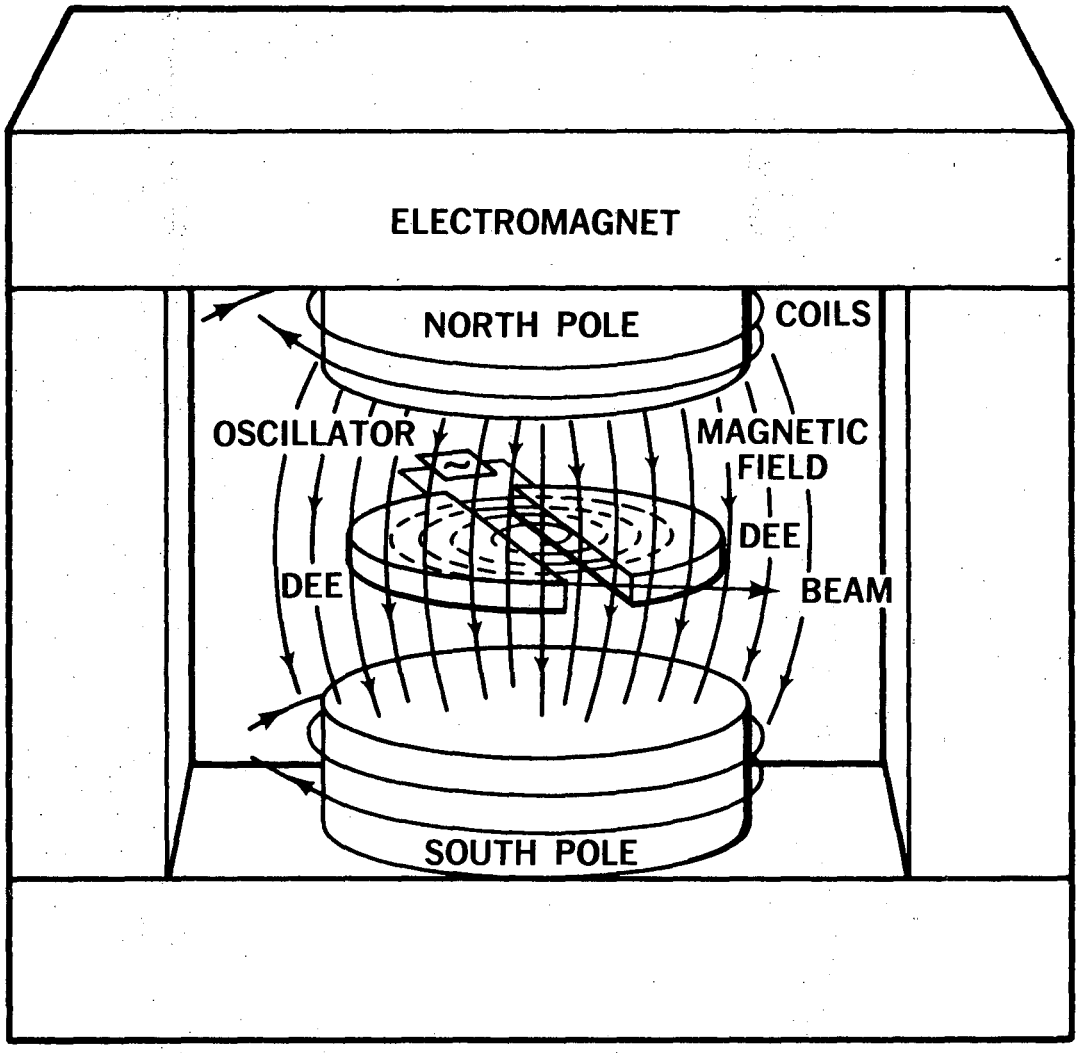

XBL 688-5797

Fig. 26

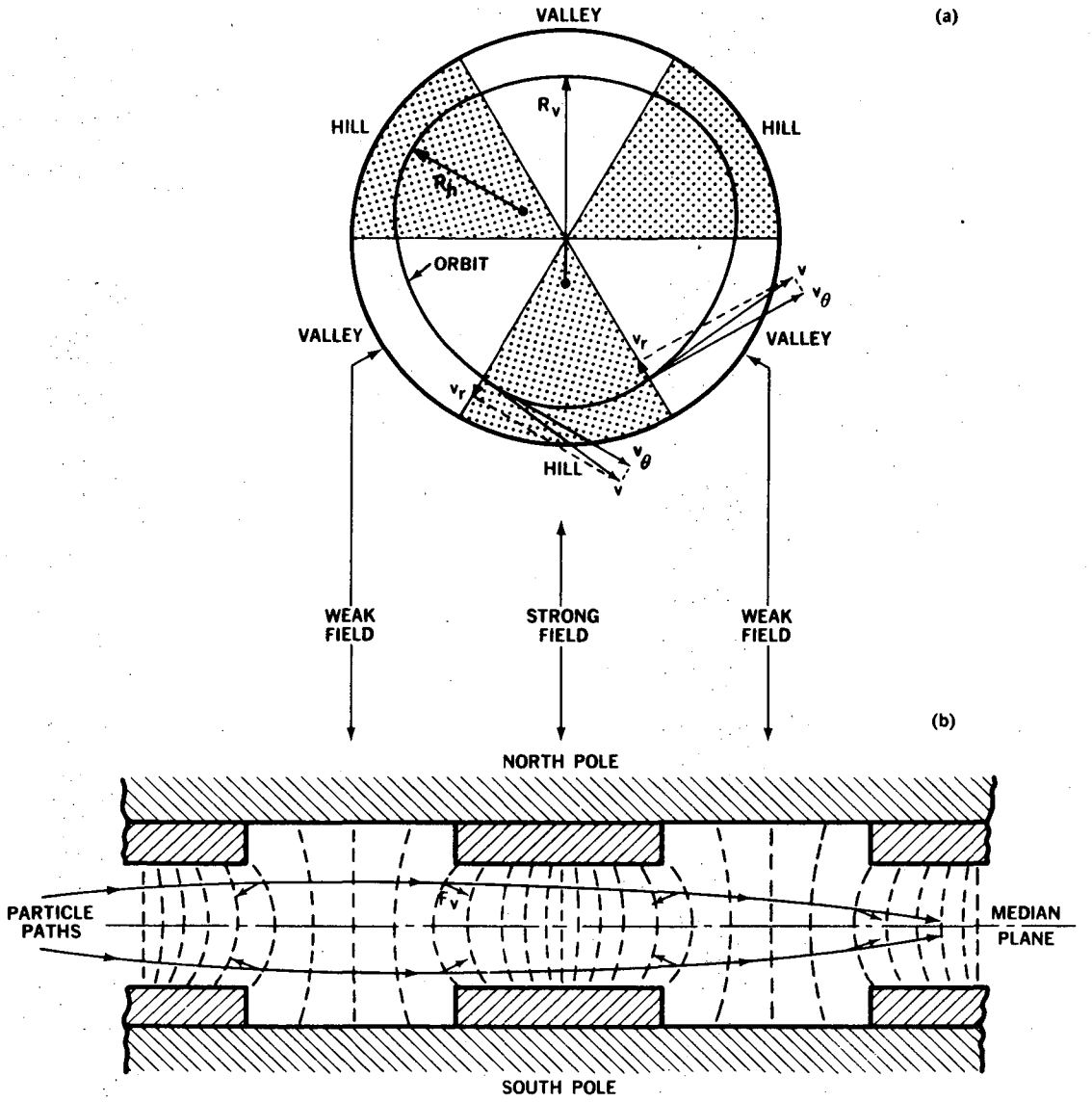

XBL 688-5802A

Fig. 27

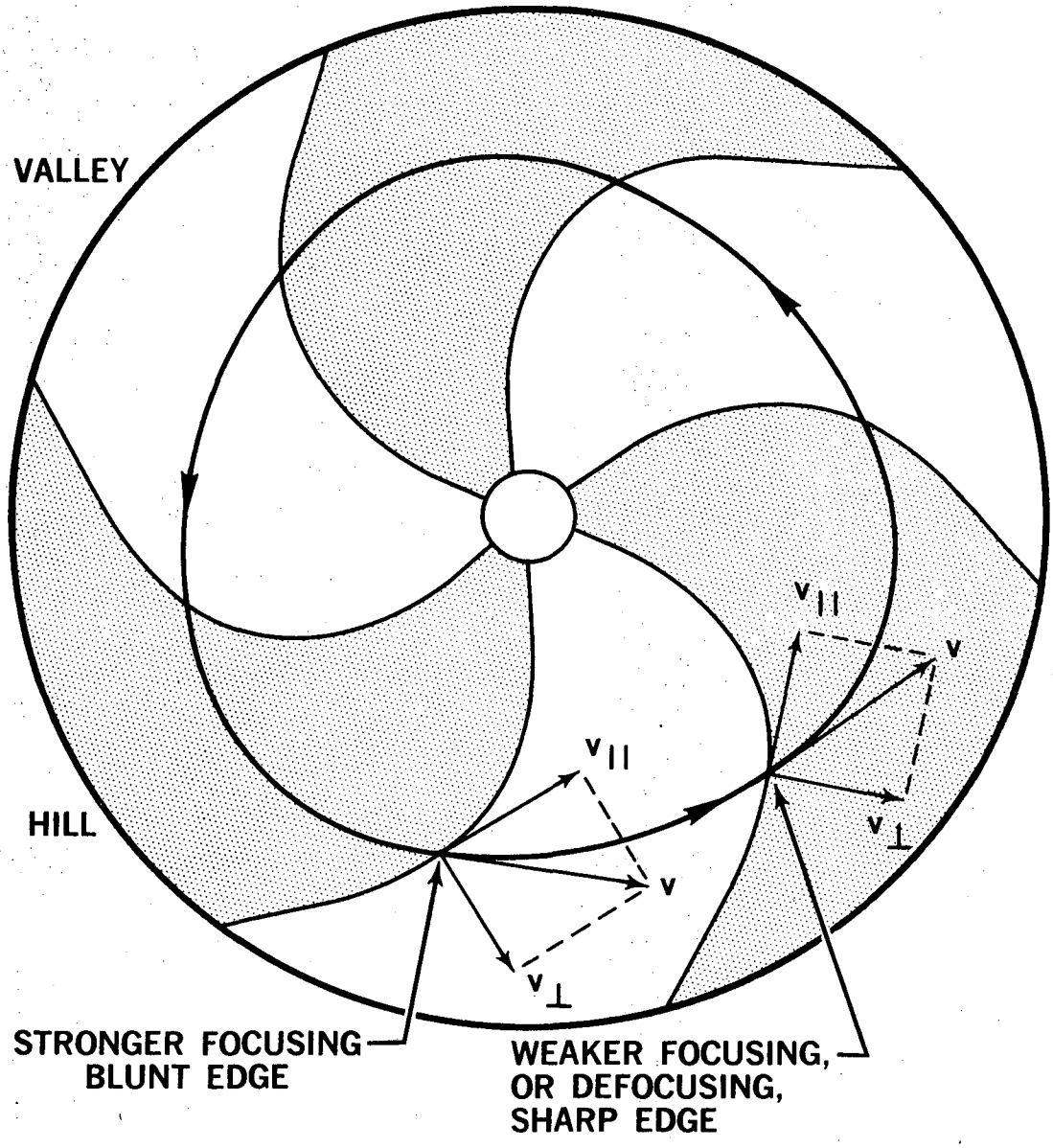

XBL 688-5804

Fig. 28

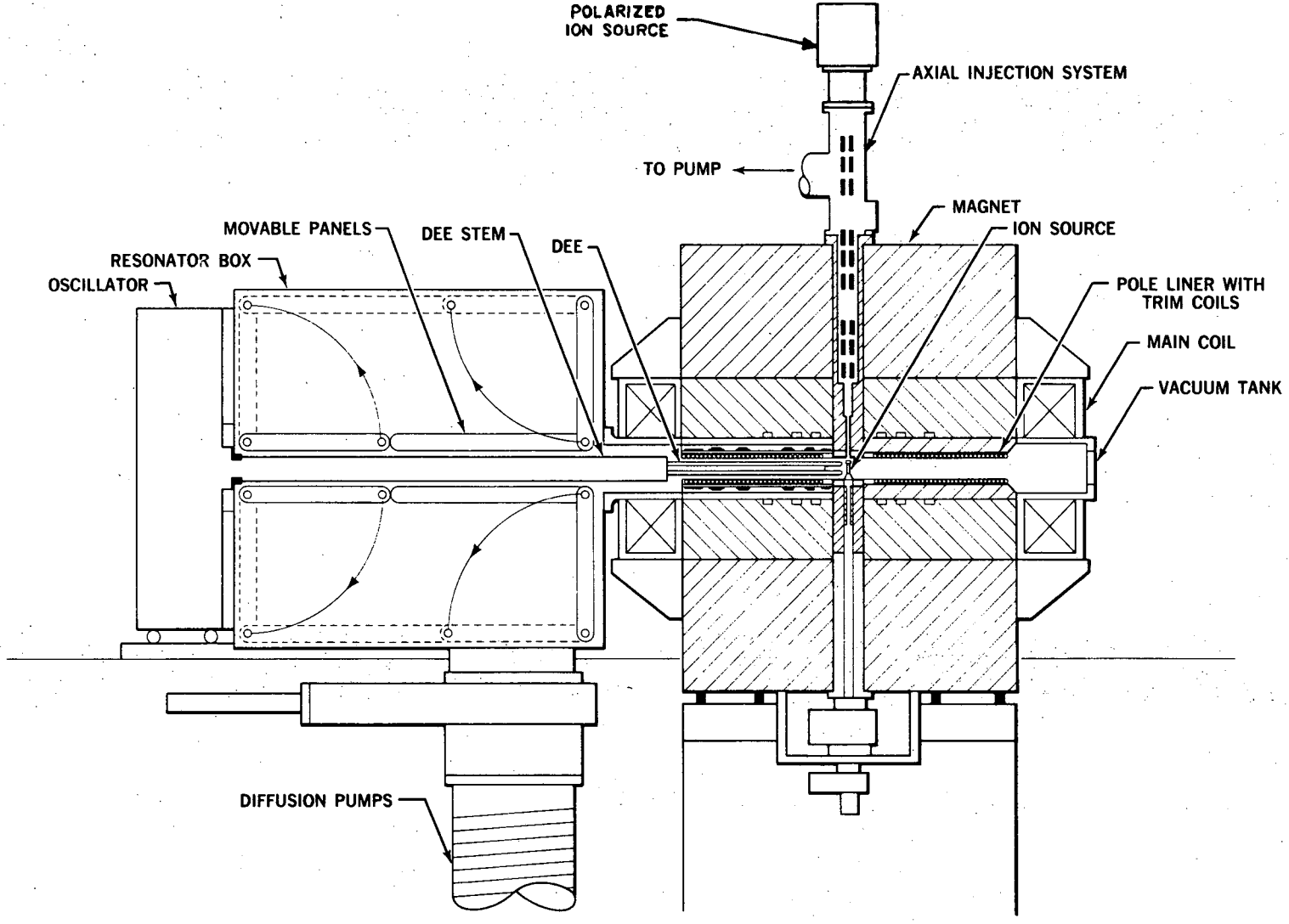
POLARIZED
ION SOURCE
AXIAL INJECTION SYSTEM
TO PUMP
MAGNET
ION SOURCE
MOVABLE PANELS
DEE STEM
DEE
RESONATOR BOX
OSCILLATOR
POLE LINER WITH
TRIM COILS
MAIN COIL
VACUUM TANK
DIFFUSION PUMPS
XBL 678-4698

Fig. 29

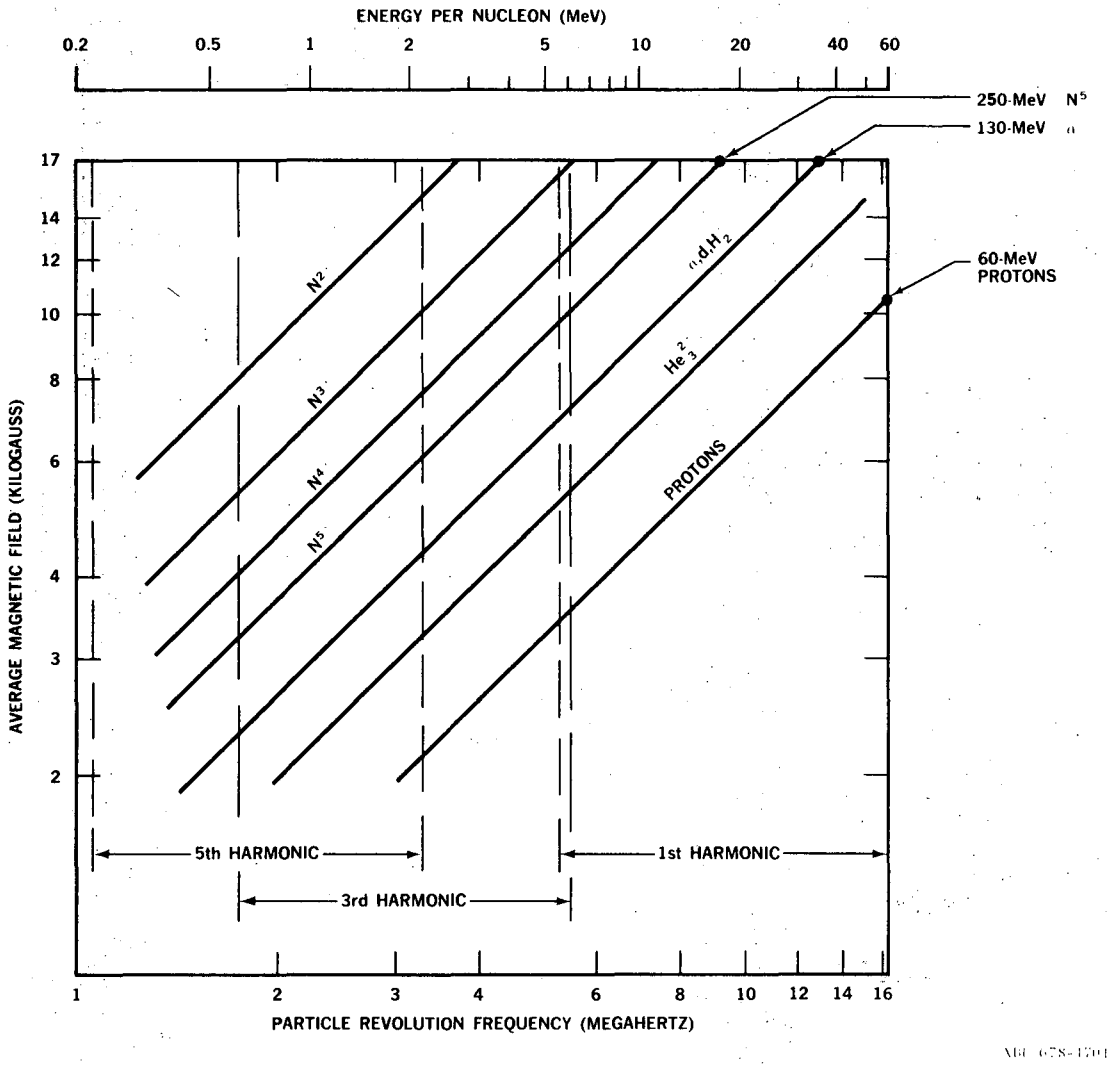
ENERGY PER NUCLEON (MeV)
0.2
0.5
1
2
5
10
20
40
60
250-MeV N5
130-MeV α
60-MeV PROTONS
N2
N3
N4
N5
α,d,H2
He3
PROTONS
5th HARMONIC
3rd HARMONIC
1st HARMONIC
AVERAGE MAGNETIC FIELD (KILOGAUSS)
17
14
12
10
8
6
4
3
2
1
2
3
4
6
8
10
12
14
16
PARTICLE REVOLUTION FREQUENCY (MEGAHERTZ)

Fig. 30

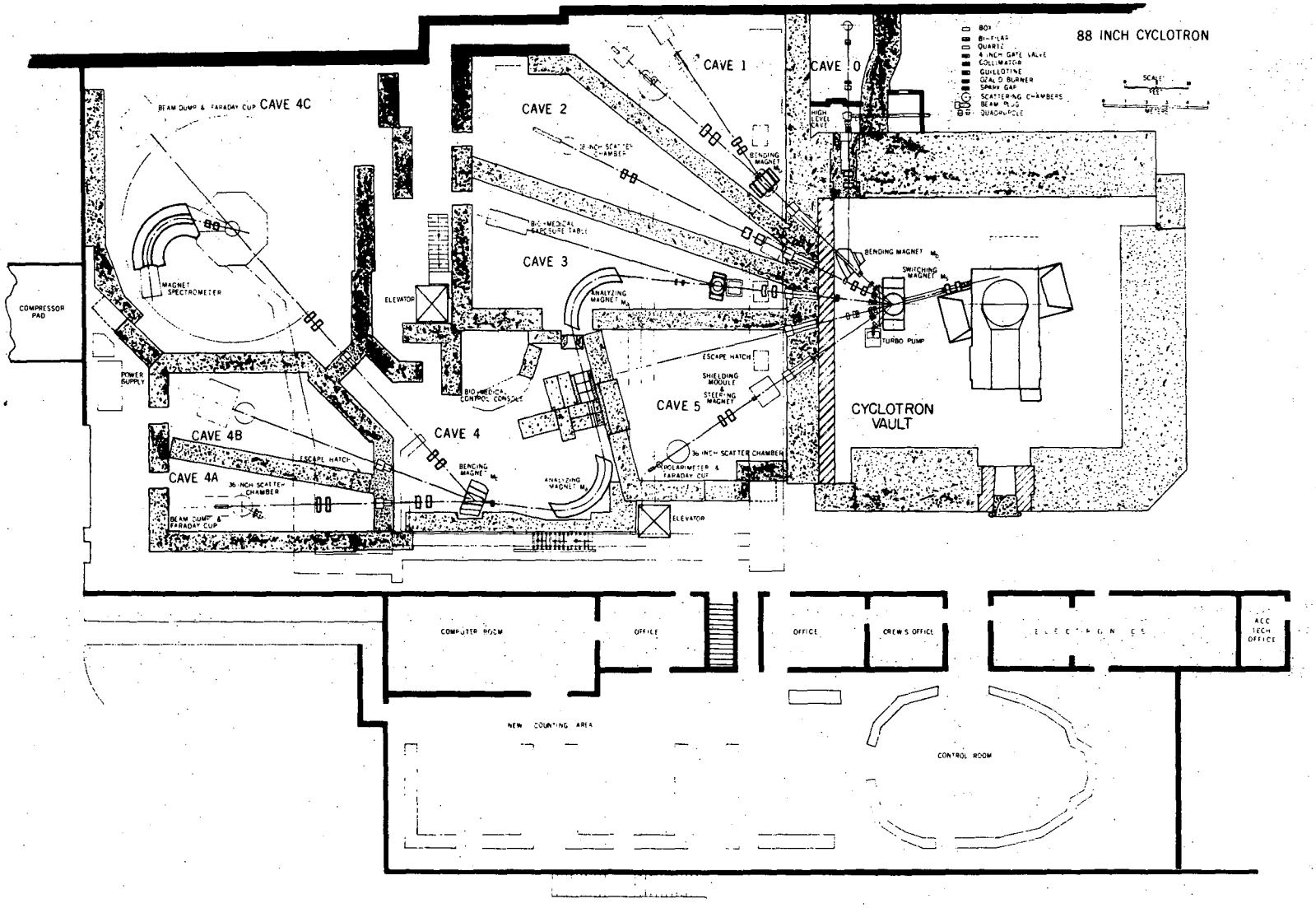

XBL 722-331

Fig. 31

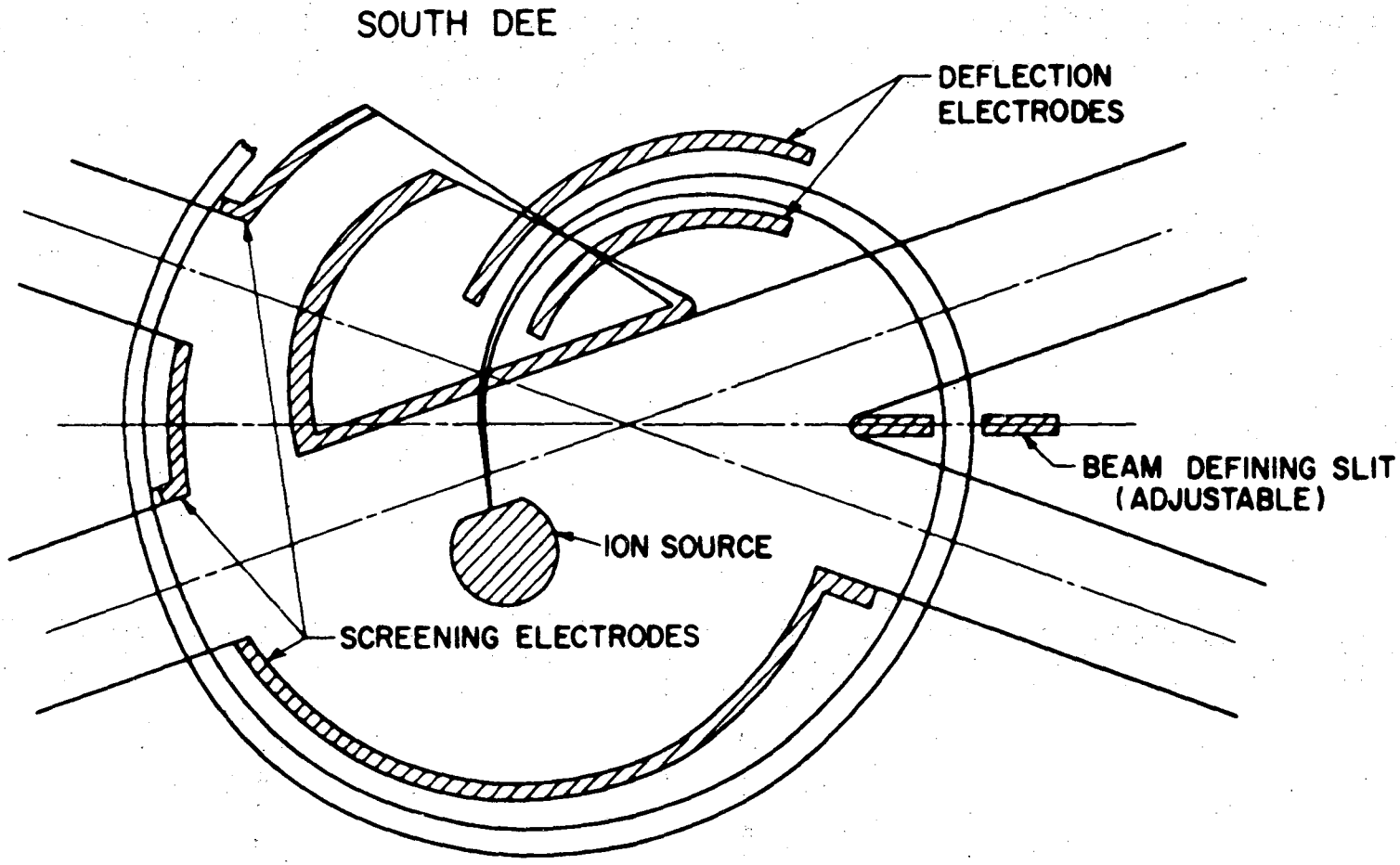

XBL 722-329

Fig. 32

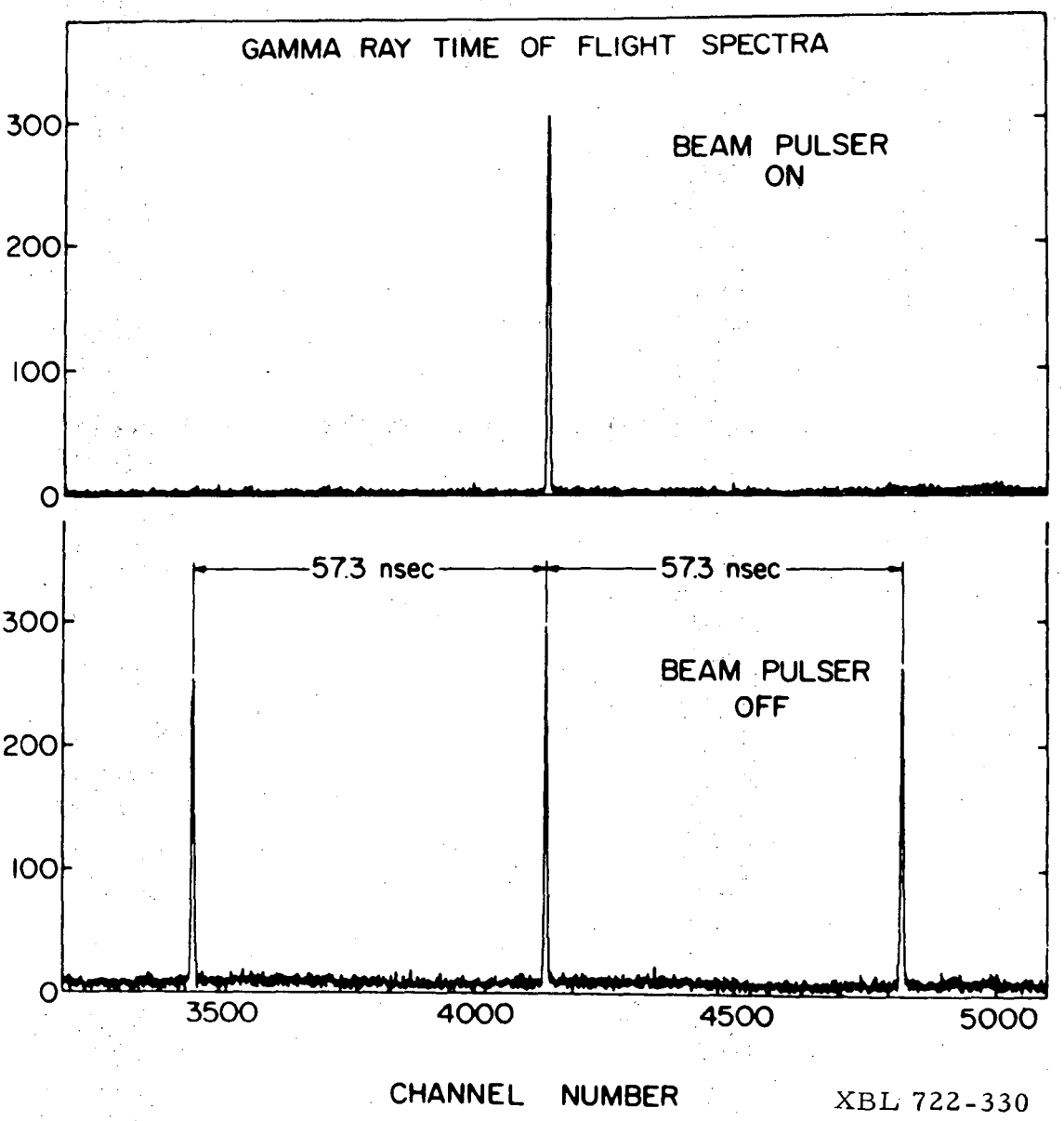
GAMMA RAY TIME OF FLIGHT SPECTRA
300
200
100
0
BEAM PULSER
ON
57.3 nsec
57.3 nsec
300
200
100
0
BEAM PULSER
OFF
3500
4000
4500
5000
CHANNEL NUMBER
XBL 722-330

Fig. 33

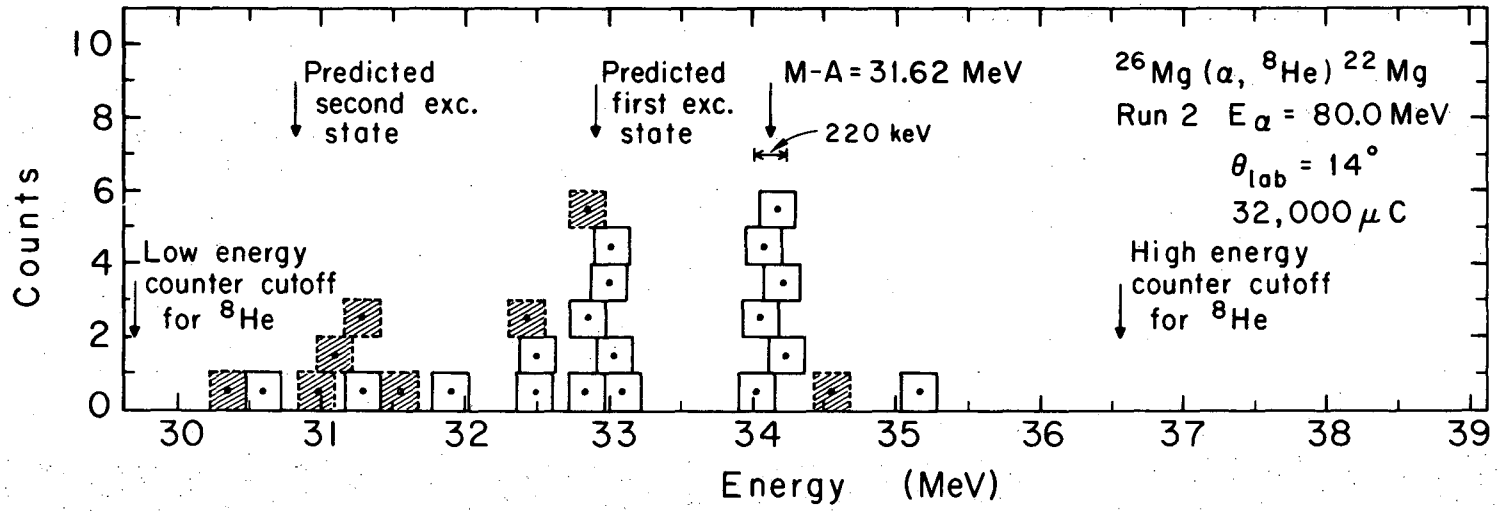

MUB 9484A

Fig. 34

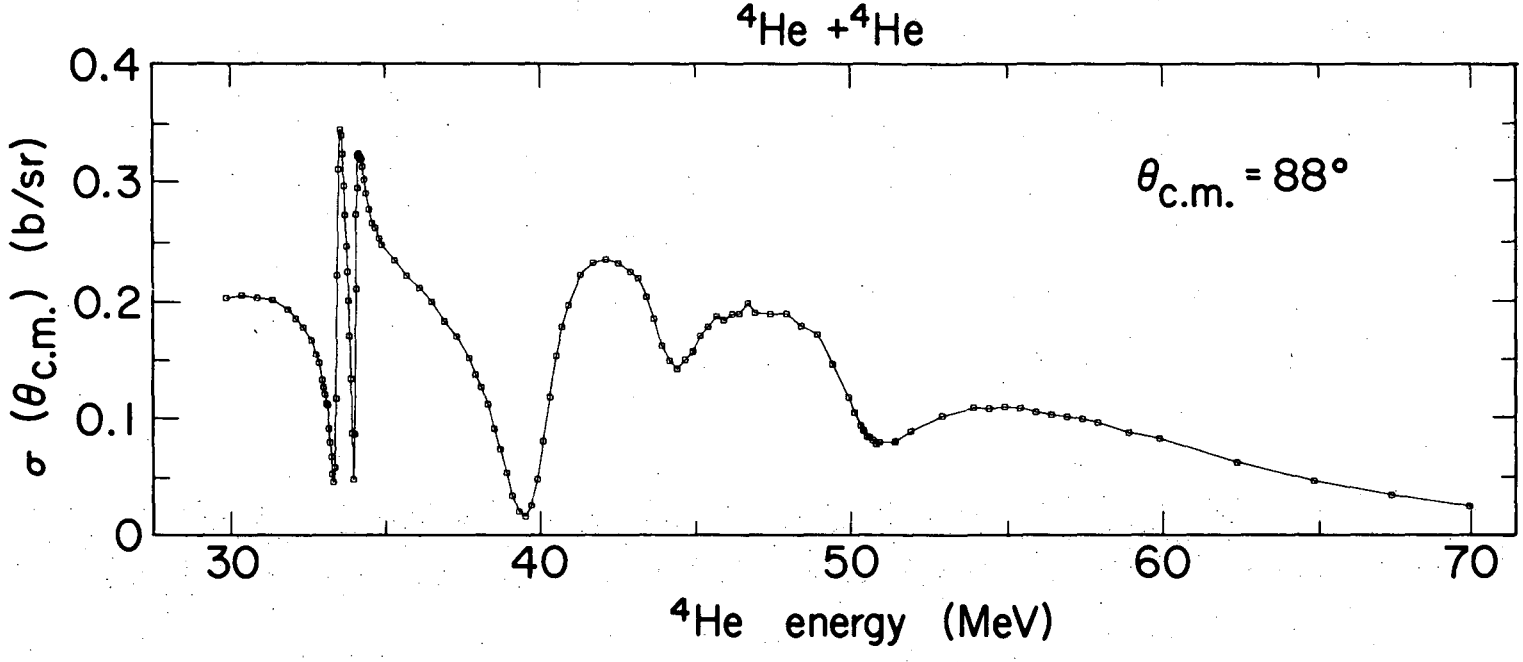
$^4He + ^4He$
$\theta_{c.m.} = 88°$
$\sigma\ (\theta_{c.m.})$ (b/sr)
0.4
0.3
0.2
0.1
0
30
40
50
60
70
^4He energy (MeV)
XBL694-2492A

Fig. 35

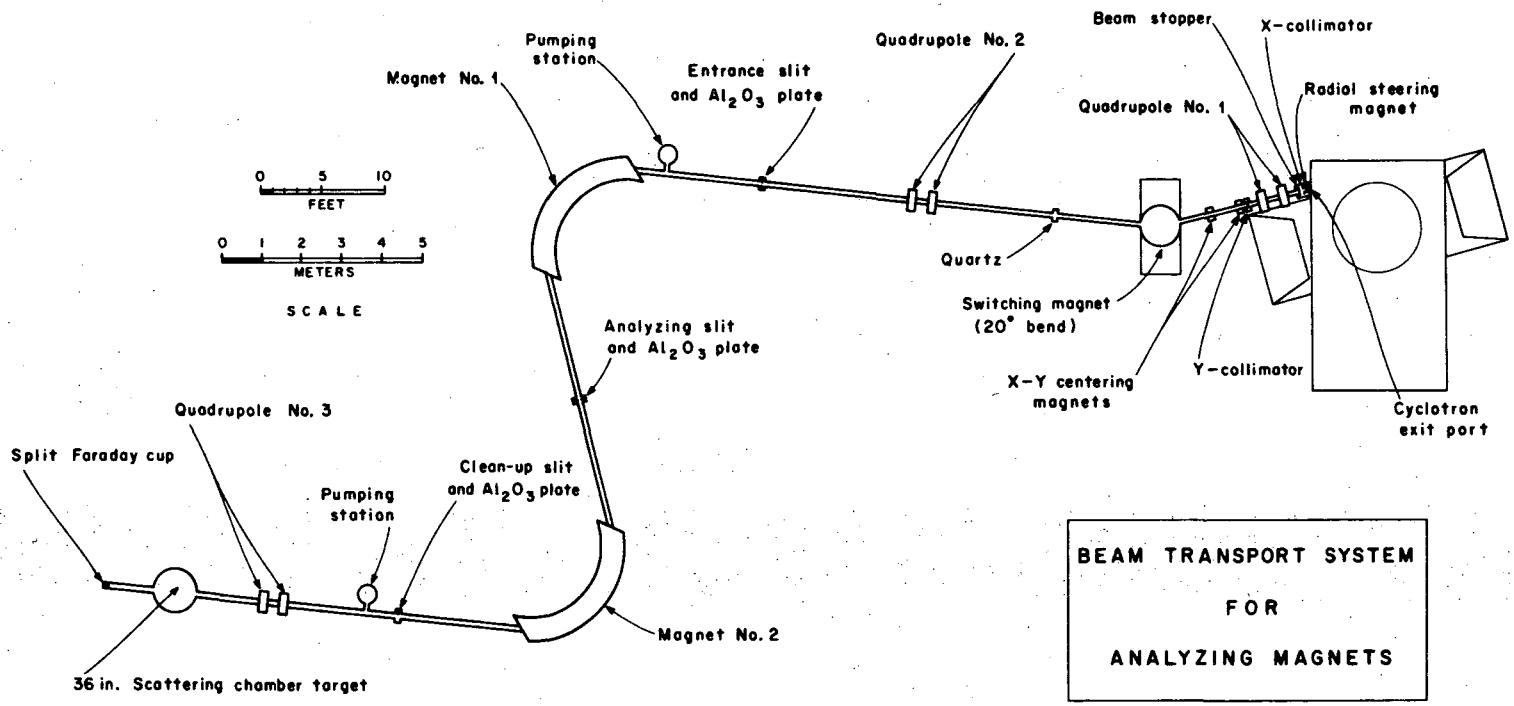
Pumping station
Magnet No. 1
Entrance slit and Al_2O_3 plate
Quadrupole No. 2
Beam stopper
X-collimator
Radial steering magnet
Quadrupole No. 1
0 5 10
FEET
0 1 2 3 4 5
METERS
SCALE
Quartz
Switching magnet (20° bend)
Analyzing slit and Al_2O_3 plate
X-Y centering magnets
Y-collimator
Cyclotron exit port
Quadrupole No. 3
Split Faraday cup
Pumping station
Clean-up slit and Al_2O_3 plate
Magnet No. 2
36 in. Scattering chamber target
BEAM TRANSPORT SYSTEM
FOR
ANALYZING MAGNETS
XBL687-3258

Fig. 36

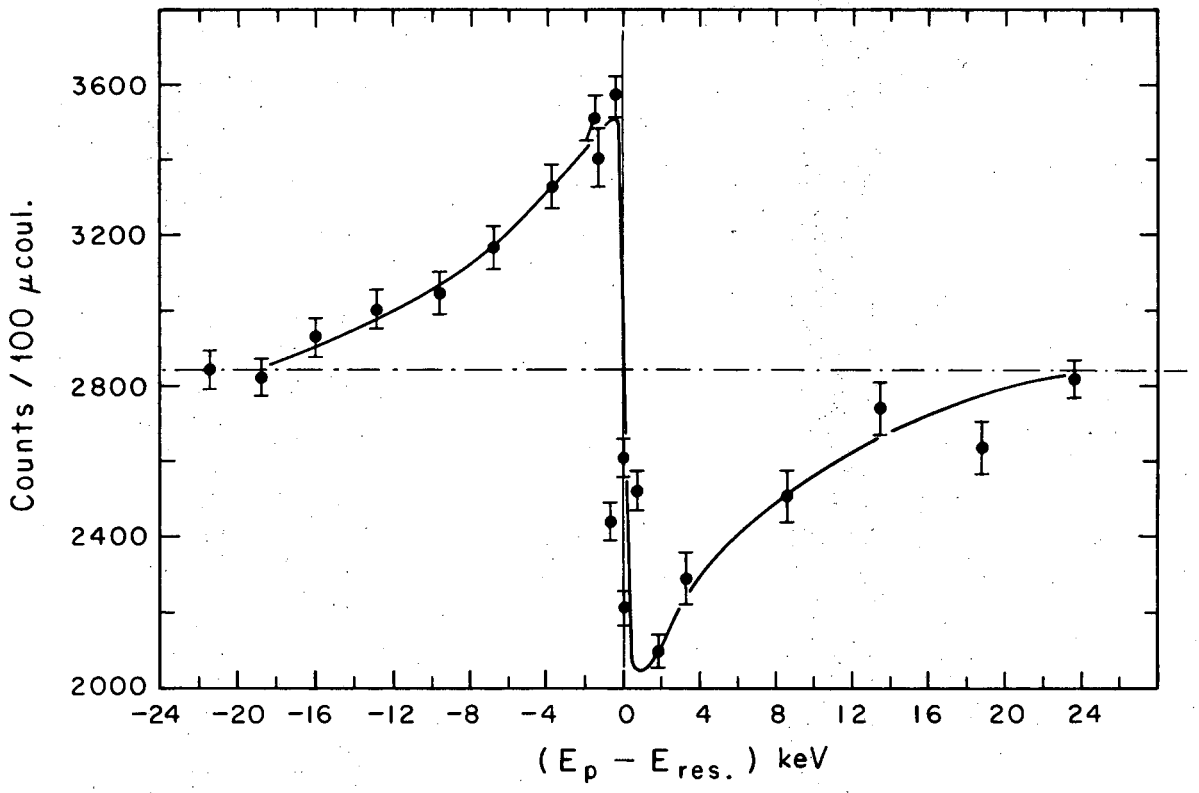
3600
3200
2800
2400
2000
Counts / 100 μcoul.
-24
-20
-16
-12
-8
-4
0
4
8
12
16
20
24
(Ep − Eres.) keV
XBL687-3260

Fig. 37

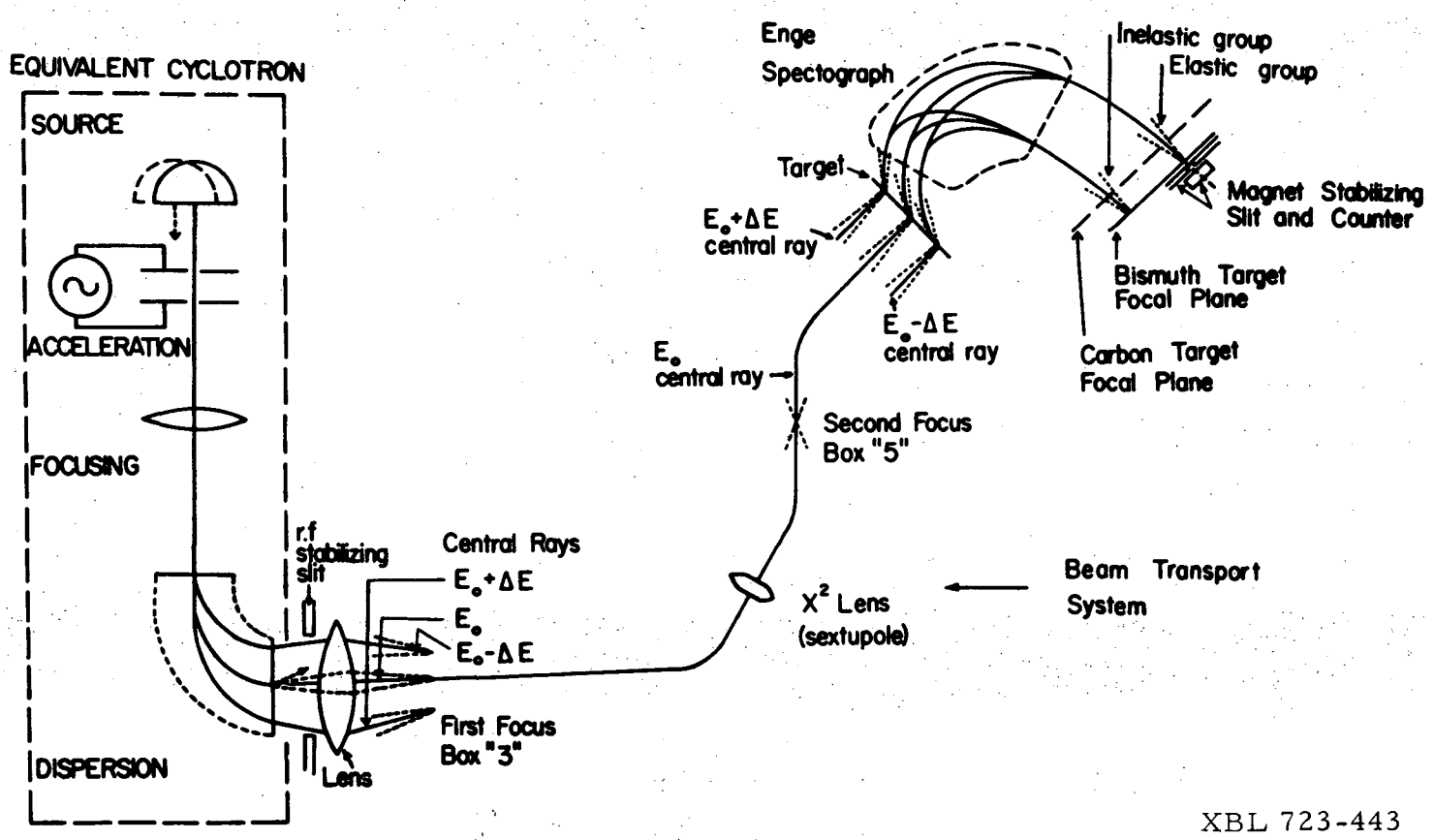
EQUIVALENT CYCLOTRON
SOURCE
ACCELERATION
FOCUSING
DISPERSION
r.f stabilizing slit
Central Rays
$E_o+\Delta E$
E_o
$E_o-\Delta E$
First Focus Box "3"
Lens
X^2 Lens (sextupole)
Second Focus Box "5"
Beam Transport System
Enge Spectograph
Target
$E_o+\Delta E$ central ray
E_o central ray
$E_o-\Delta E$ central ray
Inelastic group
Elastic group
Magnet Stabilizing Slit and Counter
Bismuth Target Focal Plane
Carbon Target Focal Plane
XBL 723-443

Fig. 38

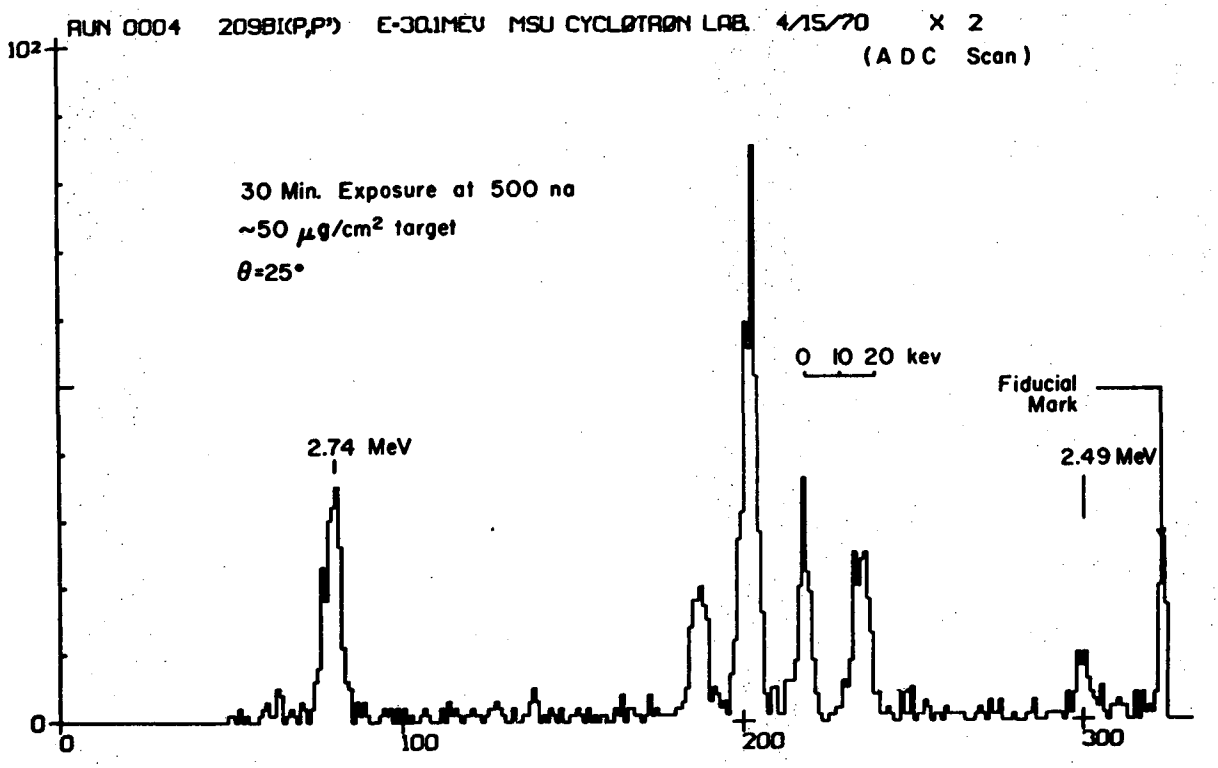

XBL 723-445

Fig. 39

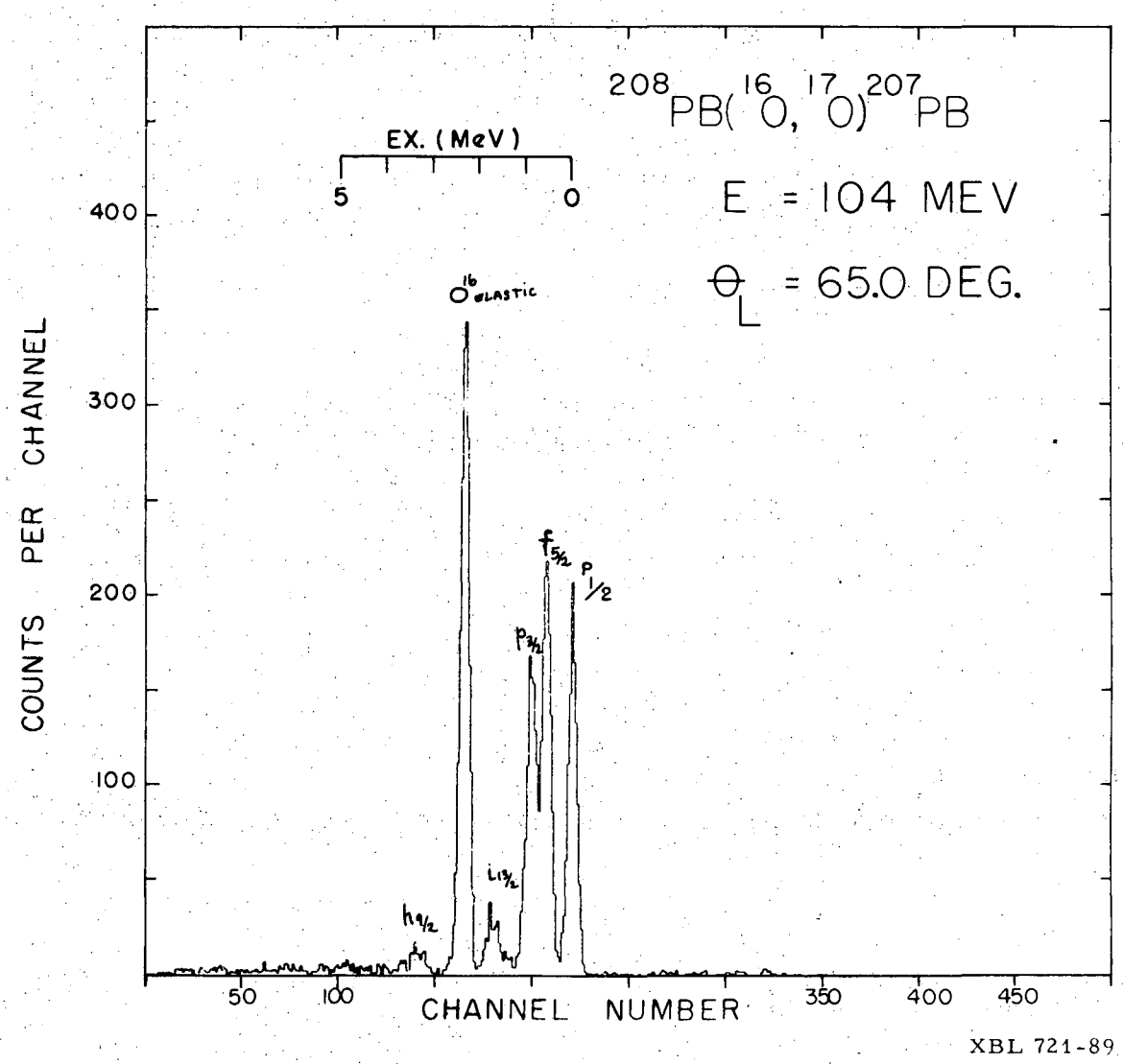
208PB(16O, 17O)207PB
E = 104 MEV
θL = 65.0 DEG.
EX. (MeV)
5
0
O16 ELASTIC
f5/2
p1/2
p3/2
i13/2
h9/2
COUNTS PER CHANNEL
400
300
200
100
50
100
350
400
450
CHANNEL NUMBER
XBL 721-89

Fig. 40

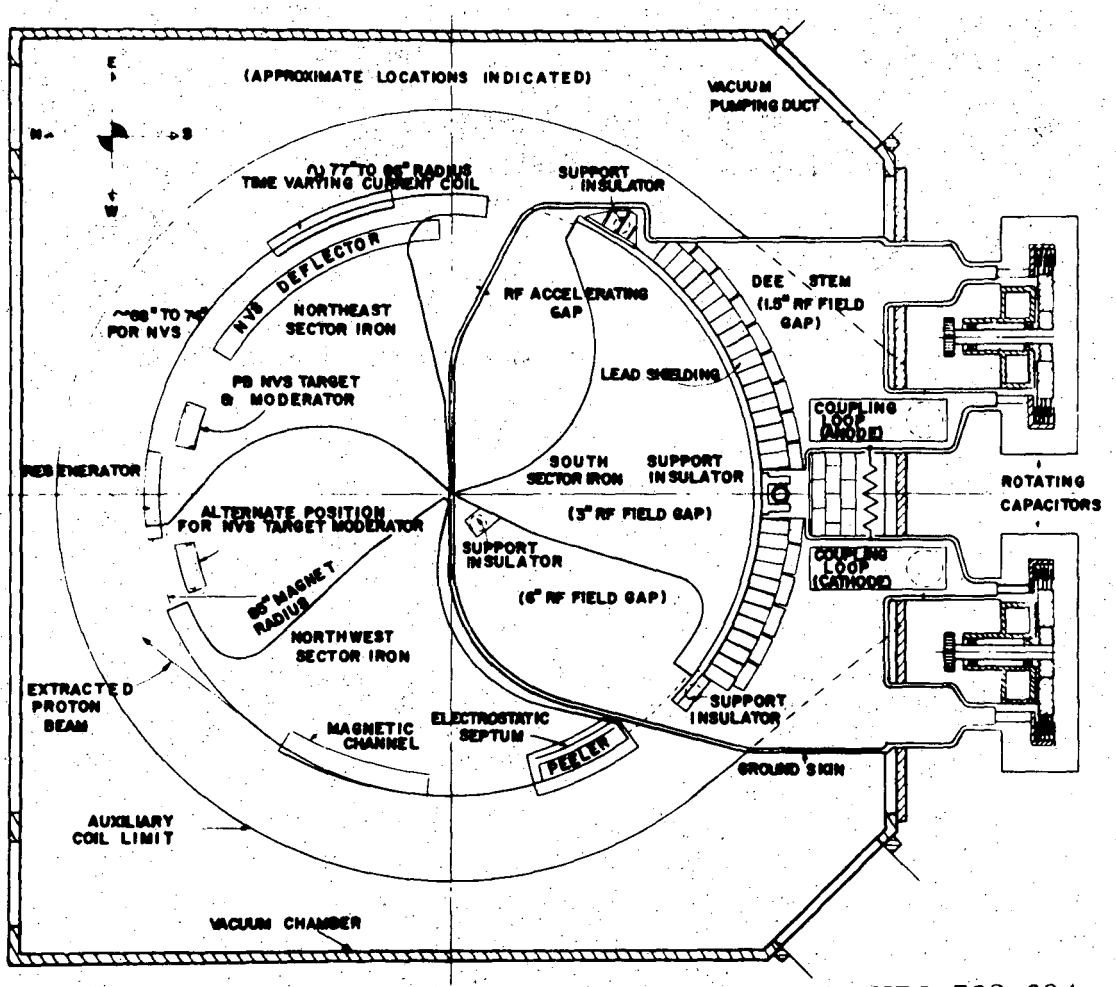

XBL 722-324

Fig. 41

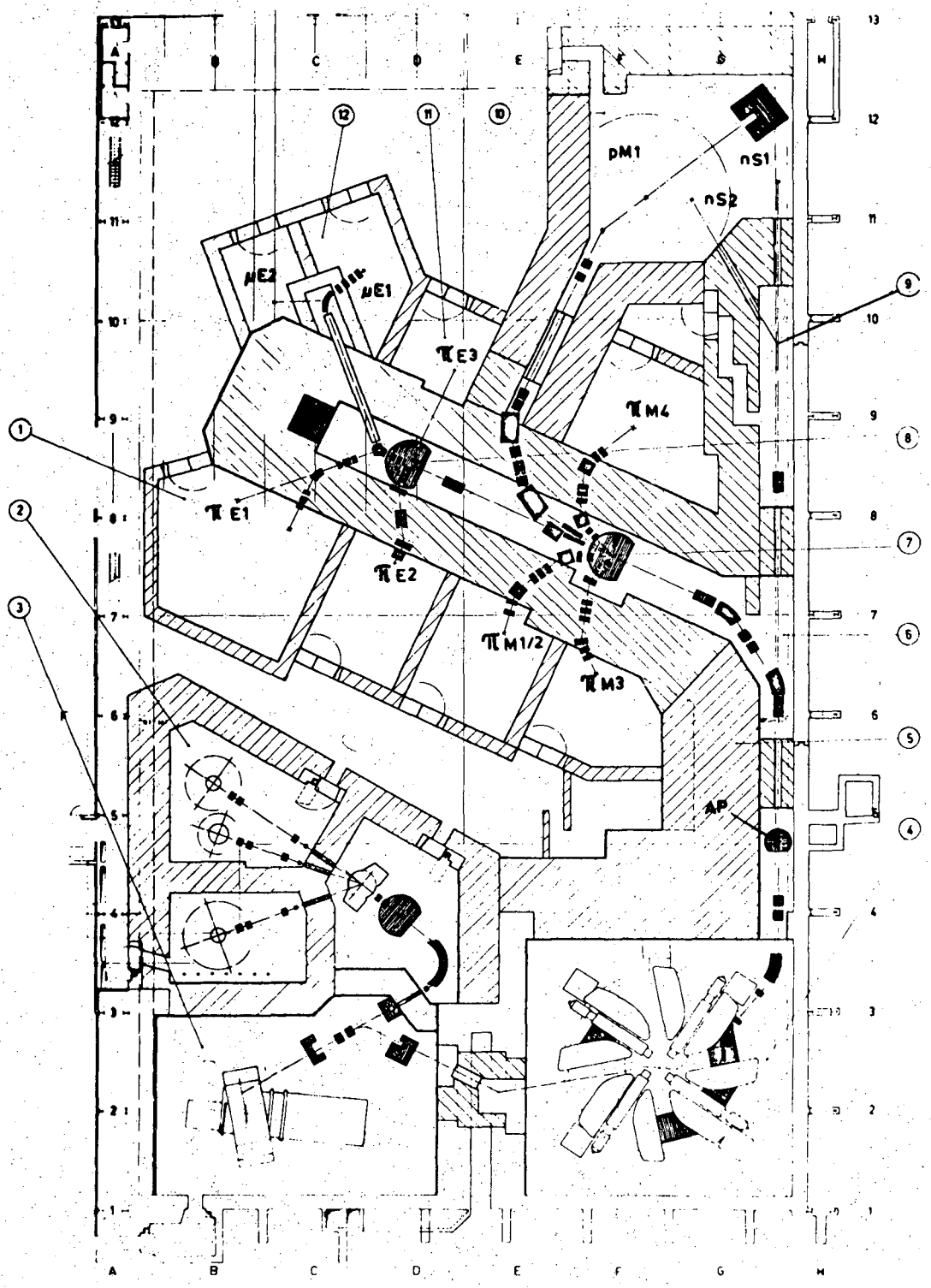

XBL 722-328

Fig. 42

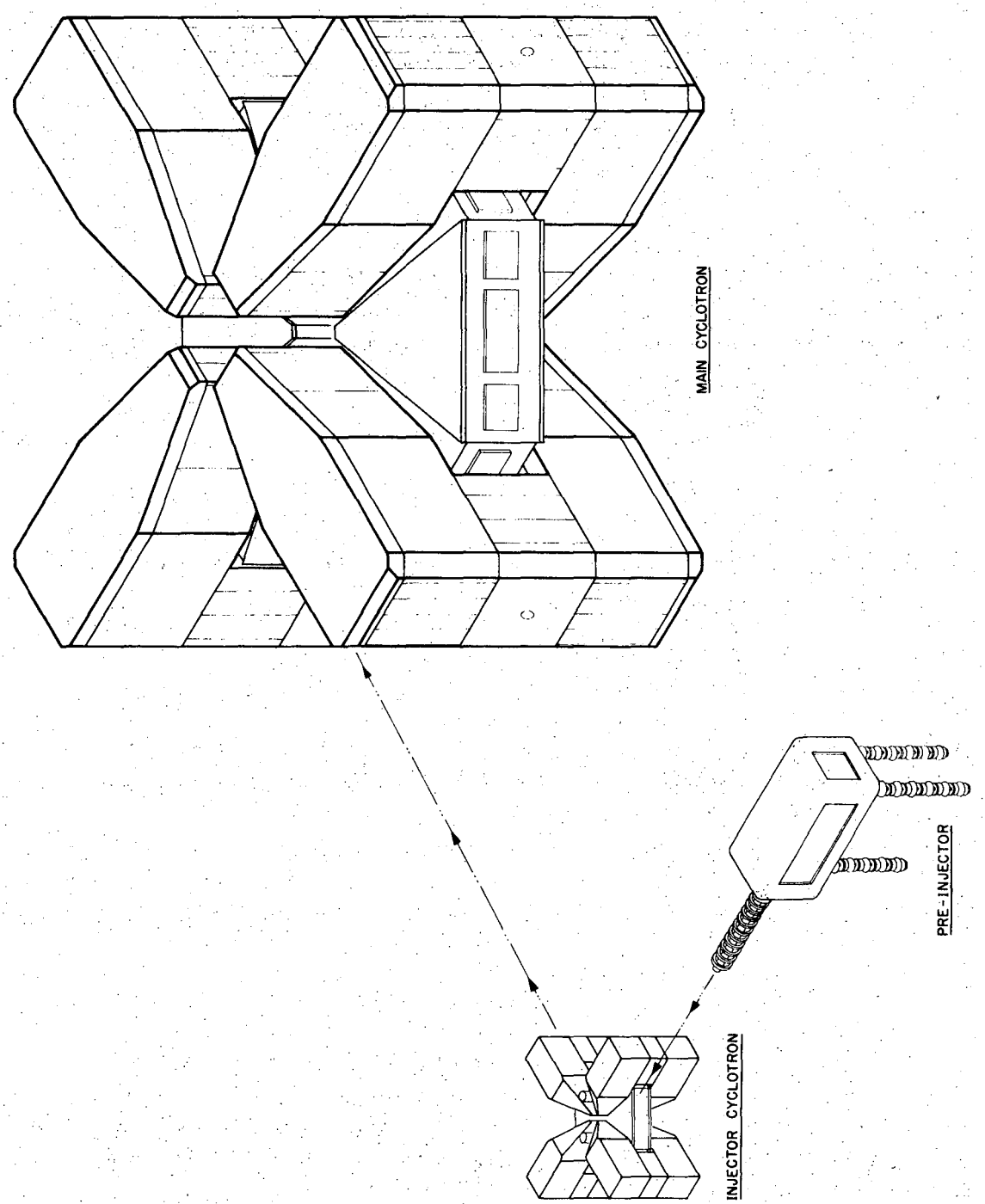

XBL 722-345

Fig. 43

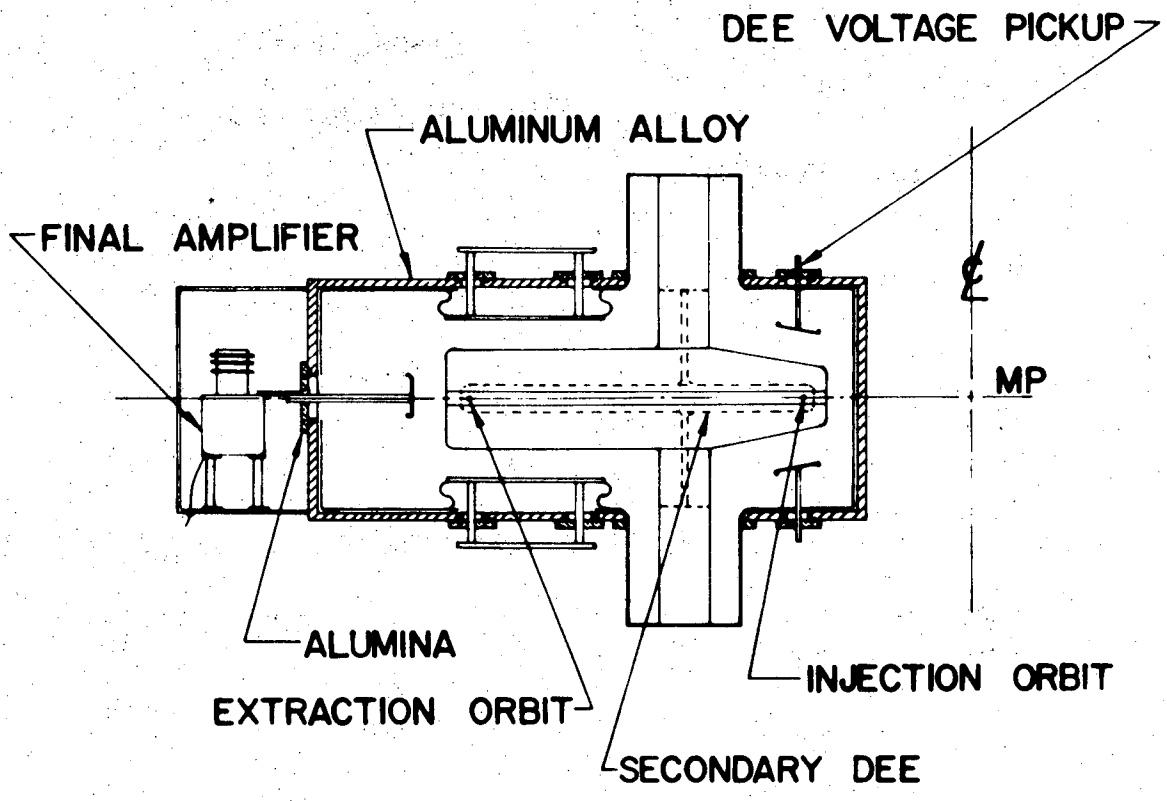

XBL 723-441

Fig. 44

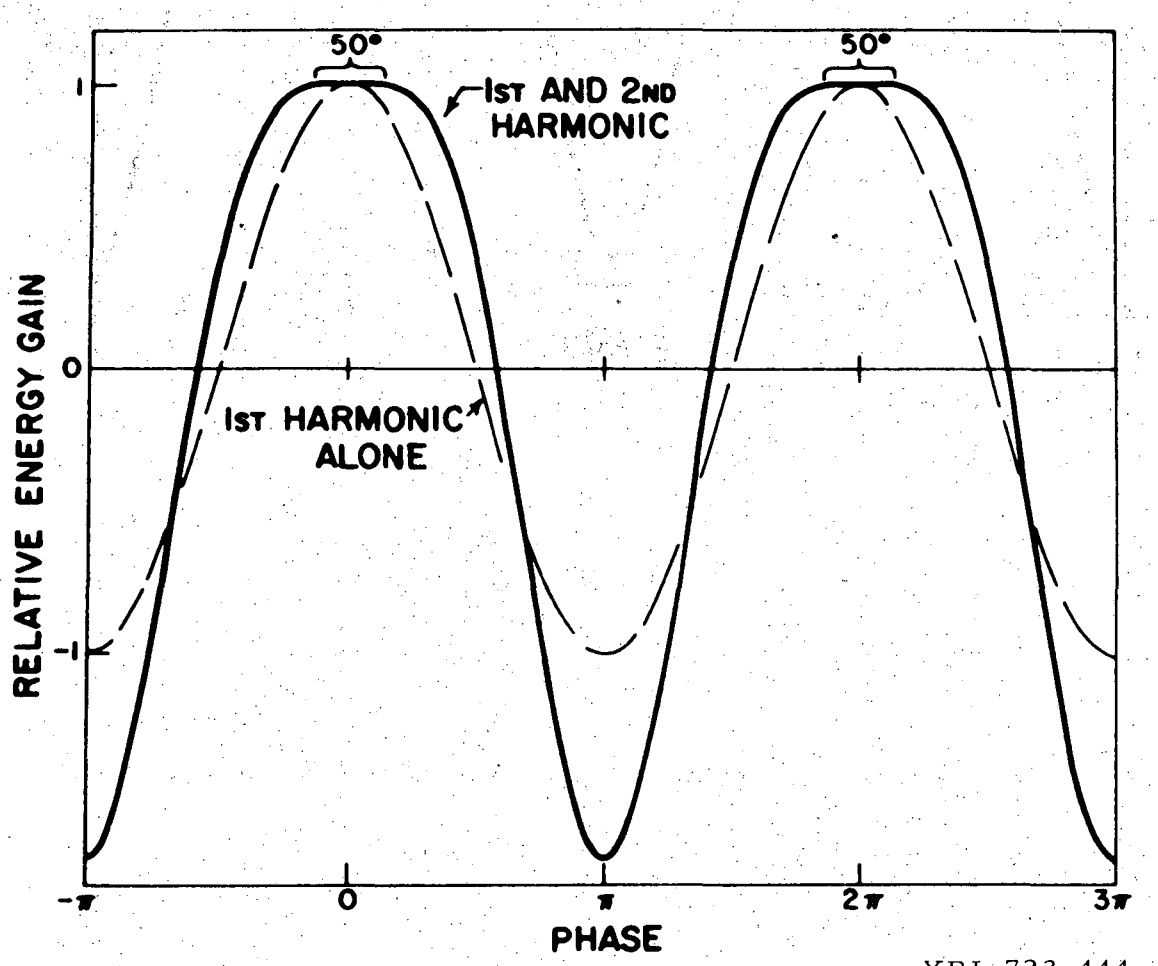

XBL 723-444

Fig. 45

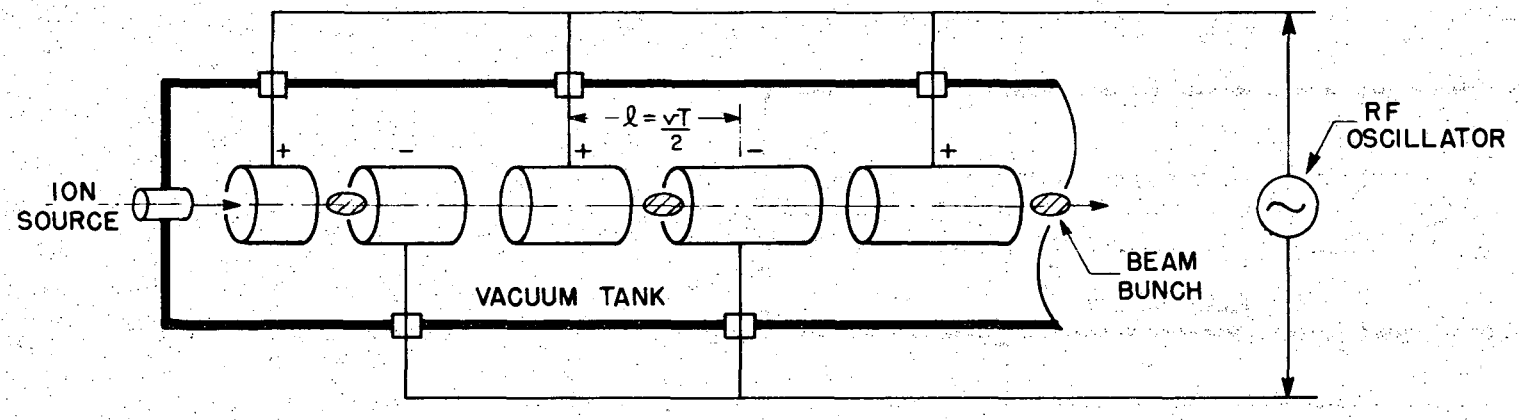

WIDERÖE LINEAR ACCELERATOR

XBL 722-349

Fig. 46

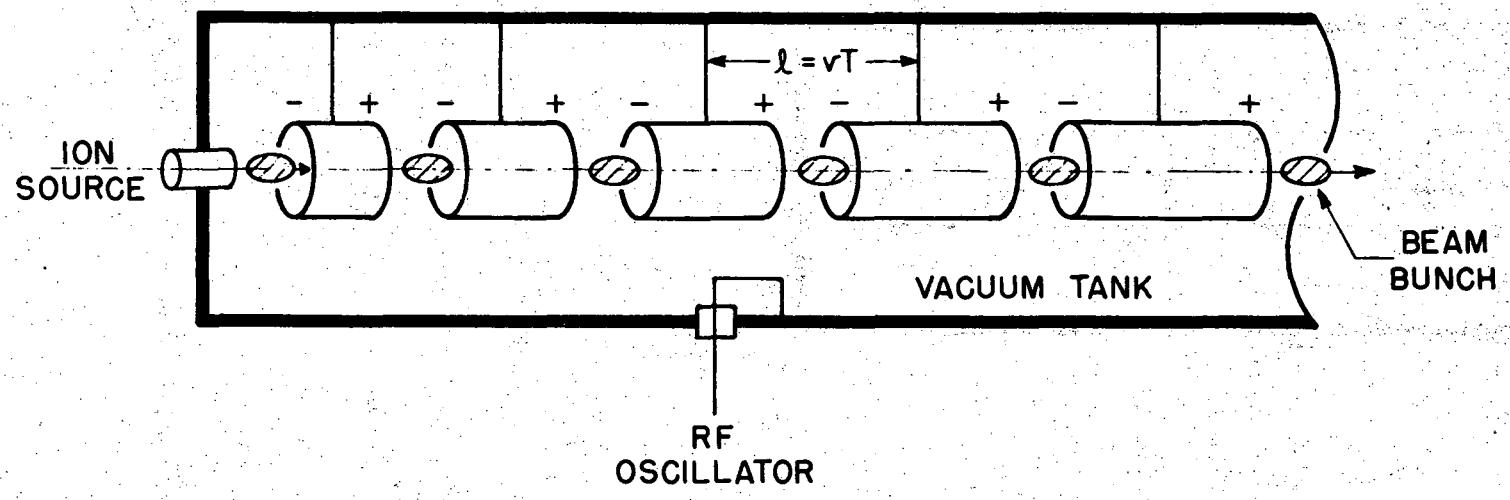

ALVAREZ LINEAR ACCELERATOR

XBL 722-348

Fig. 47

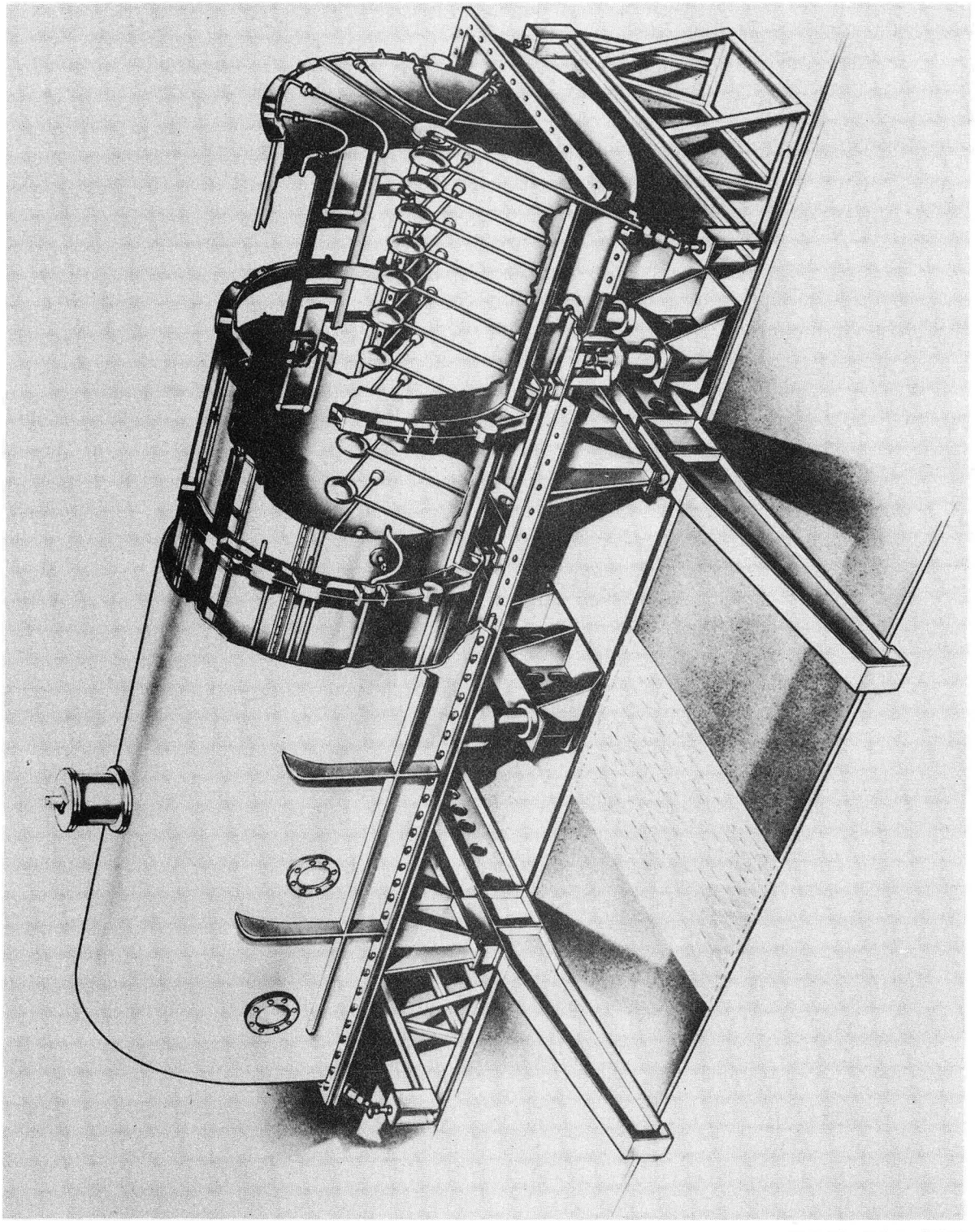

XBB-722-907

Fig. 48

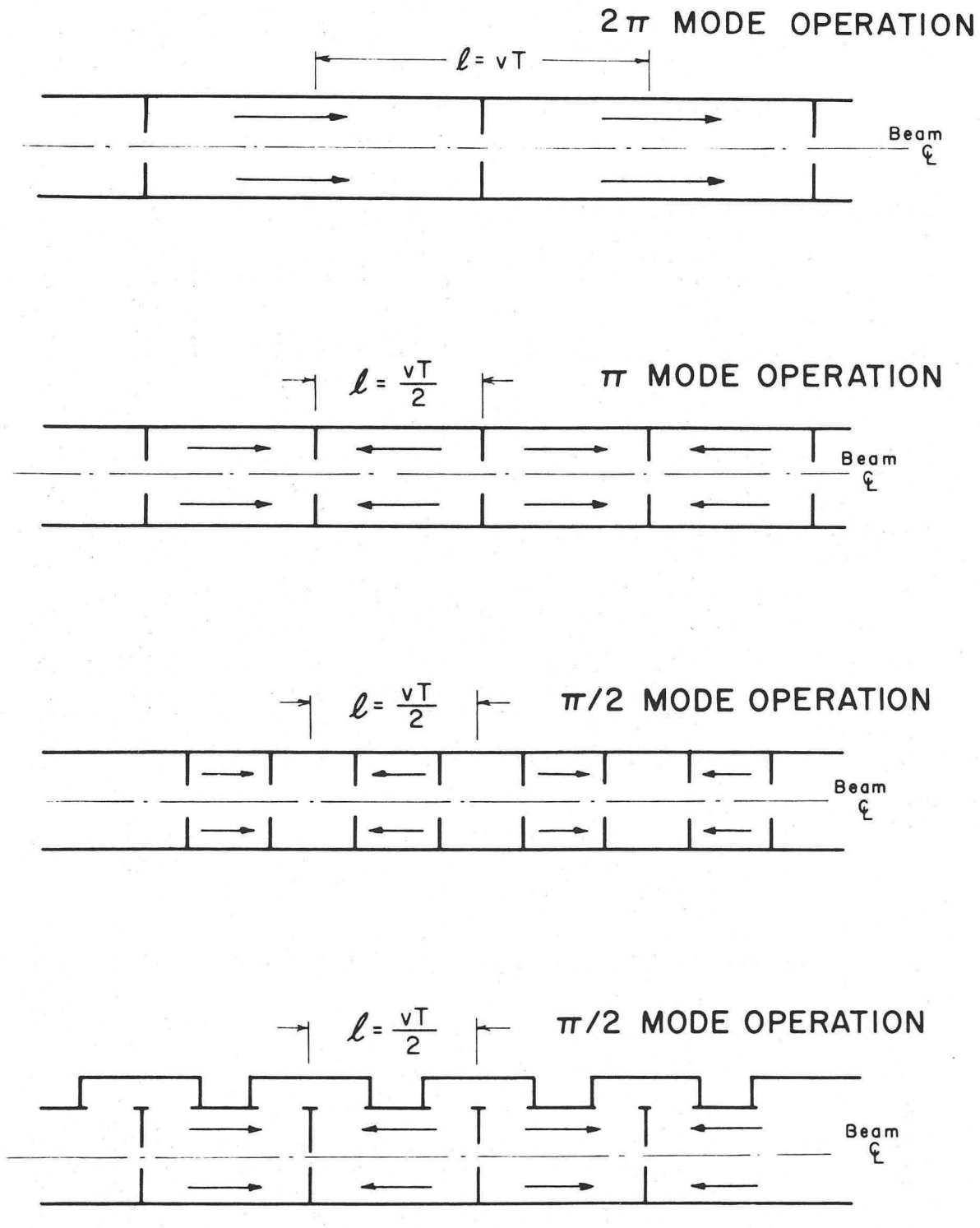

XBL 722-333

Fig. 49

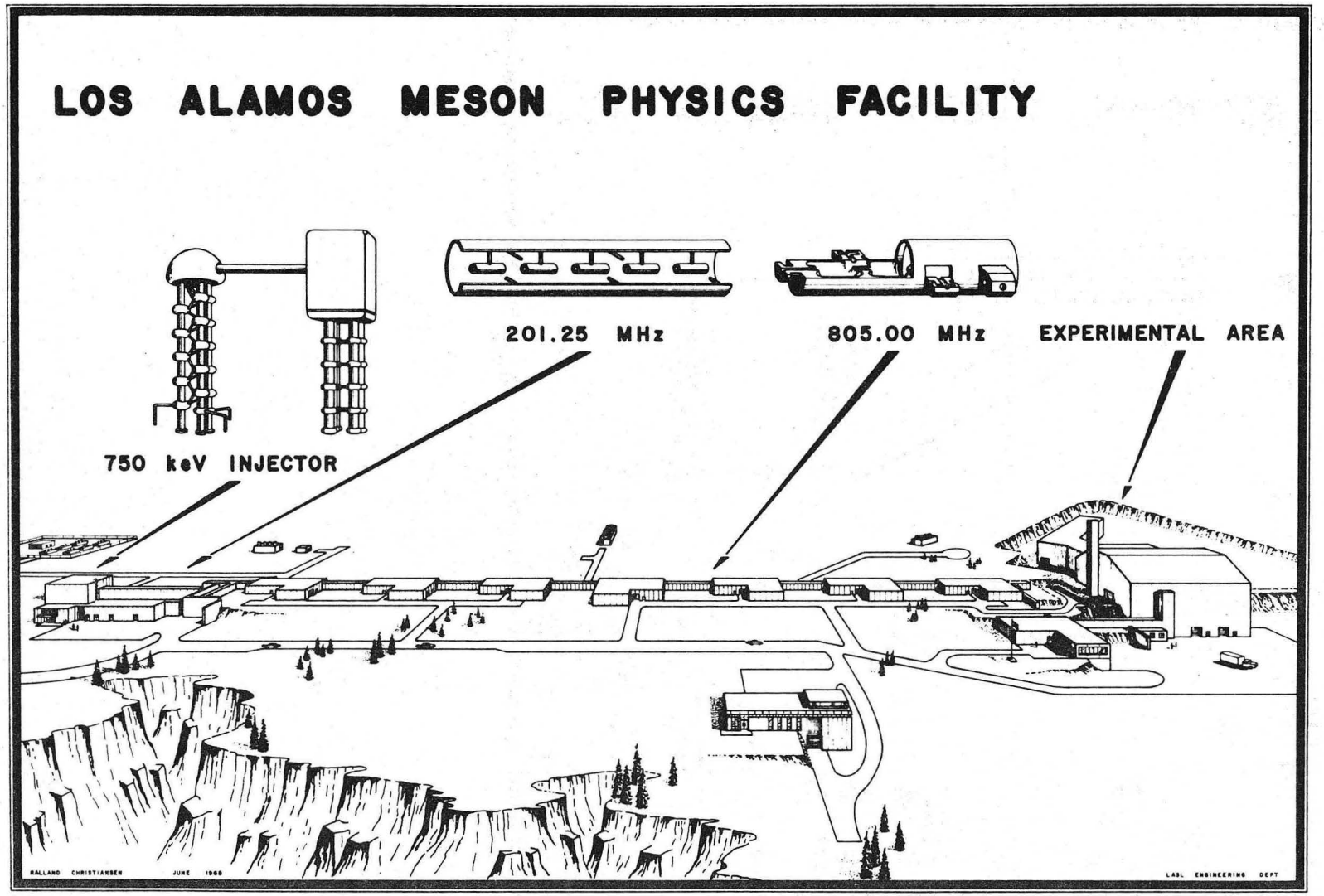

XBL 722-124

Fig. 50

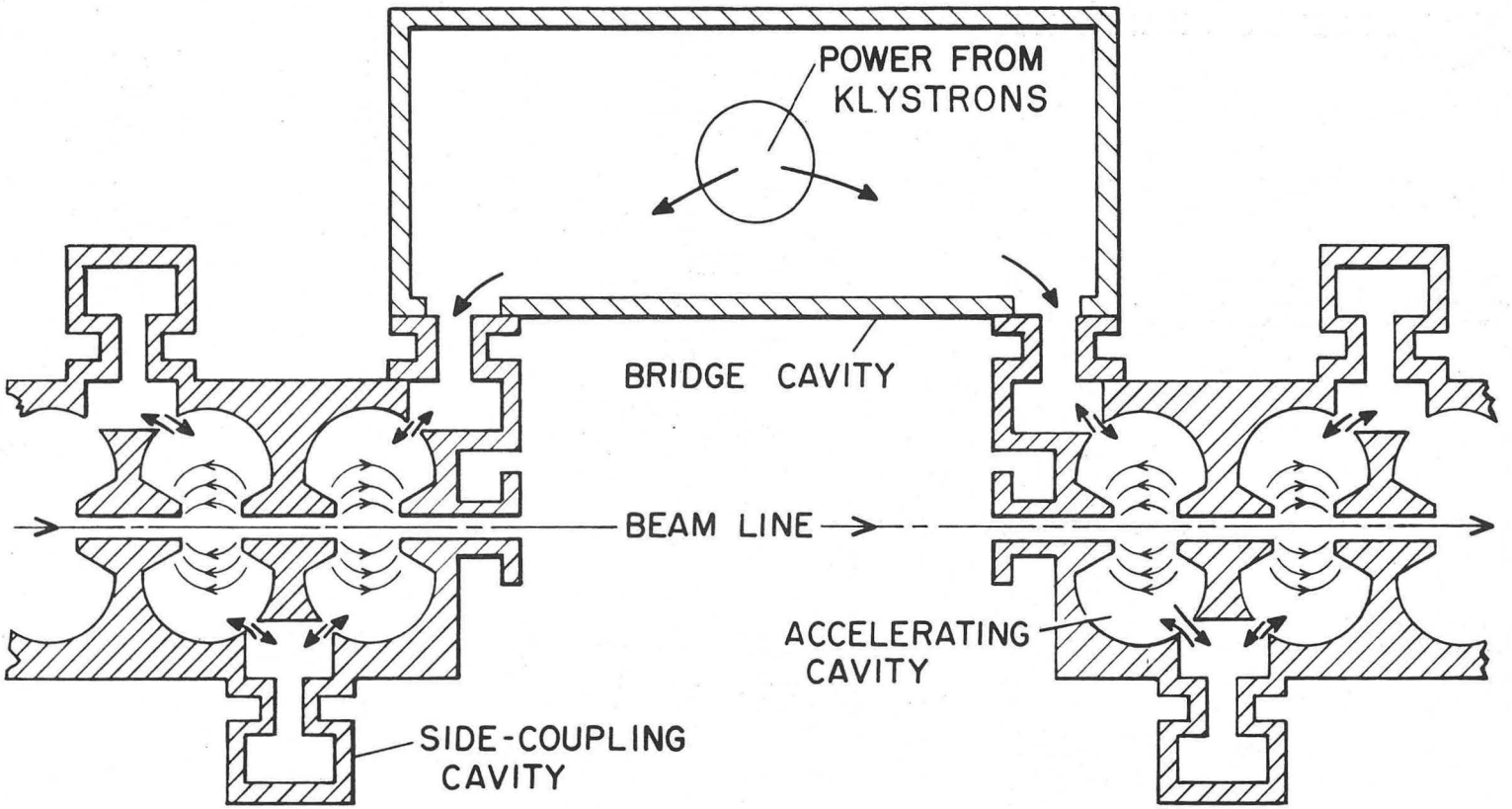
POWER FROM
KLYSTRONS
BRIDGE CAVITY
BEAM LINE
ACCELERATING
CAVITY
SIDE-COUPLING
CAVITY
XBL 722-128

Fig. 51

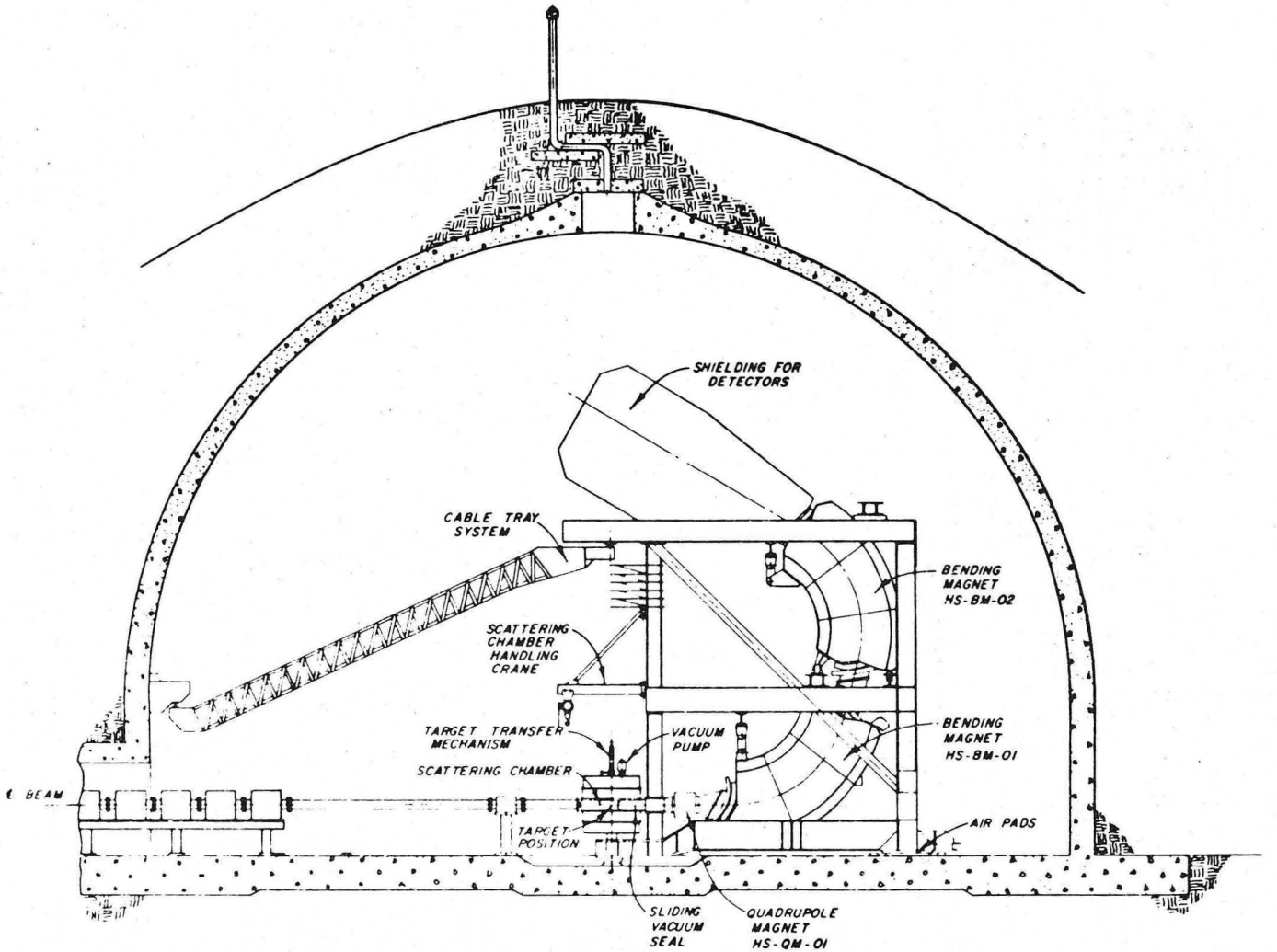

SECTION HRS FACILITY

0 5 10

GRAPHIC SCALE

XBL 722-326

Fig. 52

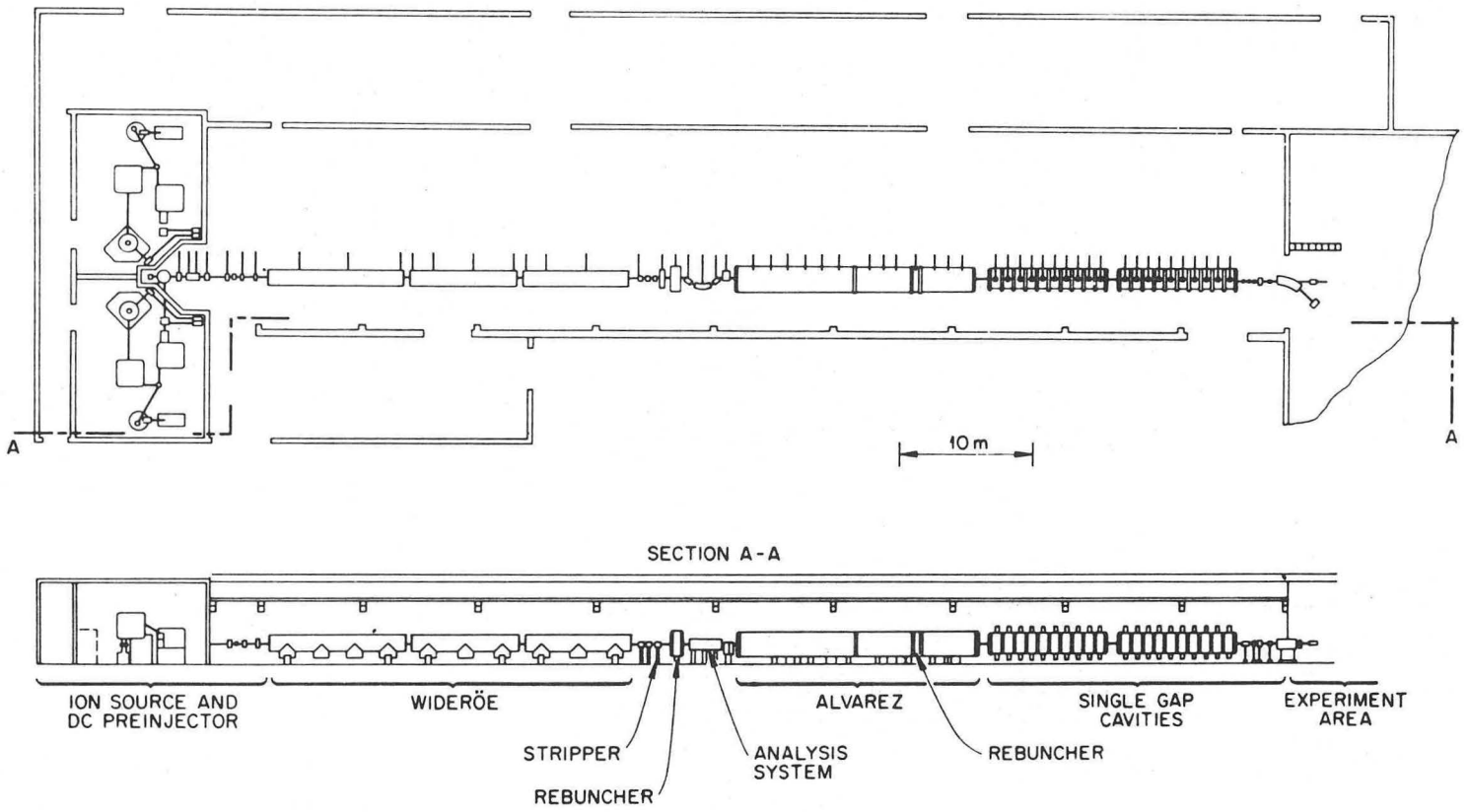

XBL 723-463

Fig. 53

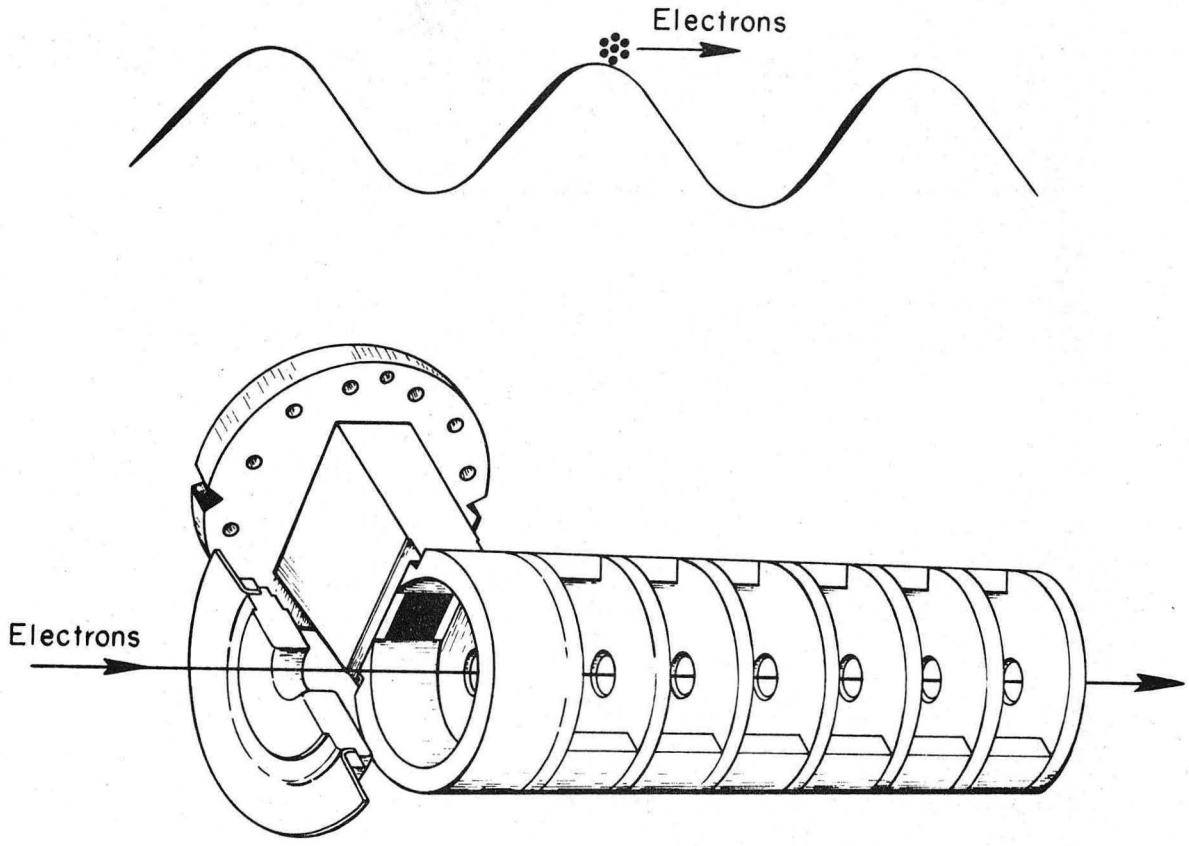

Fig. 54

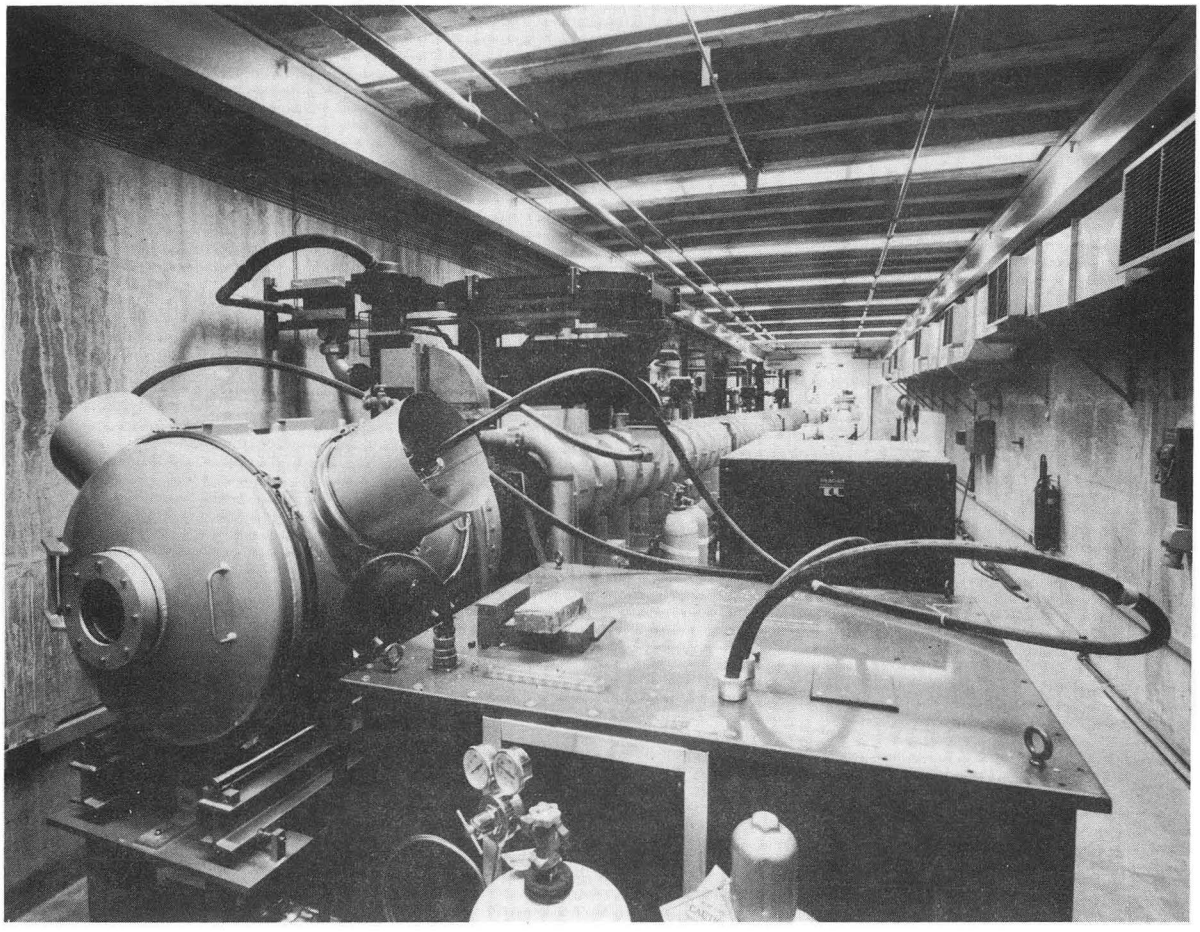

Fig. 55

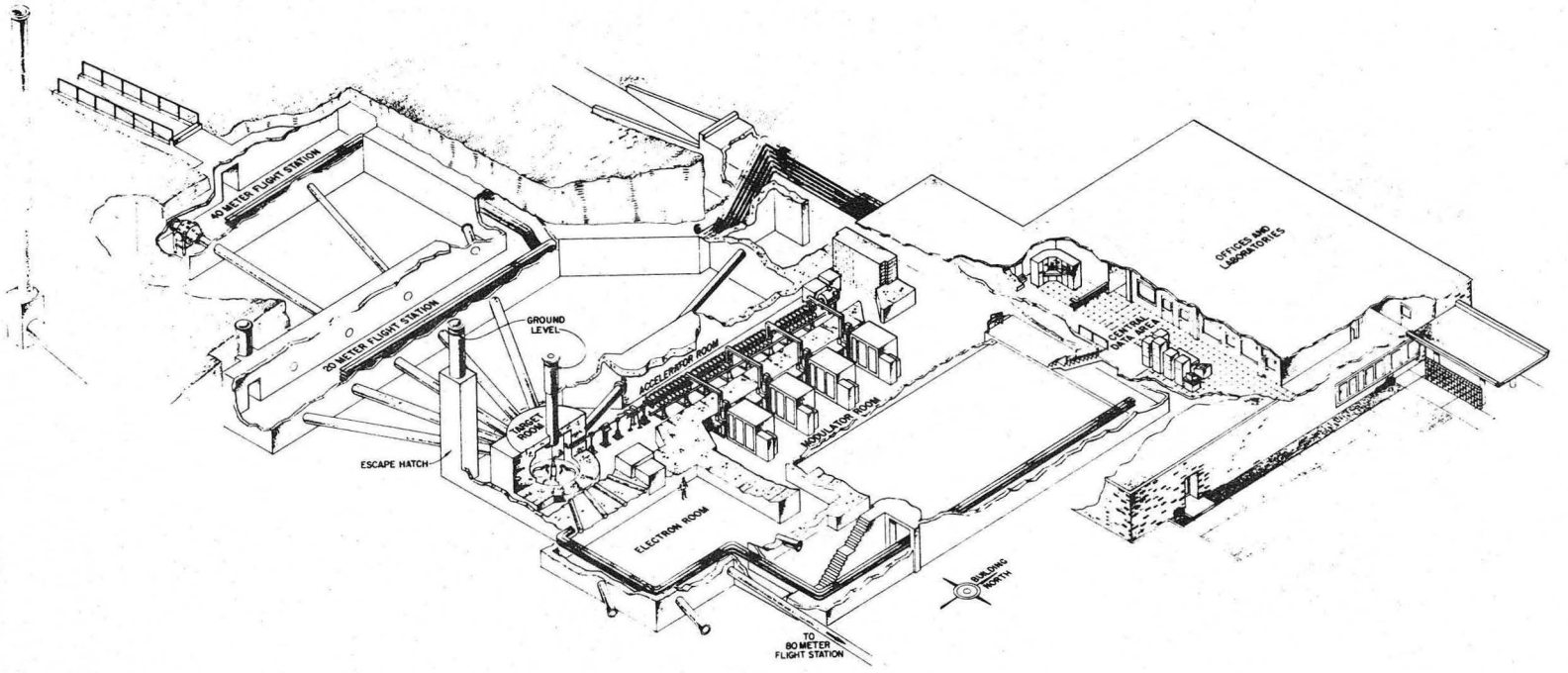

XBL 722-125

Fig. 56

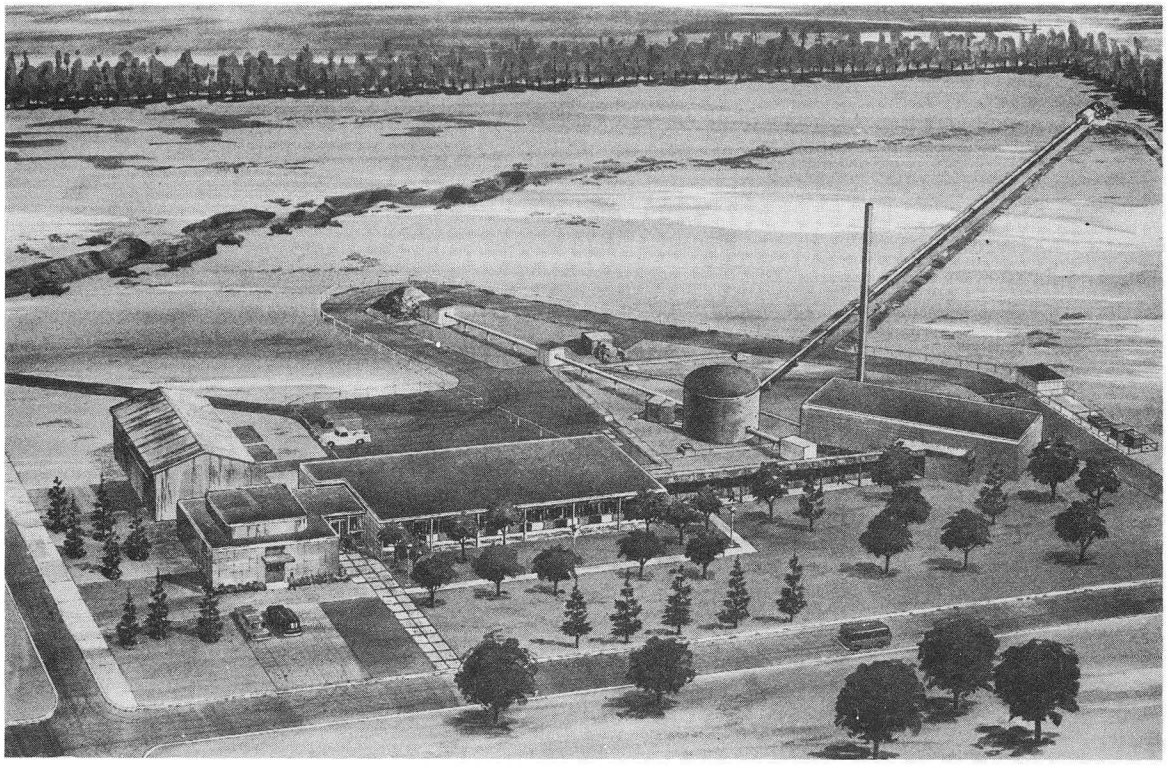

Fig. 57

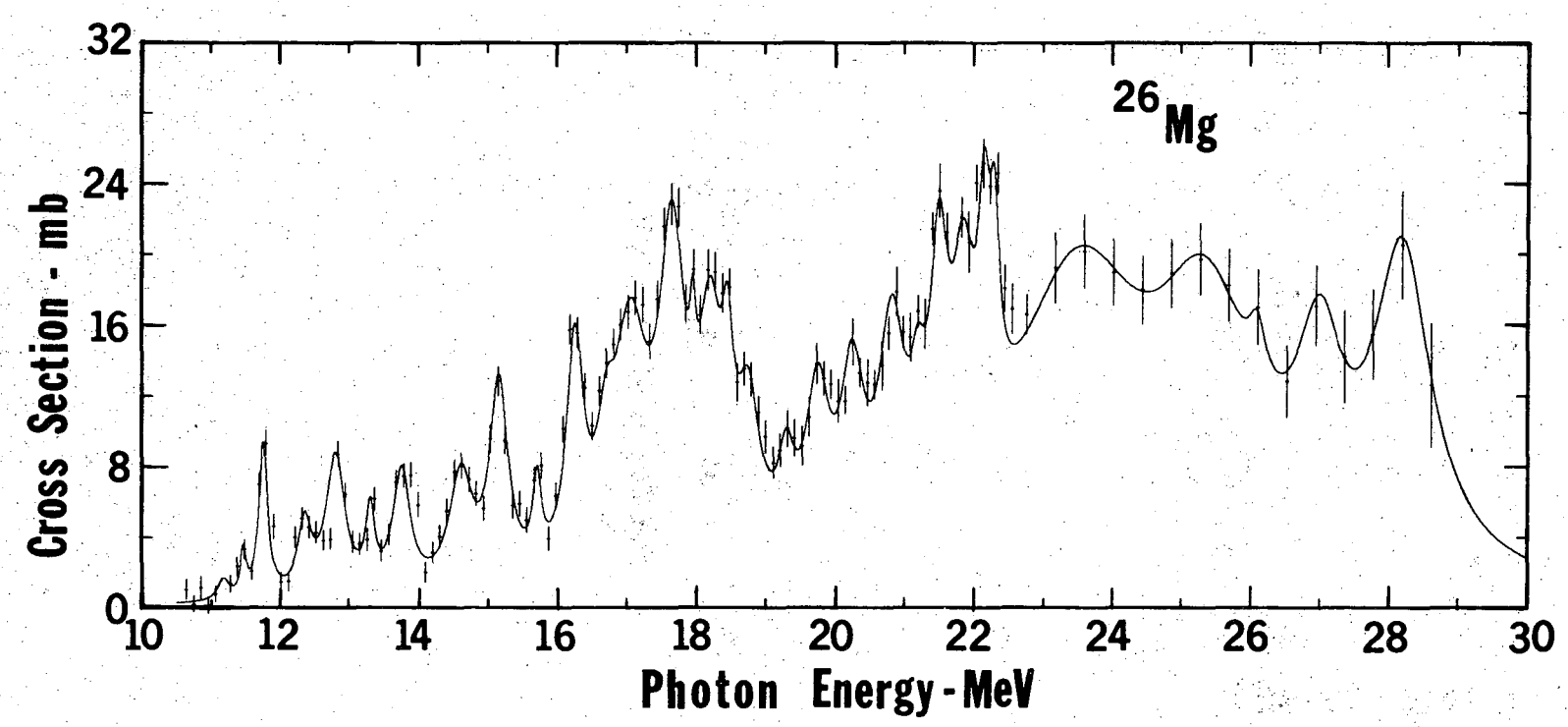

XBL 722-123

Fig. 58

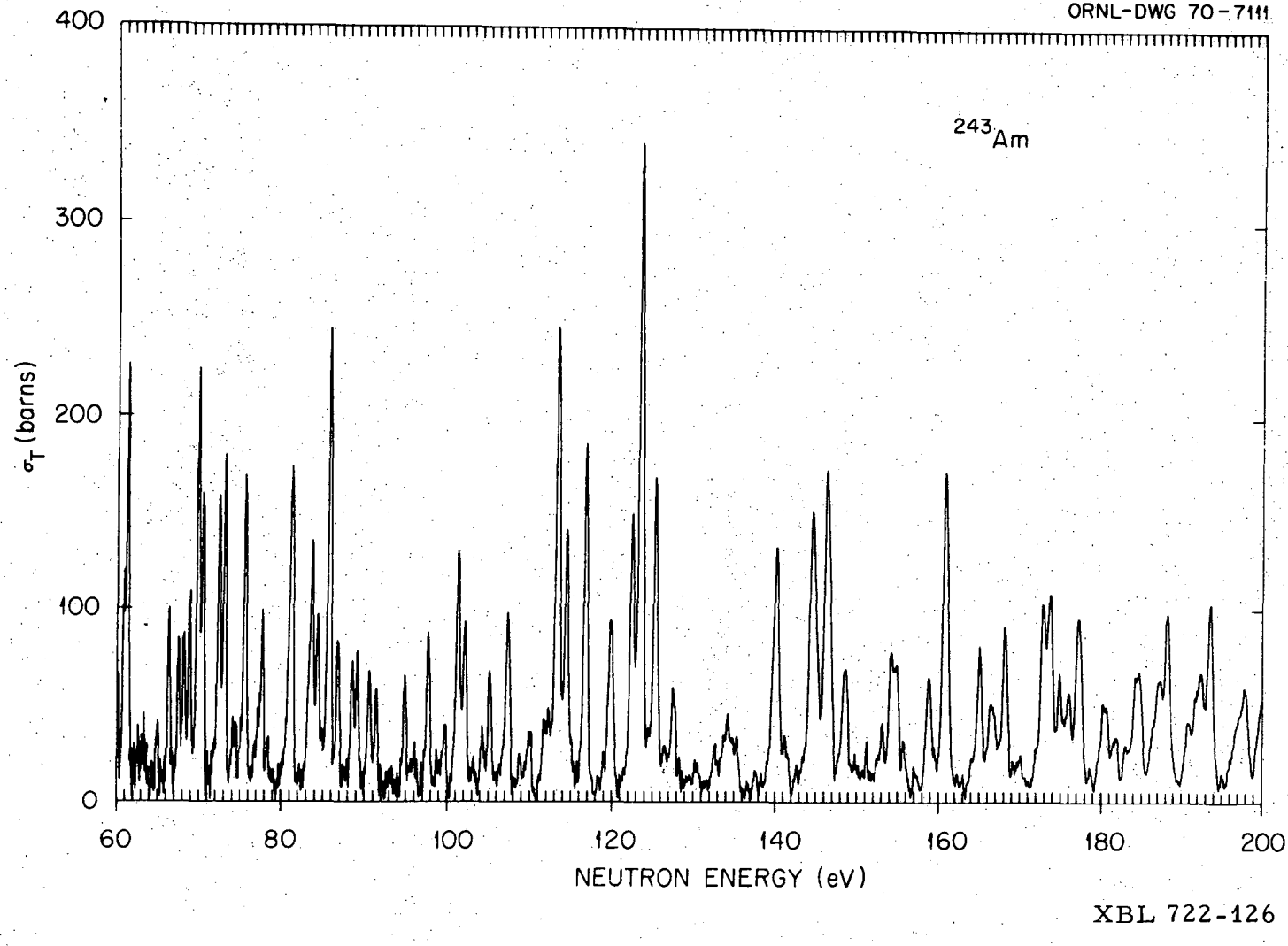
ORNL-DWG 70-7111
^{243}Am
σ_T (barns)
400
300
200
100
0
60
80
100
120
140
160
180
200
NEUTRON ENERGY (eV)
XBL 722-126

Fig. 59

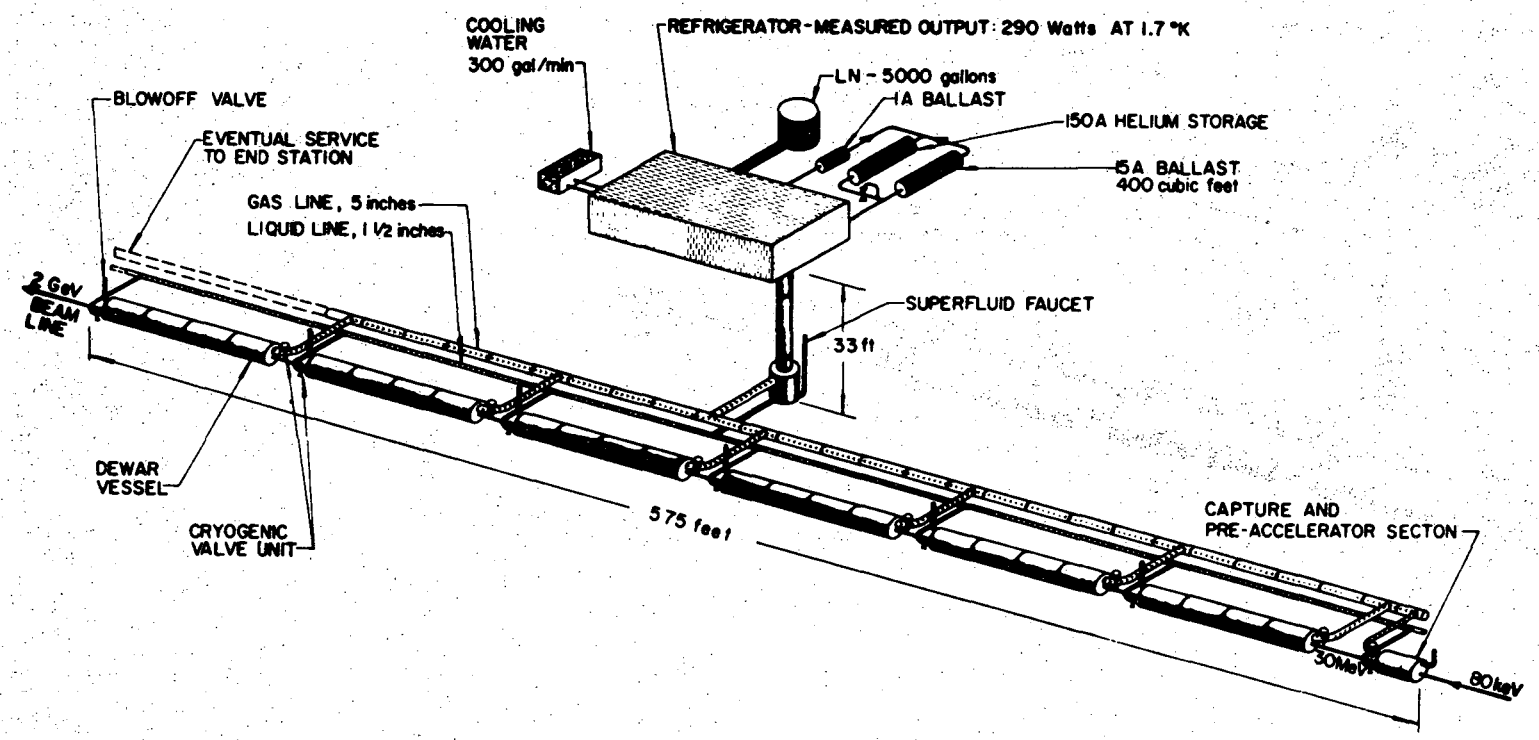

XBL 723-465

Fig. 60

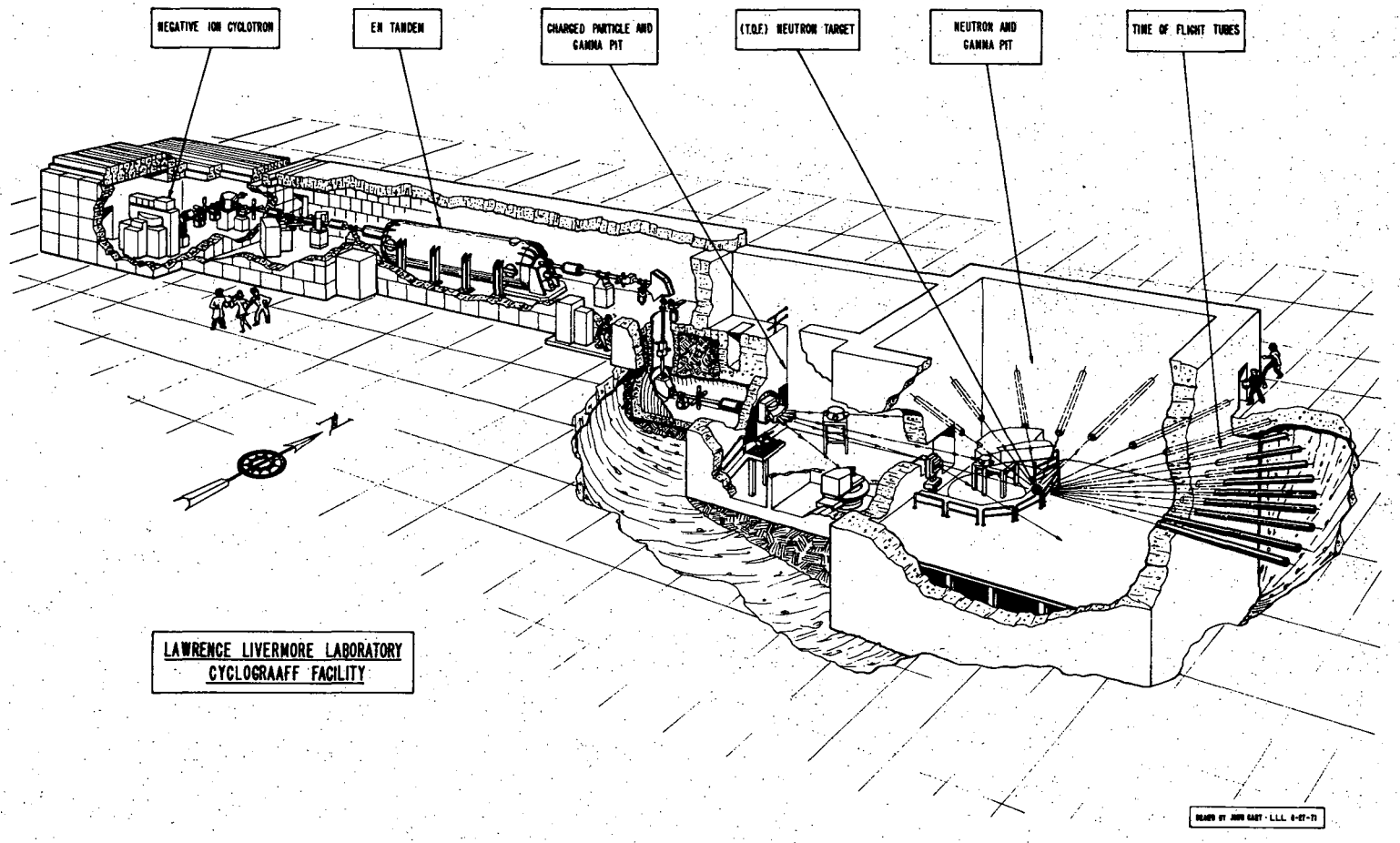

XBL 723-469

Fig. 61

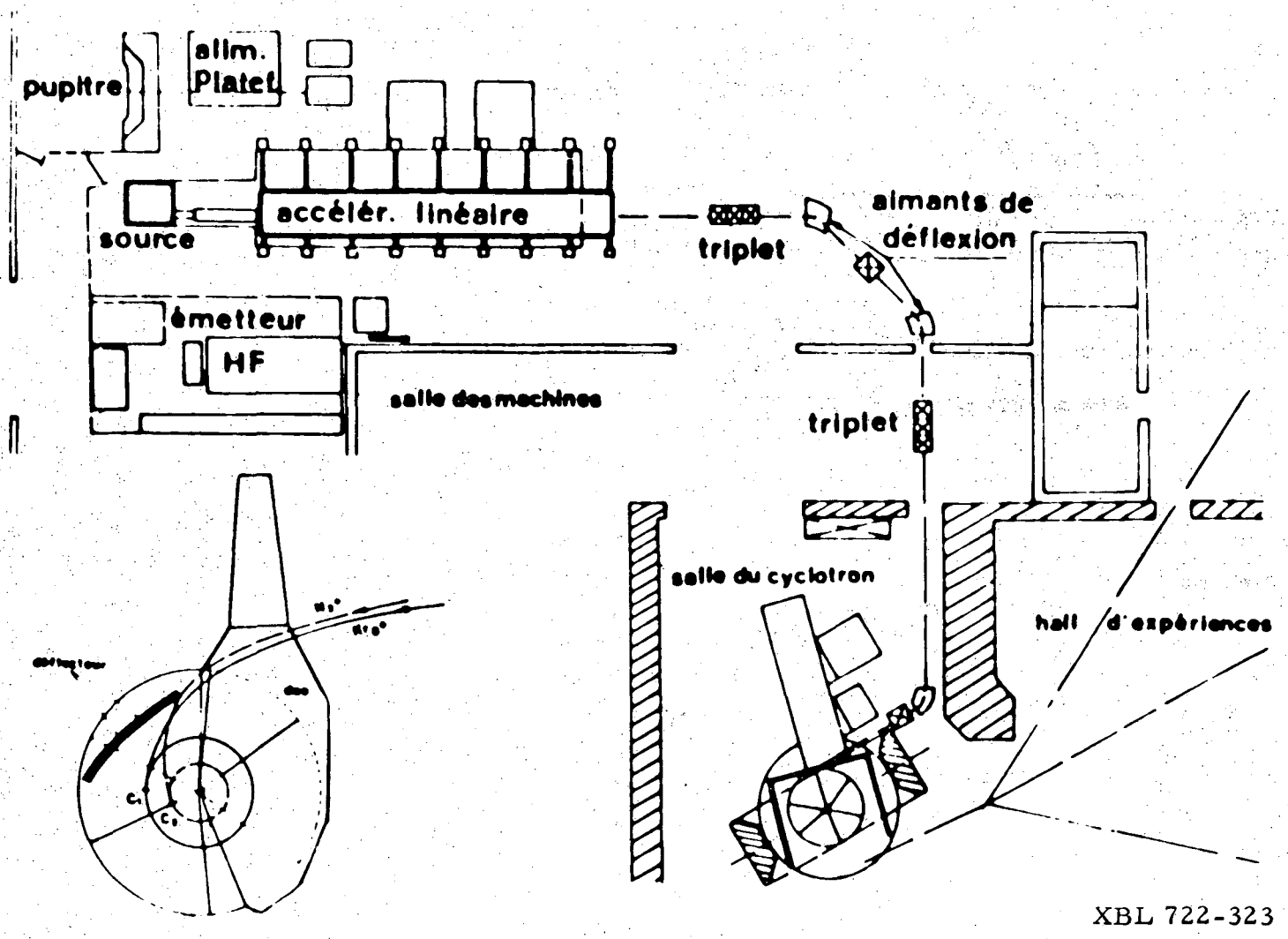
pupitre
alim. Platet
accélér. linéaire
source
triplet
aimants de déflexion
émetteur
HF
salle des machines
triplet
salle du cyclotron
hall d'expériences
XBL 722-323

Fig. 62

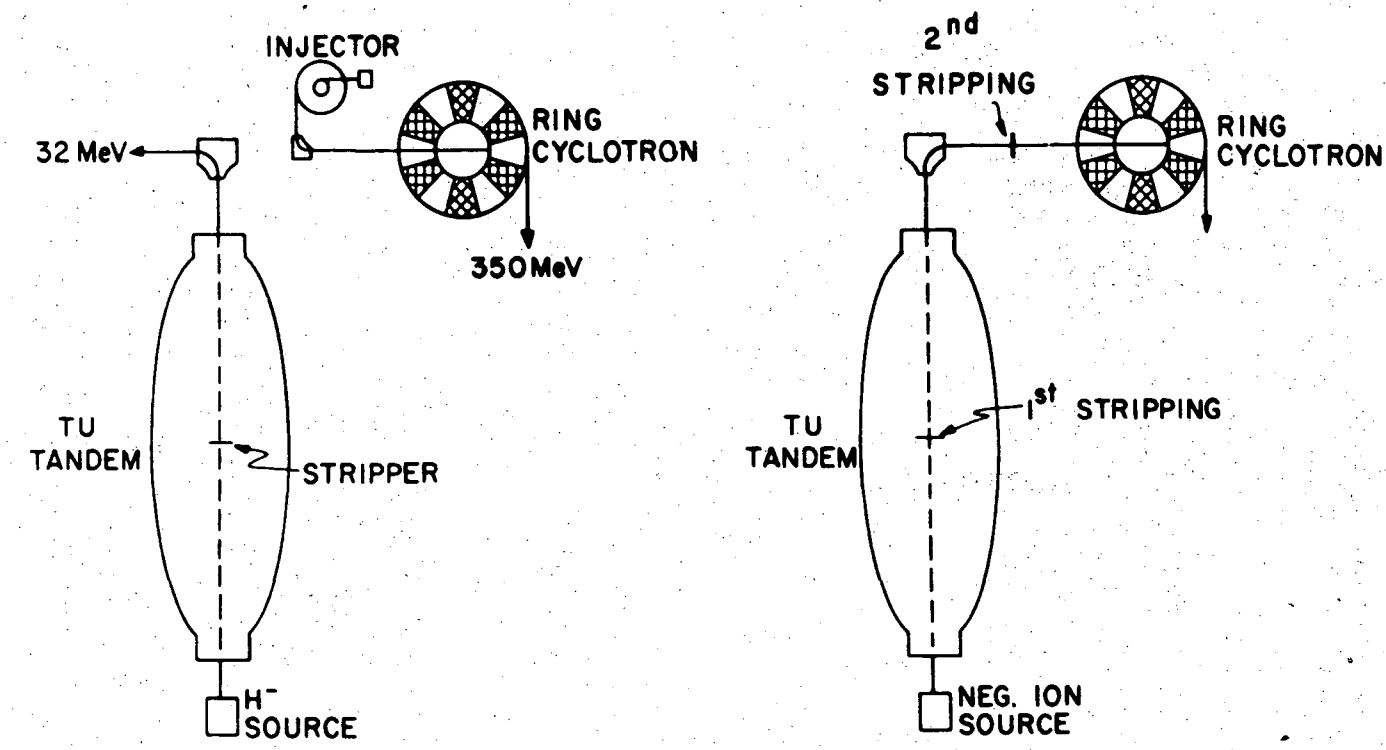

XBL 722-327

Fig. 63

TECHNICAL INFORMATION DIVISION
LAWRENCE BERKELEY LABORATORY
UNIVERSITY OF CALIFORNIA
BERKELEY, CALIFORNIA 94720